

FOREWORD

This report covers the work performed by the Analytical Mechanics Department of the Energy Controls Division of The Bendix Corporation under USAF Contract No. F33(615)-67-C-1263 from 15 December 1966 to 30 June 1967. The contract was initiated under Project No. 6M26499 (Flight Dynamics) "Development of the Shim Joint Concept for Composite Structural Members." This work was done under the technical direction of Mr. C. E. Booker of the Flight Dynamics Laboratory Research and Technology Division Air Force Systems Command, Wright-Patterson Air Force Base, Ohio. The manuscript was released August 1967.

This work was performed under the direction of A. L. Courtney, Project Engineer, and B. W. Cole, Senior Analyst. Important contributions were made by Dr. J. P. Wong, analysis, and F. P. Weldy, Processing and Fabrication Techniques. Dr. C. S. Ades, Dr. L. H. N. Lee, Dr. R. A. Ridha, and R. V. Cervelli have served as consultants in the area of analysis and design.

This technical documentary report has been reviewed and is approved.

*K. H. Digges*

Kennerly H. Digges  
Chief, Mechanical Branch  
Vehicle Equipment Div.  
AF Flight Dynamics Laboratory

ABSTRACT

Several methods have been proposed for attaching to the ends of structural tubes fabricated from composite materials, but few have been studied in detail. This program was initiated to study the shim joint concept in detail as subjected to tension loads. The shim joint concept permits a conventional pin joint between the composite tube end and a mating metal fitting by reinforcing the composite material with thin metallic layers. Shim joints were studied during this program as applied to glass reinforced plastic tubes. Corrosion resistant steel (AM 355, 260 ksi) was used as a reinforcement material.

An attempt was made to extend shim joint technology by (a) defining through analyses the critical failure modes and pertinent design parameters for tension loads, (b) establishment of design allowables for each of the failure modes through tensile testing of single pin, flat plate specimens, (c) development of a rational design procedure for the shim reinforced tube end, (d) development of improved methods for fabrication and machining of the reinforced tube end, and (e) fabrication and test of full scale tubular joints in test weight end fittings.

It was shown during this program that glass composite tubes can be successfully reinforced with AM 355 foil to develop the ultimate load in the tube without prohibitive attachment weight penalties. An optimization routine was used in the design procedure to aid in determining the minimum weight configuration. The bond joint strength was increased significantly during the program by incorporating an adhesive film between the metallic and fibrous layers. A joint, designed to transmit 150 kips to a 3.0 inch OD tube, added only 0.35 pound to the basic tube weight.

TABLE OF CONTENTS

| Section |  | Page |
|---------|--|------|
| I       | INTRODUCTION . . . . .                             | 1    |
|         | 1.1 History . . . . .                              | 1    |
|         | 1.2 Program Objectives . . . . .                   | 2    |
| II      | ANALYSIS OF ATTACHMENT AREA . . . . .              | 4    |
|         | 2.1 Design Variables . . . . .                     | 4    |
|         | 2.2 Failure Modes . . . . .                        | 6    |
|         | 2.2.1 Net Area Tension . . . . .                   | 7    |
|         | 2.2.2 Pin Hole Bearing . . . . .                   | 8    |
|         | 2.2.3 Hoop Tension . . . . .                       | 9    |
|         | 2.2.4 Shear Bearing . . . . .                      | 9    |
|         | 2.2.5 Bond . . . . .                               | 10   |
|         | 2.2.6 Wall Thickness Transition Zone . . . . .     | 16   |
|         | 2.2.7 Pin Shear . . . . .                          | 17   |
| III     | FLAT PLATE TESTS . . . . .                         | 18   |
|         | 3.1 Purpose . . . . .                              | 18   |
|         | 3.2 Description . . . . .                          | 18   |
|         | 3.3 Flat Plate Test Results . . . . .              | 18   |
|         | 3.3.1 Net Tension Area . . . . .                   | 18   |
|         | 3.3.2 Pin Bearing . . . . .                        | 20   |
|         | 3.3.3 Hoop Tension . . . . .                       | 21   |
|         | 3.3.4 Bond . . . . .                               | 21   |
|         | 3.3.5 Transition Zone . . . . .                    | 22   |
|         | 3.3.6 Staggered Shim Length . . . . .              | 22   |
| IV      | SHIM JOINTS FOR STRUCTURAL TUBES . . . . .         | 35   |
|         | 4.1 Design Procedure . . . . .                     | 35   |
|         | 4.1.1 Design Constraints . . . . .                 | 35   |
|         | 4.1.2 Objective Function . . . . .                 | 36   |
|         | 4.2 Design of Tubular Test Joint . . . . .         | 37   |
|         | 4.3 Efficiency of the Shim Joint Concept . . . . . | 38   |
| V       | MATERIALS AND FABRICATION . . . . .                | 42   |
|         | 5.1 Filament Composites . . . . .                  | 42   |
|         | 5.2 Metal Shims . . . . .                          | 42   |
|         | 5.3 Cleaning . . . . .                             | 43   |
|         | 5.4 Adhesives . . . . .                            | 45   |
|         | 5.5 Drilling . . . . .                             | 45   |
|         | 5.6 Flat-Plate Specimens . . . . .                 | 46   |
|         | 5.7 Tubes . . . . .                                | 46   |

LIST OF ILLUSTRATIONS

| Figure | Title   | Page |
|--------|---|------|
| 1      | Tubular Shim Joint Design Variables . . . . .   | 5    |
| 2      | Effect of Overlap Length on Adhesive Maximum Shear Stress Concentration Factor . . . . .  | 14   |
| 3      | Effect of Adhesive Thickness on Shear Stress Concentration Factor for Bonded Joints . . . . .   | 15   |
| 4      | Typical Flat Plate Specimen . . . . .   | 19   |
| 5      | Flat Plate Specimens - Rupture through Net Tension Area . . . . .   | 23   |
| 6      | Net Tension Test Results vs. $D_{op}/W$ . . . . .   | 24   |
| 7      | Flat Plate Specimens - Pin Bearing Failure . . . . .  | 25   |
| 8      | Pin Bearing Test Results vs. $D_{op}/t_s$ . . . . .   | 26   |
| 9      | Flat Plate Specimens - Rupture through Hoop Tension Area . . . . .  | 27   |
| 10     | Hoop Tension Test Results vs. $a/D_{op}$ . . . . .  | 28   |
| 11     | Flat Plate Specimens - Failure of BR-1009-49 Adhesive Joint . . . . .   | 29   |
| 11a    | Flat Plate Specimens - Failure of AF-111 Adhesive Joint . . . . .   | 30   |
| 12     | Average Adhesive Shear Strength vs. Effective Joint Length . . . . .  | 31   |
| 13     | Flat Plate Specimens - Rupture by Combination of Failure Modes . . . . .  | 32   |
| 14     | Flat Plate Specimens with Thickness Transition - Failure by Delamination . . . . .  | 33   |
| 15     | Flat Plate Specimen with Staggered Shim Length - Combination Glass and Bond Failure . . . . .   | 34   |
| 16     | Increase in Weight of Structural Member Due to Joint vs. Number of Pins used in Joint . . . . .   | 40   |
| 17     | Weight Comparison of Constant Strength Tubes vs. Tube Length<br>Fiber Glass Tube Weights Include Steel End Reinforcement and Steel Pins . . . . . | 41   |
| 18     | Bend Radius vs. Residual Bend Radius for AM-355 Sheet 0.02 Inch Thick . . . . .   | 44   |
| 19     | Flat Plate Specimen Winding Mandrel . . . . .   | 47   |
| 20     | Winding Longitudinal Filament . . . . .   | 48   |
| 21     | Winding Transverse Filament . . . . .   | 49   |
| 22     | Location of Metal Shim . . . . .  | 50   |
| 23     | Tube with Shim Reinforced End . . . . .   | 52   |
| 24     | Shim Reinforced End of Tube . . . . .   | 53   |
| 25     | Joint End Test Adapter (Nonflight Weight) . . . . .   | 55   |
| 26     | Tension Fixture Assembly . . . . .  | 56   |
| 27     | Tubular Joint which was Fabricated for Testing . . . . .  | 58   |
| 28     | Tubular Shim Joint Specimen - After Tension Test . . . . .  | 60   |
| 29     | Tubular Shim Joint Specimen - After Compression Test . . . . .  | 61   |
| 30     | Effect of n ratio on the Shear Stress Concentration Factor . . . . .  | 85   |
| 31     | Effect of Joint Length on Distribution of Shear Stress . . . . .  | 86   |
| 32     | Effect of Joint Length on Distribution of Shear Stress Concentration Factor . . . . .   | 87   |

DEFINITIONS

- A - Cross sectional area, in.<sup>2</sup>.
- D - Diameter, in.
- E - Young's Modulus, ksi.
- $f_c$  - Compressive stress, ksi.
- $f_t$  - Tensile stress, ksi.
- $f_{ht}$  - Hoop tension stress, ksi.
- $f_s$  - Shear stress, ksi.
- $f_n$  - Normal stress, ksi.
- $F_{tu}$  - Ultimate tensile strength of the shim material, ksi.
- $F_{xt}$  - Ultimate tensile strength of the composite laminate in the longitudinal direction.
- $F_s$  - Allowable average shear stress in adhesive layer, ksi.
- $F_{su}$  - Ultimate shear strength of pin material, ksi.
- $G_a$  - Shear modulus of adhesive material, ksi.
- $K_{tu}$  - Net tension area efficiency factor, ( $f_t/F_{tu}$ ).
- $K_{ht}$  - Hoop tension efficiency factor ( $f_{ht}/F_{tu}$ ).
- $K_{br}$  - Pin bearing efficiency factor ( $f_{br}/F_{tu}$ ).
- L - Length, in.
- $N_s$  - Number of shim reinforcement layers.

SECTION I  
INTRODUCTION

1.1 HISTORY

Energy Controls Division (ECD) of The Bendix Corporation explored in an earlier program the feasibility of utilizing composite materials for structural components in such mechanical assemblies as aircraft landing gear. The criteria for feasibility in that program were confined to cost and weight considerations. The feasibility program was performed under the authority of USAF Contract Number AF33(615)-3080 and the findings were documented in report number AFML-TR-66-309, dated December, 1966.

It was determined during the feasibility program that structural tubes fabricated of composite materials would be lighter than tubes made from more conventional materials such as steel, aluminum, or titanium alloys.

The earlier study had indicated that the greatest potential weight savings could be obtained with components designed primarily to support torsion or axial compression and tension. Typical of such components are torsion shafts and aircraft landing gear restrictor support tubes, spacer tubes, side braces, and drag braces.

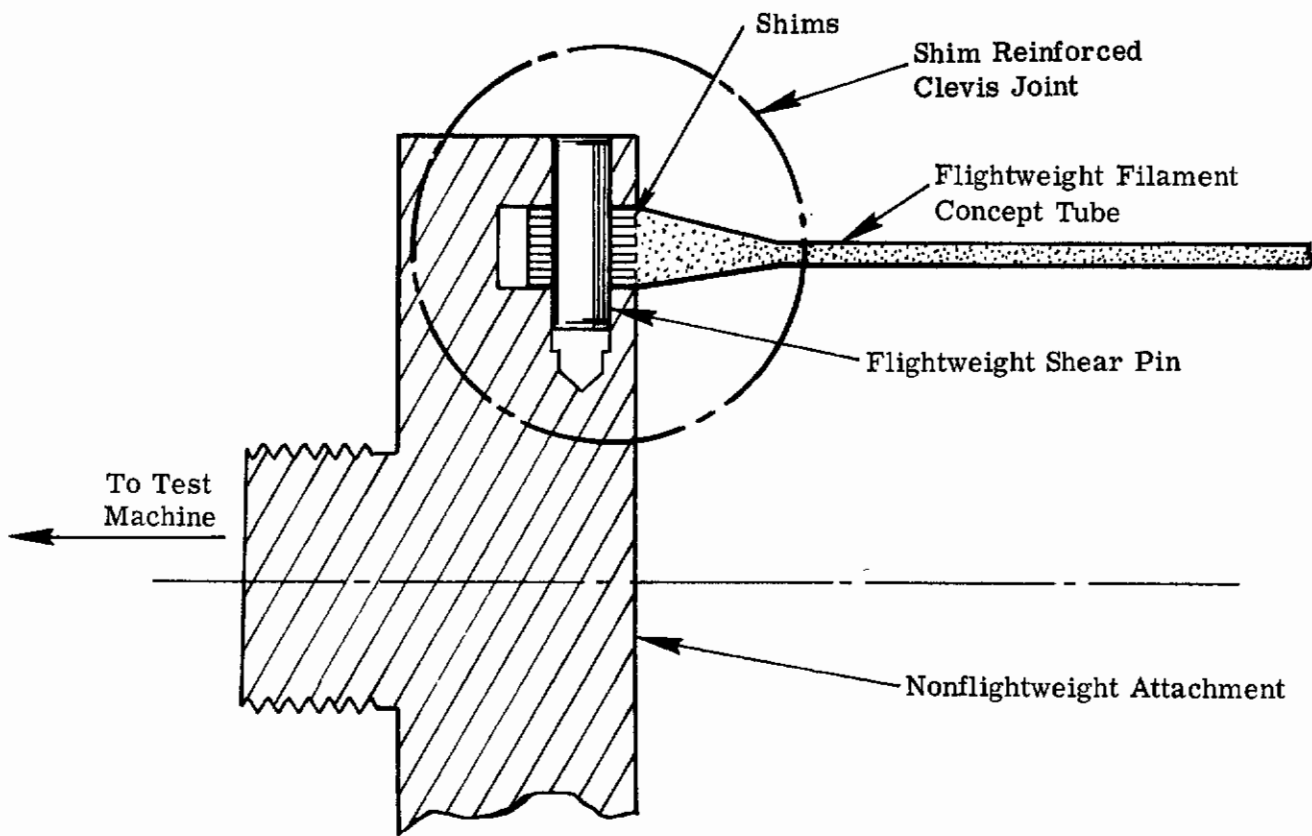
An important recommendation of the feasibility study was that lightweight methods of joining composite tubes to metal end fittings be developed. The design of metal end fittings, per se, is well within the capability of existing technology and does not require elaboration. However, even though structural members can be made lighter with composite materials than with the more common metal alloys, the weight of reinforcing composite tube ends and joining them to metal end fittings will impose penalties. As a result, the significant weight saving potential of composite materials may tend to be offset somewhat by the weight penalties imposed by joining the tubes to metal end fittings. The design of efficient, lightweight joints between composite tubes and metal end fittings is, therefore, a necessary element in the development of composite material landing gear components and requires formulation of design data and analysis techniques.

During the feasibility study, several different types of joints were considered which offered promise and warranted further development. The metal-shim-reinforced joint for tension and compression members showed considerable promise of providing a joint suitable for use in aircraft applications.



1.2 PROGRAM OBJECTIVES

The program documented in this report is an extension of the earlier program summarized briefly above. The program reported herein had as its objective the development of a shim reinforced clevis joint between a lightweight, filament concept tube and a nonflightweight attachment as shown below:



The objective of the subject program was achieved in accordance with the following program plan:

- A. Determine pertinent design variables by analysis of the shim joint concept.
- B. Conduct a literature search to locate applicable information pertaining to (1) bonded joint design, (2) mechanical joint design, (3) materials selection for shims and adhesives, (4) processing methods for bonding and machining shim materials, and (5) fabrication techniques for shim joints.
- C. Perform tests of shim reinforced flat-plate specimens to obtain ultimate strength design allowables.
- D. Employ an optimization procedure to perform minimum weight studies for shim joints.
- E. Fabricate and test the resulting joint design in two, three-inch outside diameter structural tubes structural adhesive.



SECTION II  
ANALYSIS OF ATTACHMENT AREA

2.1 DESIGN VARIABLES

Advanced concepts such as tapered shims, staggered shim lengths, and multiple rows of rivets can all be incorporated into the shim joint concept. In this program, however, a simple configuration was chosen for initial study. The shim layers were of uniform thickness and constant length in the longitudinal direction. A single circumferential row of pins was used to transfer loads from the composite tube to the mating metal part. Figure 1 illustrates the configuration which was studied.

Analysis of this simple attachment configuration resulted in an extensive list of potential design parameters. Each of the potential parameters must be considered in the design process to ensure that a minimum weight configuration is approached. Most of the geometric variables are defined in Figure 1. A complete listing of geometric variables is presented below:

- $N_s$  - Number of metallic shim layers.
- $N_p$  - Number of pins along the tube circumference.
- $N_c$  - Number of filament layers in tube wall that do not extend into the attachment area.
- $D_{op}$  - Outside pin diameter.
- $D_{ip}$  - Inside pin diameter.
- $W$  - Circumferential distance between pin centerlines.
- $a$  - Distance from pin row centerline to tube end.
- $l$  - Distance from pin row centerline to back edge of shims.
- $t_s$  - Thickness of metallic shim layers.
- $L_s$  - Longitudinal length of metallic shim layers ( $l + a$ ).

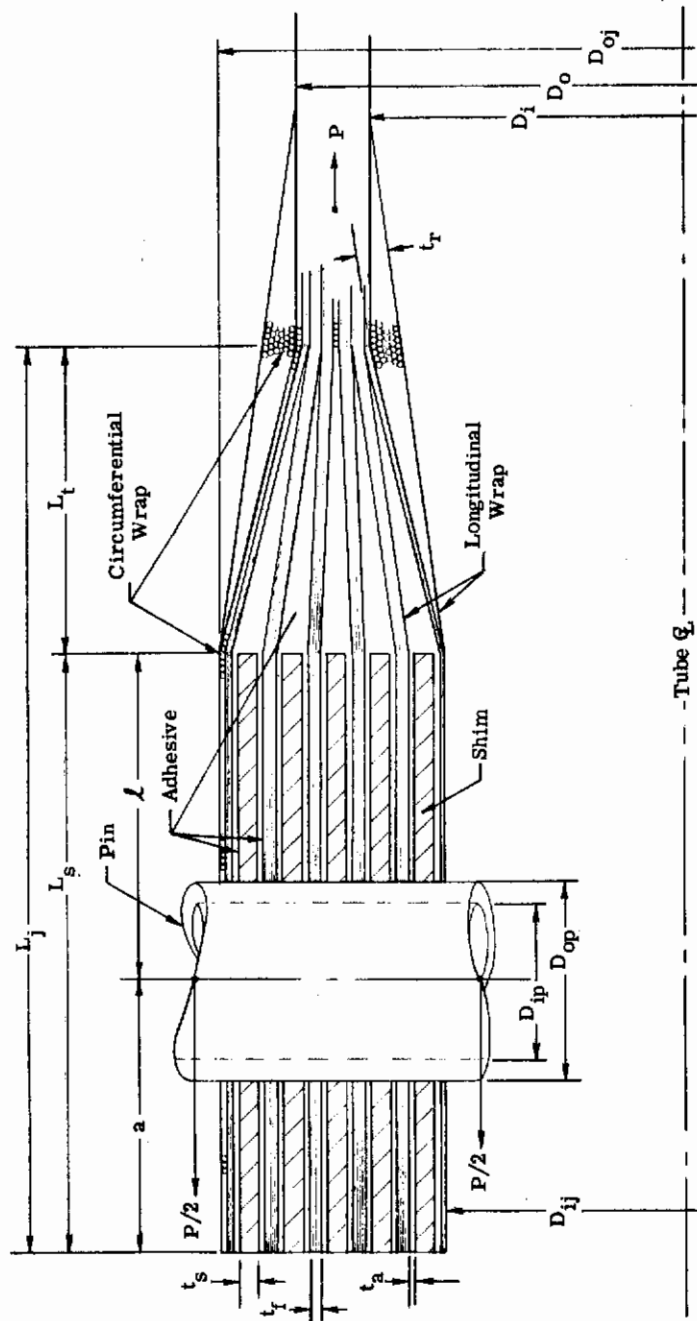


Figure 1. Tubular Shim Joint Design Variables

- $t_a$  - Thickness of the adhesive layer joining the metallic shim to the composite material.
- $t_f$  - Thickness of composite layers between shims.
- $t_c$  - Thickness of composite layers which do not extend between shims.
- $D_{oj}$  - Outside tube diameter in attachment area.
- $D_{ij}$  - Inside tube diameter in attachment area.
- $L_t$  - Wall thickness transition length.
- $t_r$  - Maximum thickness of the transition length circumferential reinforcing rings.
- $L_r$  - Length of reinforcing rings.
- $L_j$  - Total length of reinforced attachment area ( $L_s + L_t$ ).

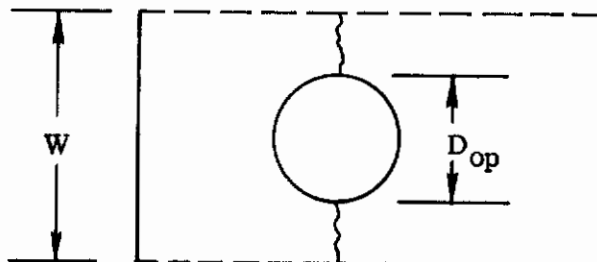
The efficiency of the joint design is also a function of the materials used in the various joint components. The effect of utilizing various component materials is studied by including in the design procedure the design allowables and weight densities associated with the materials of interest. The material weight densities are also considered as design variables and are denoted in the design procedure as follows:

- $\omega$  - Density of the composite material.
- $\omega_s$  - Density of the metallic shim material.
- $\omega_a$  - Density of the adhesive material.
- $\omega_f$  - Density of the filler material.
- $\omega_p$  - Density of the pin material.

## 2.2 FAILURE MODES

Mechanical fasteners in shim reinforced composite materials produce much the same failure modes as in metals. The following analysis considers those potential failure modes resulting from axial tension loads on the joint. Net area tensile failure, pin hole bearing failure, hoop tension failure, shear bearing tear-out failure, and pin shear failure can all be produced in the attachment by proper manipulation of the joint geometry. Failure can also occur due to excessive shear in the bond joint between the shim and composite material, or by delamination of the fibrous layers in the tube wall thickness transition length.

2.2.1 Net Area Tension



Joint failure may occur in tension along the pin row centerline if the net tension area becomes sufficiently small. The ultimate strength of the net tension area depends on the ductility of the metallic shim material when a low elastic modulus composite is used. The composite material in the net tension area can support high stresses if the shim can be strained sufficiently to develop the stress. The AM 355 shim stock which was used in this program has an ultimate strain range of 13 to 21 percent.\* The AF-994 glass filament requires a strain of only 3.25 percent to develop a fiber stress of 400 ksi, and the experimental work of this program has verified that the filament layers are highly stressed at the time of rupture through the net tension area. Using the combined areas of the shim and filament layers, tensile stresses as high as 320 ksi have been obtained in flat plate specimens during this program.

Laboratory tests on AM 355 shim stock determined the ultimate tensile strength of this material to be in the range of 255-260 ksi.\* This would indicate that the filament layers were active at a very high stress level. For this reason the combined steel and composite areas were utilized in calculating the net tension area stress.

$$A_t = (W - D_{op}) \left( \frac{D_o - D_i}{2} - .006N_c + N_{st_s} \right) \quad (1)$$

$$\text{where } W = \frac{\pi D_{oj}}{N_p}$$

The ultimate tension load is given by

$$P_{ult} = N_p K_{tu} A_t F_{tu} \quad (2)$$

where  $K_{tu}$  is the ultimate tensile efficiency factor.

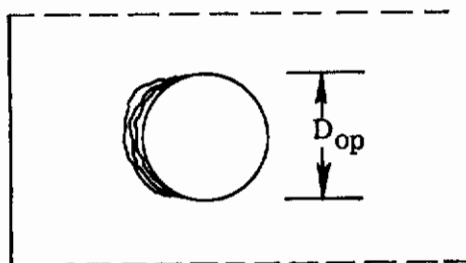
---

\*Refer to Appendix VI.

The allowable tensile stress is a function of the  $D_{op}/W$  ratio as in lug strength analysis. For high  $D_{op}/W$  ratios, the tensile area is quite narrow and the elastic stress concentration factor is relatively ineffective in the plastic range. The strain distribution becomes nearly constant across the tension area of the metallic shims when loaded into the plastic range. For lower  $D_{op}/W$  ratios, however, the tension area is wide enough that a strain gradient exists across the shim material even in the plastic range. The metallic layers are less efficient because they are subjected to a plastic stress concentration factor.

The filament layers are also less efficient since they are not uniformly strained across the tension area. Flat plate tests were conducted to determine tensile allowables and the results are presented in Section III of this report.

## 2.2.2 Pin Hole Bearing



The basic reason for employing metal shims in the composite tube attachment area was to increase the pin hole bearing strength. The bearing strength of nonreinforced composite materials are far too low to support pins with the high loading intensities experienced in major structural components.

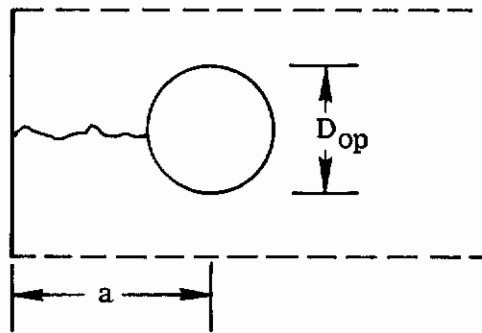
Test results have indicated that bearing failure of shim reinforced composites normally occurs as a result of shim buckling. Buckling strength is a function of individual shim thickness,  $t_s$ , and the unsupported metal span length,  $D_{op}$ . The bearing allowables are presented in Section III of this report as a function of the ratio  $D_{op}/t_s$ . The allowable pin bearing load is the product of the bearing efficiency factor  $K_{br}$ , the total projected metal-to-metal bearing area, the ultimate tensile strength of the shim material, and the number of pins used in the tubular joint.

$$A_{br} = N_s t_s D_{op} \quad (3)$$

$$P_{ult} = N_p K_{br} A_{br} F_{tu} \quad (4)$$

Since the failure mode is actually one of stability, the degree of restraint due to clamping must also be considered in establishing allowables for this failure mode. A joint which is tightly clamped by a threaded nut on the pin will produce much higher bearing stresses than an identical joint which is not clamped or restricted in any way. Clamping of the flat plate tests described in this report was adjusted to duplicate that expected in the composite tube attachment.

## 2.2.3 Hoop Tension



Hoop tension is a term used to describe one of two failure modes which can occur when the pin row is placed too close to the tube end. The material between the pin hole and the tube end is subjected to tension stresses which act perpendicular to the direction of the applied load. During this program, unidirectional plies only were utilized between the metallic shims. Since the tensile strength of the glass epoxy system is quite low in the transverse direction, the composite material was not considered to be effective in transmitting hoop stress during the establishment of allowables for this program. Metallic area only was considered in calculating hoop tension stresses. Further testing would be required to establish allowables for attachments which incorporate plies oriented at an angle to the tube axis.

Determination of the stress distribution along the hoop tension critical plane would be a difficult analysis problem. For this reason, a fictitious stress obtained by dividing the axial load applied to each pin by the hoop tension area is used in the analysis of this failure mode. The allowable is defined in terms of the shim material ultimate tensile strength and is a function of the  $a/D_{op}$  ratio. The hoop tension area is given by the following expression:

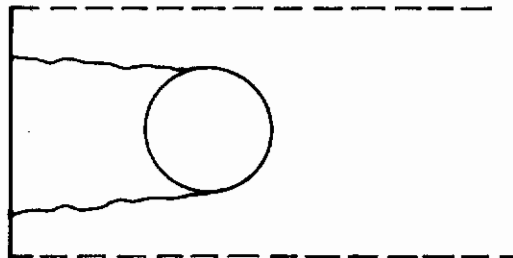
$$A_{ht} = N_s t_s \left( a - \frac{D_{op}}{2} \right) \quad (5)$$

The ultimate load for the joint is

$$P_{ult} = N_p K_{ht} A_{ht} F_{tu} \quad (6)$$

The hoop tension efficiency factor is further explained in Section III of this report.

## 2.2.4 Shear Bearing





Past experience with lug design would indicate that shear bearing failure could also occur if the pin row is placed too close to the tube end. In the shear bearing mode, the metal slug between the pin hole and the tube end is forced from the tube end in double shear due to the pin bearing pressure. There were no clearly defined occurrences of shear bearing failure during the flat plate test series of this program. The hoop tension mode predominated in specimens fabricated with a short "a" distance.

In some specimens involving a combination of shim failure modes, however, individual shims have been found to fail in the shear bearing mode, but there was not sufficient data to form allowables. It has been suggested that the tubular members may be more susceptible to shear bearing failures than hoop tension failures since the tubular geometry lends some transverse support in the direction of hoop failures which is not present in flat plate specimens. Only tubular test data can ascertain this fact. Also, these failure modes may be functions of the  $a/t_s$  ratio as well as the  $a/D_{op}$  ratio, but further testing would be required to affirm this theory.

## 2.2.5 Bond

The quality of the bond joint is highly sensitive to cleaning, fabrication and machining procedures. The analysis which follows assumes that these procedures have been performed at a near optimum level, and that the quality of bond is high.

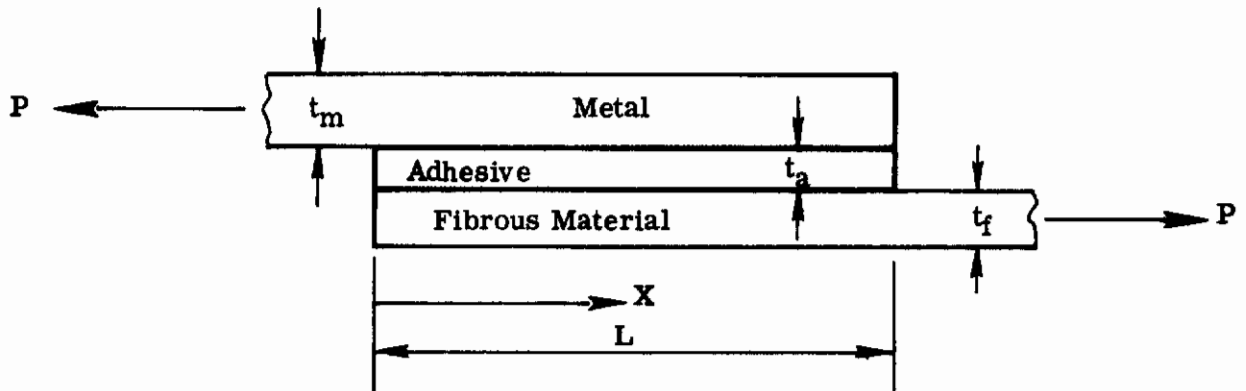
To better understand the mechanics of a bonded lap joint, a detailed continuum analysis was conducted. The analysis considered a joint connecting two members of dissimilar materials in which the load is transferred by shear stress through an adhesive layer at the member interface. The analysis assumes:

- (a) That all elements are linearly elastic,
- (b) That the effects of bending due to eccentricity in the joint may be neglected, and
- (c) That the fibrous member is of uniform thickness.

The analysis does not fully duplicate the shim joint used in this project. It was extended to consider a bonded joint of several layers, but did not consider application of load to the metal layers through pin holes within the bonded joint length. Also, the primary interest of this program was the ultimate strength of a multi-layer bonded joint. Ultimate strength information would have required a plastic analysis of the joint which was beyond the scope of this program. The elastic analysis was quite useful, however, in defining the parameters which affect stress levels and stress concentrations within the bonded joint.

Details of the bonded joint analysis are presented in Appendix II. Before proceeding, however, it would be well to discuss some results of that analysis. To obtain a closed-form solution for the joint it was necessary to assume that both members were of constant thickness. Equations 7 and 8 show the resulting shear stress at each end of the adhesive.





at  $x = 0$

$$f_{s \max} = P \left[ \frac{G_a E_f t_f}{t_a E_m t_m (E_f t_f + E_m t_m)} \right]^{1/2} \quad (7)$$

at  $x = L$

$$f_{s \max} = P \left[ \frac{G_a E_m t_m}{t_a E_f t_f (E_f t_f + E_m t_m)} \right]^{1/2} \quad (8)$$

where  $E_f$  = Elastic modulus of fibrous material.

$E_m$  = Elastic modulus of metal.

$G_a$  = Shear modulus of adhesive material.

The shear stress concentration factors at the corresponding points are given by equations 9 and 10.

at  $x = 0$

$$S_a = L \left[ \frac{G_a E_f t_f}{t_a E_m t_m (E_f t_f + E_m t_m)} \right]^{1/2} \quad (9)$$

at  $x = L$

$$S_a = L \left[ \frac{G_a E_m t_m}{t_a E_f t_f (E_f t_f + E_m t_m)} \right]^{1/2} \quad (10)$$

Most interesting is the fact that the maximum stress concentration factors,  $S_a$ , are linear functions of the joint length, but that the maximum shear stress value is independent of joint length. A longer joint length will certainly reduce the average shear stress, but it will not decrease the maximum shear stress. Therefore, bond joints become less efficient with increased length because the mid portion of longer joints transfer very little load. The flat plate tests of this program have verified that the allowable shear stress does decrease as the joint length increases (Figure 13). Figure 2 illustrates the effect of overlap length on the stress concentration factor in a typical bonded joint. The analysis strongly indicates that lengthening a bond joint may not be the most efficient means of increasing the joint ultimate strength.

Examination of equations 7, 8, 9, and 10 also reveal that both maximum shear stress and the stress concentration factors are inversely proportional to the square root of the adhesive thickness,  $t_a$ . The validity of this result was illustrated during the latter part of this program when AF-111 (3M Corporation) adhesive film was incorporated in the joint in lieu of the BR-1009-49 tack primer (American Cyanamid Corporation) to increase the thickness of the adhesive layer. The original tack primer thickness was about 0.0045 inch. The ultimate bond strength of flat plate specimens was increased on the average by 45 percent with substitution of the AF-111 adhesive film which produced an adhesive thickness of 0.009 inch. The decrease in the elastic stress concentration factor is proportional to the ratio of the square roots of the two adhesive thicknesses:

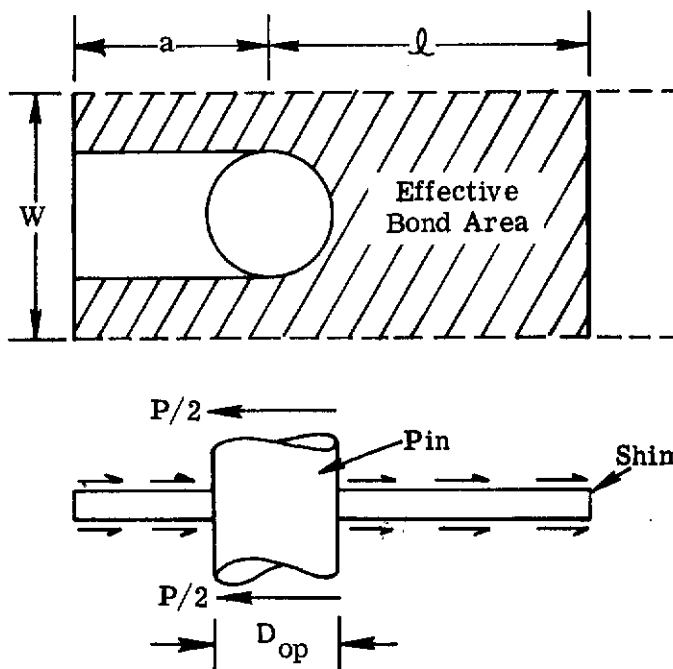
$$\frac{\sqrt{0.009}}{\sqrt{0.0045}} = 1.414 \quad (11)$$

The 41.4 percent decrease in stress concentration factor corresponds well with the 45 percent increase in ultimate strength. Figure 3 illustrates how the stress concentration varies with adhesive thickness for a typical bonded joint. Fatigue loadings may require that the adhesive thickness be increased for the joint in this study since fatigue strength is much more sensitive to stress concentration factors than ultimate strength. Increasing the adhesive thickness would be a more efficient and effective means of improving fatigue strength than lengthening the joint.

Equations 7, 8, 9, and 10 also indicate that maximum shear stress as well as the stress concentrations are functions of the ratio  $E_m t_m / E_f t_f$ . The discussion of the significance of this ratio is complex and has been placed in Appendix II. For materials of widely different moduli but similar tensile strengths, the ratio  $E_m t_m / E_f t_f$  is highly significant in limiting the strength of the bonded joint.

Bonded joints in high modulus composites (boron, carbon, etc.) would be superior to a glass-epoxy composite in this respect.

To actually design a bonded (shim) joint for ultimate loading, it was necessary to use average shear strength allowables obtained from flat plate tests. The presence of high stresses in the fibrous layers through the net tension area indicated that the part of the bond area between the pin row and the tube end was effective in transferring stress from the shims to the fibrous material. The shim area which was considered to be effective in bond is shown below to be a function of both  $a$  and  $l$ .



An effective bond length,  $l_e$ , was defined by dividing the shaded bond area by the width,  $W$ .

$$l_e = \frac{A_s}{W} \quad (12)$$

where

$$A_s = W(l + a) - N_p \alpha D_{op} - 0.4 D_{op}$$

$$W = \pi/2 (D_{oj} + D_{ij})$$

The ultimate load for a shim joint is given by:

$$P_{ult} = 2N_s A_s F_s \quad (13)$$

where  $F_s$ , the allowable shear stress, is defined in terms of the effective bond length,  $l_e$ .

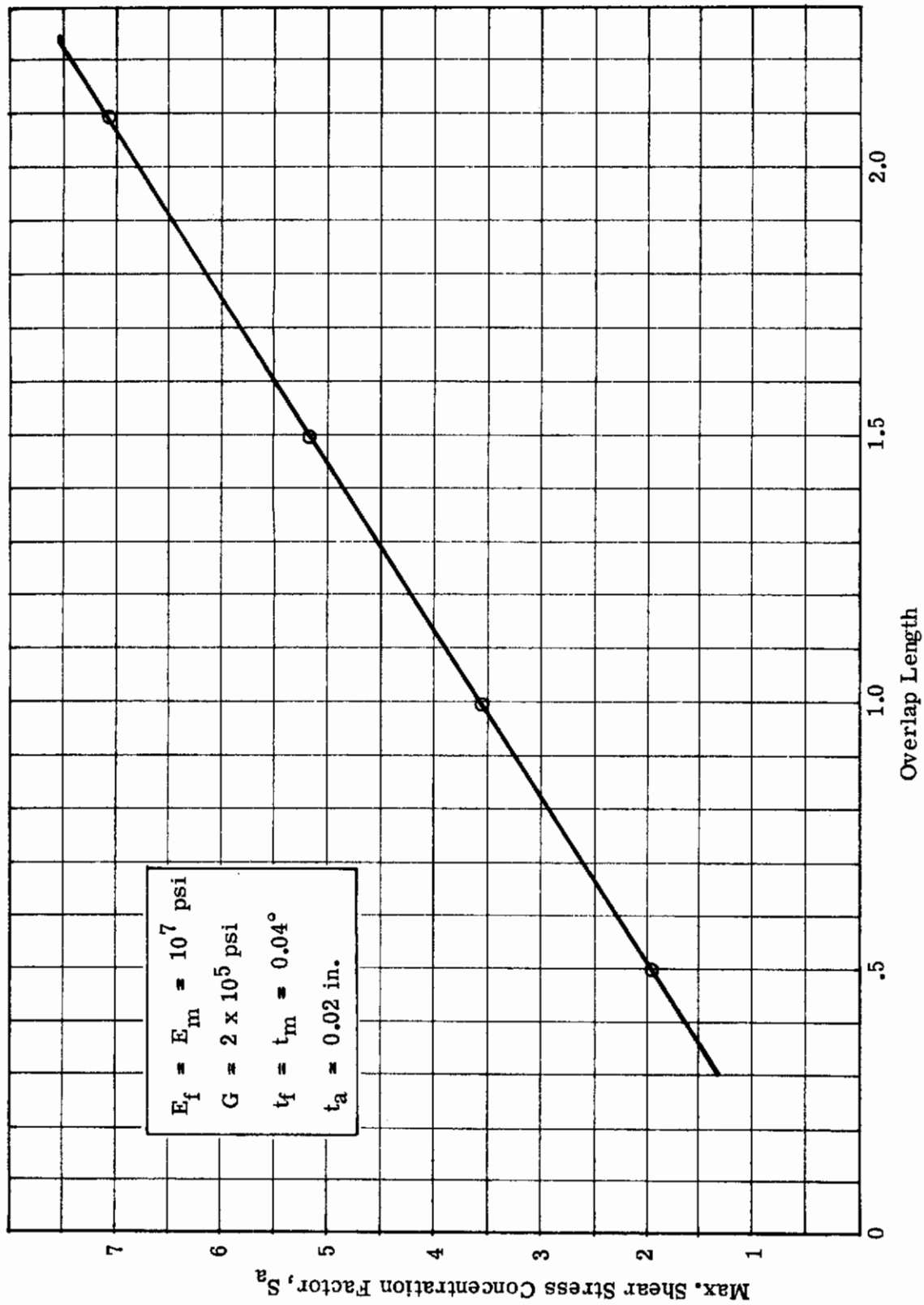


Figure 2. Effect of Overlap Length on Adhesive Maximum Shear Stress Concentration Factor

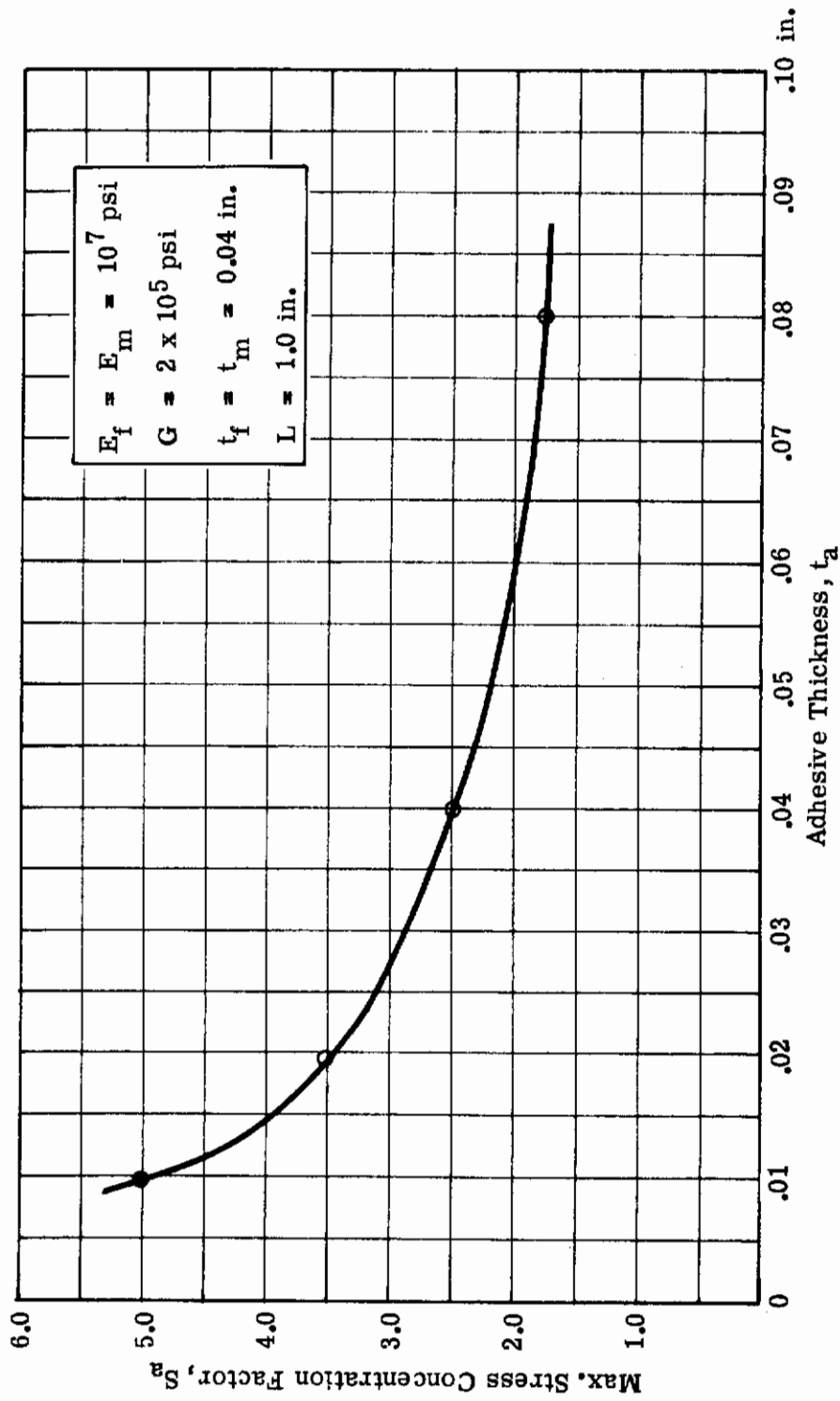
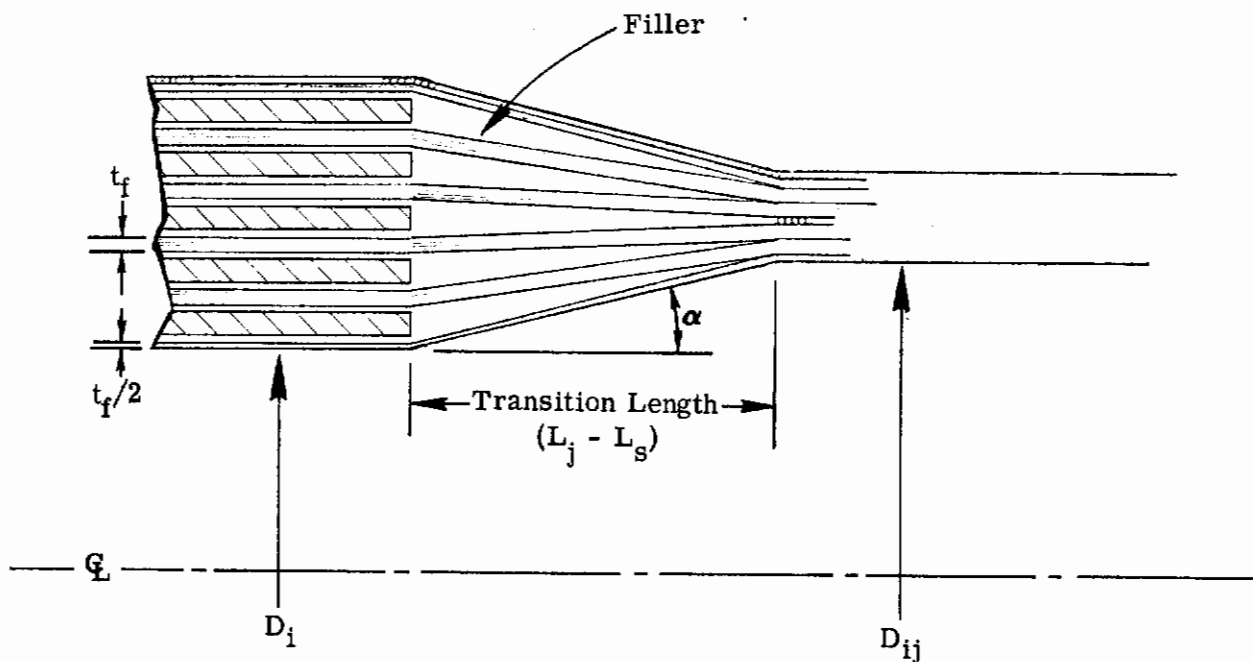


Figure 3. Effect of Adhesive Thickness on Shear Stress Concentration Factor for Bonded Joints

## 2.2.6 Wall Thickness Transition Zone.

Flat-plate specimens were fabricated during this project with excess transverse or circ layers to maintain a constant thickness throughout the specimen length. In a structural tube however, it would not be economical to use more circ layers than required to maintain the laminate strength. A tapered transition length is required to flare the tube wall into the thicker reinforced tube end as shown below:



From a weight standpoint, it is desirable to make the transition length as short as possible. As shown above, a filler material is required between the fibrous layers, and the total filler weight is proportional to the transition length. As the transition length becomes shorter, however, the radial force component which tends to separate the fibrous layers (delaminate) at the base of the transition length becomes greater. These radial forces create tensile strain concentrations at the initial separation point of adjacent layers which must not exceed the ultimate tensile strain for the resin in the composite. The tensile strain at the separation point can be controlled by designing circ wrap reinforcement rings at both the inside and outside diameters to restrict radial movement.

The transition zone was analyzed by using a finite element model of beams and springs. Details of the analysis are presented in Appendix III. As long as adjacent layers through the wall thickness do not separate at exactly the same distance from the shim pack, delamination will occur at the exterior layer. The analysis indicated that the radial force on the exterior layer,  $P'_i$ , is about 85 percent of the force obtained by ignoring the continuity of adjacent layers.

$$P_i' = 0.85 P_i \sin \alpha \quad (14)$$

where

$P_i$  = Axial force carried by exterior layer.

$P_i'$  = Radial force on outside layer at separation point.

$\alpha$  = Angle of exterior layer to the tube axis.

The average allowable tensile strain  $\epsilon_a$ , was determined experimentally to be 1.4 percent. The allowable radial force and the allowable radial displacement are given by

$$(P_i')_{ult} = C_1 \epsilon_a \quad (15)$$

$$y_a = \frac{(P_i')_{ult}}{C_2} \quad (16)$$

where  $C_1$  and  $C_2$  are coefficients depending on geometry and mechanical properties. The thickness of the required reinforcing ring is

$$t_r = \frac{D_o^2 [P_i' - (P_i')_{ult}]}{4E_f y_a} \quad (17)$$

### 2.2.7 Pin Shear

The pins are loaded in double shear and the design requires simply that the cross-sectional area be large enough to ensure that the shear stress does not exceed the ultimate shear strength of the material. If hollow pins are used, the ratio  $D_{ip}/D_{op}$  must be low enough to ensure that the pins will not crush or buckle. The ultimate load for the pinned joint as governed by pin shear is given by:

$$P_{ult} = 2N_p A_p F_{su} \quad (18)$$



SECTION III  
FLAT PLATE TESTS

3.1 PURPOSE

Theoretical analysis of the shim joint concept has been very beneficial to understanding the mechanics of the joint. The information resulting from this work is not adequate, however, for determination of the joint ultimate strength. Ultimate strength design data must still be obtained empirically. The flat plate test specimen (Figure 4) was developed to enable inexpensive determination of ultimate strength design allowables for the various failure modes in a shim joint. The presence of free edges on the sides of the flat plate configuration prevents exact simulation of the tubular joint, but it is felt to be adequate for most failure modes.

3.2 DESCRIPTION

The flat plate specimen used in this program is best described by Figure 4. Five 0.02 inch steel shim layers were used in each of the flat plate specimens, but the other materials were included in varying quantities to produce failure modes which were of interest. The composite material was composed of 65 percent glass, by volume, and 35 percent resin. The W dimension was fixed at 1.0 inch throughout the test program to simplify fabrication procedures. Also, tests conducted during this program have included only longitudinal fibers between the shims. Further testing will be required to determine design allowables for shim joints in laminates having fibers oriented at an angle to the loading direction.

The specimens were loaded by a pin through the shim joint and by a friction grip on the opposite end. The shim pack was clamped lightly during the test to simulate the clamping action expected from a metal fitting mating with the reinforced tube end. The specimens were loaded to rupture to obtain ultimate strength design allowables. Several photographs of flat plate specimens after test follow in this section.

3.3 FLAT PLATE TEST RESULTS

3.3.1 Net Tension Area

Tension failures were promoted in flat plates by increasing the pin diameter,  $D_{op}$  to reduce the net tension area. Since all specimen widths were identical ( $W = 1.0$  inch), the design parameter,  $D_{op}/W$ , varied directly with the pin diameter. Figure 5 shows four flat plate specimens subsequent to failure in the tension mode. The AF-111 adhesive

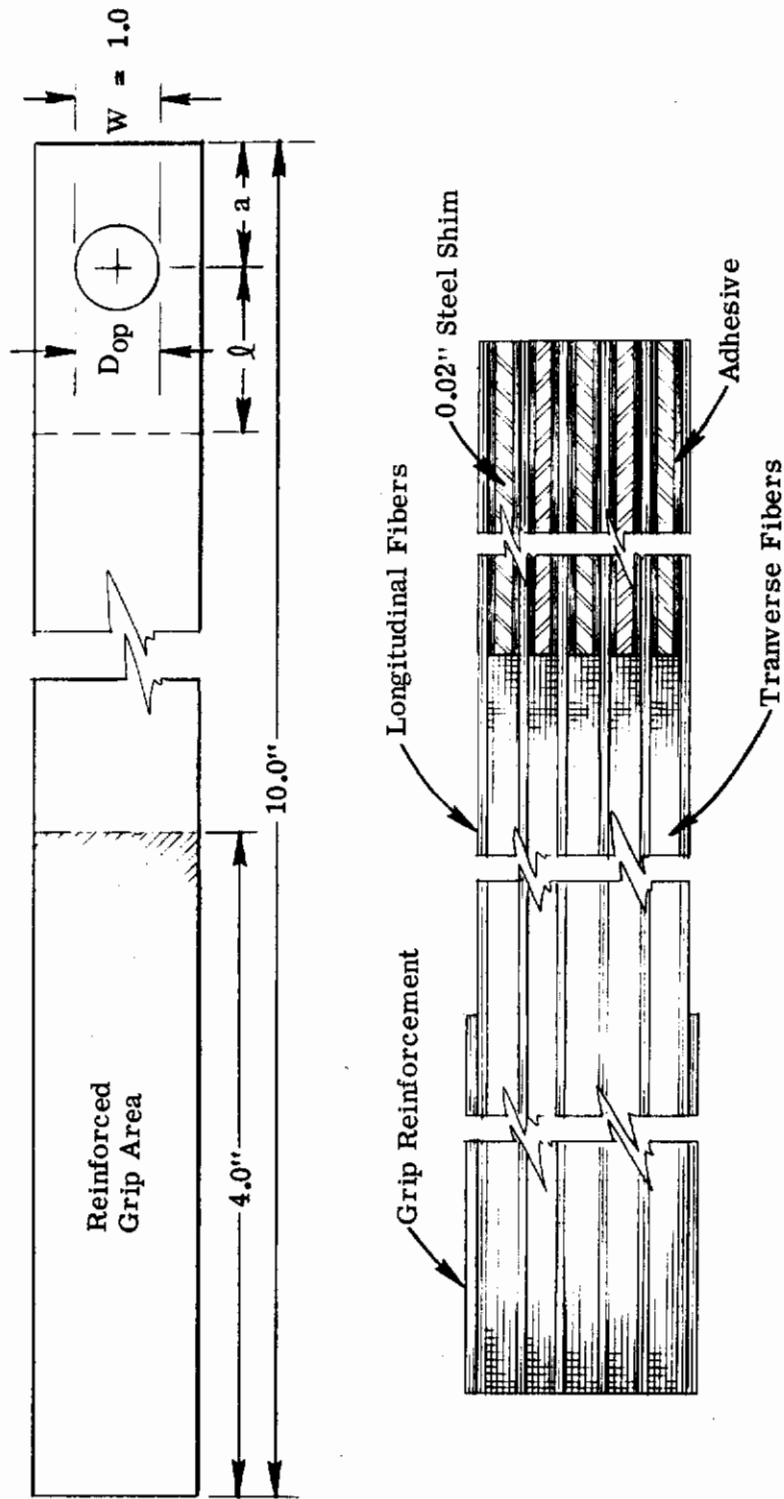


Figure 4. Typical Flat Plate Specimen

was used in the Series V specimens, but had little effect on the tensile strength of flat plates.

The net tension data is shown in Figure 6 plotted versus the ratio  $D_{op}/W$ . The calculated stress values were divided by the ultimate tensile strength of the shim material ( $f_t/F_{tu}$ ) to form the net tension efficiency factor,  $K_{tu}$ .

A mean allowable curve is shown superimposed on the test data. The mean allowable is defined in terms of  $D_{op}/W$  by the expression:

$$K_{tu} = \frac{79.327}{143.75 - 100 D_{op}/W} \quad (19)$$

which was used as the net tension area failure envelope in the automated design procedure.

Data points denoted as "lower bound" values arise from tests in which failure occurred either in a different mode, or in a combination of modes which included the one of interest. These specimens did experience relatively high stresses in the mode being plotted, however, and it was decided to use these stress values to aid in defining the lower bound of the failure envelope. These stresses represent a strength which can be expected in that mode without failure.

### 3.3.2 Pin Bearing

Pin bearing failure was induced in the flat plate specimen by decreasing the pin diameter to reduce the metal-to-metal contact area. Only one shim thickness was used during the flat plate program, so it is not known how shim thickness alone effects the pin bearing allowable stress. It was found, however, that the pin bearing allowable stress varied significantly with the  $D_{op}/t_s$  ratio. Figure 7 shows a typical pin bearing failure, and Figure 8 shows the flat plate pin bearing strength data plotted versus the  $D_{op}/t_s$  ratio. The bearing ultimate stress values have been divided by the ultimate tensile strength of the shim material ( $f_b/F_{tu}$ ) to form the pin bearing efficiency factor,  $K_{br}$ . In this form, the data is applicable to any high strength steel shims. A mean allowable curve is shown superimposed on the test data in Figure 8. The curve was derived empirically and is defined by:

$$K_{br} = 3.0 - \frac{123.8}{107 - D_{op}/t_s} \quad (20)$$

Equation 20 was used as the pin bearing failure envelope in the optimum design procedure.

Pin bearing failure is of special interest because it is more ductile than other failure modes. Very large strains can be absorbed without destroying the joint. When structural members are fabricated from brittle materials such as fiber glass, it may be desirable to design the assembly such that initial failure occurs in the attachment by pin bearing to avoid catastrophic failure of the assembly.

### 3.3.3 Hoop Tension

Hoop tension failures are a function of the ratio  $a/D_{op}$  and were controlled in the flat plate series by both the "a" and  $D_{op}$  dimensions. Hoop tension failures are fairly sudden in nature. Typical hoop tension specimens are shown after test in Figure 9. Note that some shim layers failed in the shear bearing mode in specimens having larger pin diameters.

The total hoop tension test results are plotted in Figure 10 as a function of the  $a/D_{op}$  ratio. Again a mean allowable curve has been derived to fit the test data. The data is presented in terms of a hoop tension efficiency factor ( $f_{ht}/F_{tu}$ ) such that it can be used for shim materials of any tensile strength. The mean allowable curve is defined by:

$$K_{ht} = \frac{3.173}{a/D_{op} + 0.65} \quad (21)$$

which was used as the hoop tension failure envelope in the design procedure.

### 3.3.4 Bond

Bond failures were produced in the flat plate specimens by decreasing the  $l$  distance to raise the average shear stress in the adhesive. Since it was determined that the area between the pin and the specimen end was also effective in load transfer, the "a" value was also varied during the flat plate bond tests. The effective length of bond, for flat plates,  $l_e$ , was defined in terms of both "l" and "a" by:

$$l_e = (l + a) - a D_{op} - 0.4 D_{op} \quad (22)$$

Typical bond failures in early flat plate specimens are shown in Figure 11. . As the photographs indicate, this failure mode results in a very sudden release of the load. Figure 11a shows bond failures which occurred later in the program after adoption of the AF-111 adhesive tape. As the photographs indicate, there was a marked improvement in shear strength with the thicker adhesive. The total shear strength data for both adhesive systems are plotted versus "effective bond length" in Figure 12. The data indicates that the AF-111 not only results in higher average shear strengths, but also in less scatter of strength data.

An algebraic equation was derived to fit the AF-111 shear strength. The curve, which is shown superimposed on the test data in Figure 12, is defined by

$$f_s = \frac{5130}{l_e + 1.95} \quad (23)$$

Equation 23 was used to define the bond joint failure envelope in the optimum design procedure.

Fifty percent additional fiber glass was placed between the shims in the Series V specimens in an effort to obtain ultimate strength data for longer bond joints. The 0.02 inch shim layers, however, were unable to resist the increased stress levels generated by the fiber glass. The series resulted primarily in the combination failure modes shown in Figure 13. Since shim stock of increased thickness was not readily available, adhesive shear strength data for effective lengths greater than 1.4 inches was not obtained. The combination mode failure data was useful in forming lower bounds for the other failure envelopes.

### 3.3.5 Transition Zone

Two flat plate specimens were fabricated without the excess transverse fiber glass layers to study the delamination failure mode in the thickness transition zone. The specimens were fabricated with a transition length of 0.5 inch. The specimens did fail by delamination as expected, and the data was used to establish allowable stress levels in the circumferential, reinforcing ring, design procedure. One of the specimens is shown in Figure 14.

### 3.3.6 Staggered Shim Length

Two additional flat plate specimens were fabricated without excess transverse material. They were two of the Series III specimens which incorporate staggered shim lengths and the AF-111 adhesive film. The attachment area of the specimens did not fail in the bonded joint as anticipated. The geometry of staggered shims apparently resulted in increased stress concentrations in the outer layers of fiber glass causing a sudden failure in the filament material at the tips of the metallic shims. Subsequent tests utilizing the AF-111 adhesive film have shown, however, that shims of constant length which are shorter than the shortest staggered shims tested in Series III, are capable of developing a higher shear load than the fiber glass (400 fibers per inch of width between shims) can transmit to the joint. Further tests designed to eliminate failure in the filament material might indicate an improvement in bond strength by using the staggered shim geometry. Figure 15 shows one of the staggered shim specimens after test.



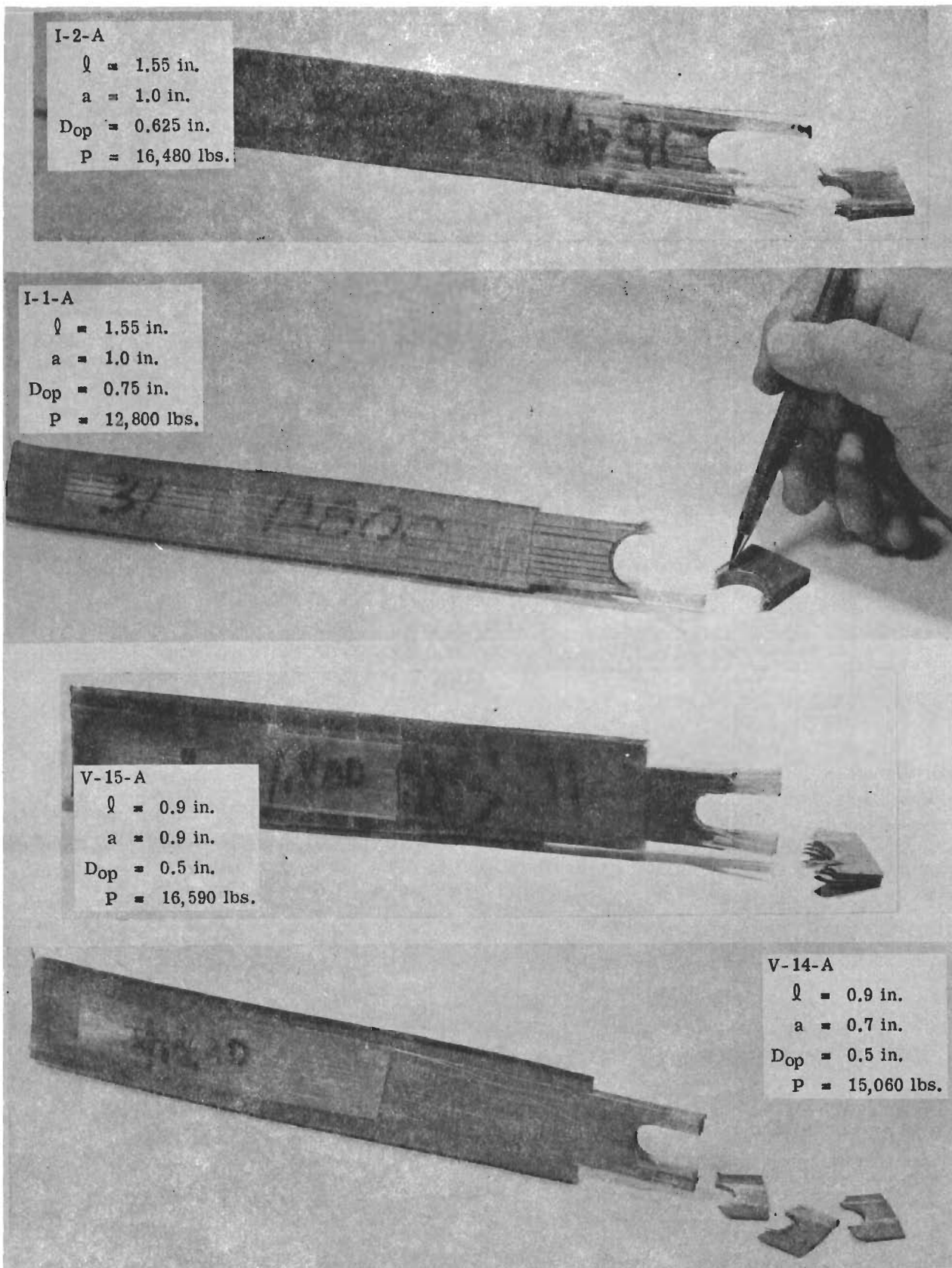


Figure 5. Flat Plate Specimens-Rupture Through Net Tension Area

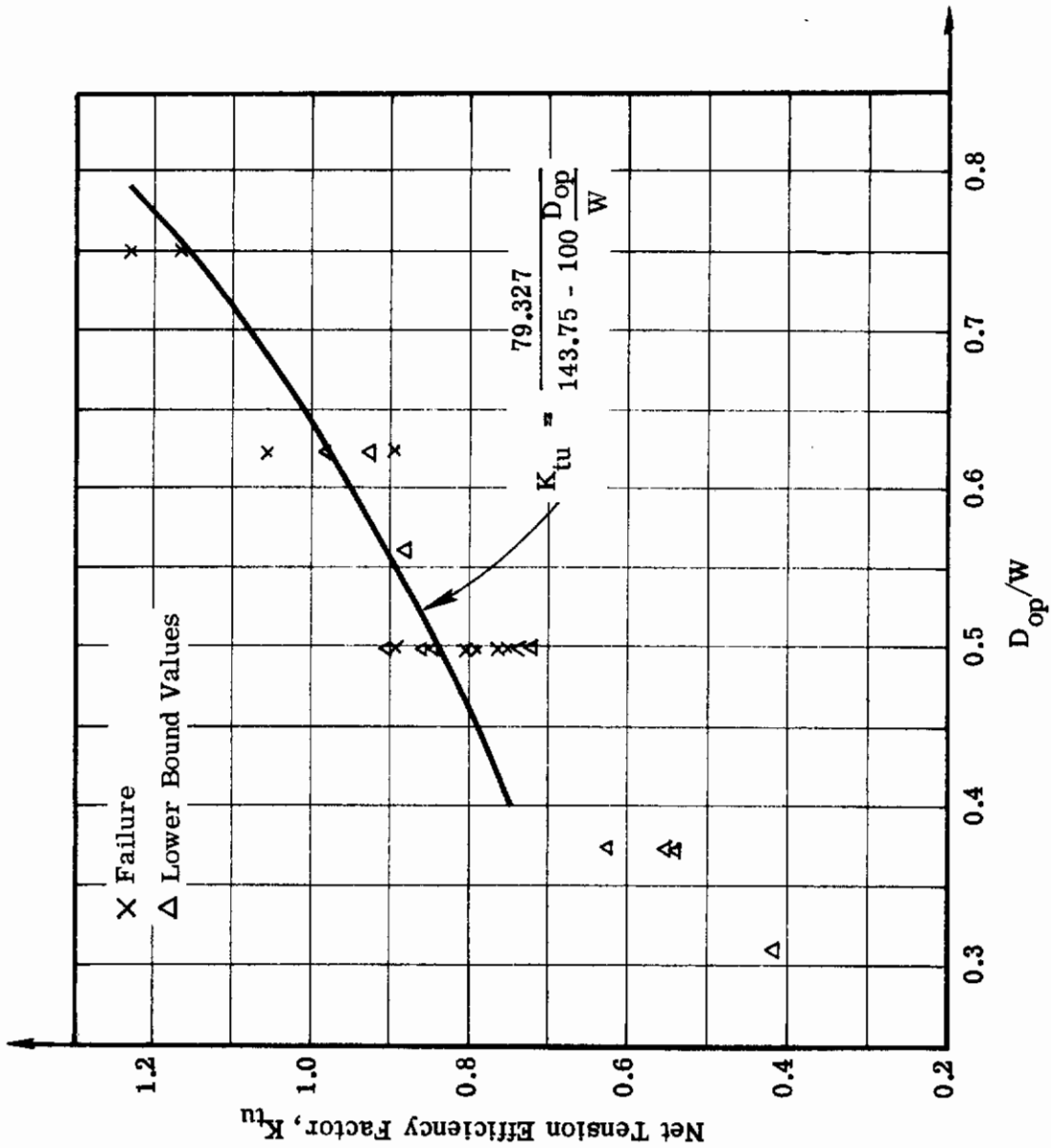


Figure 6. Net Tension Test Results vs.  $D_{op} / W$



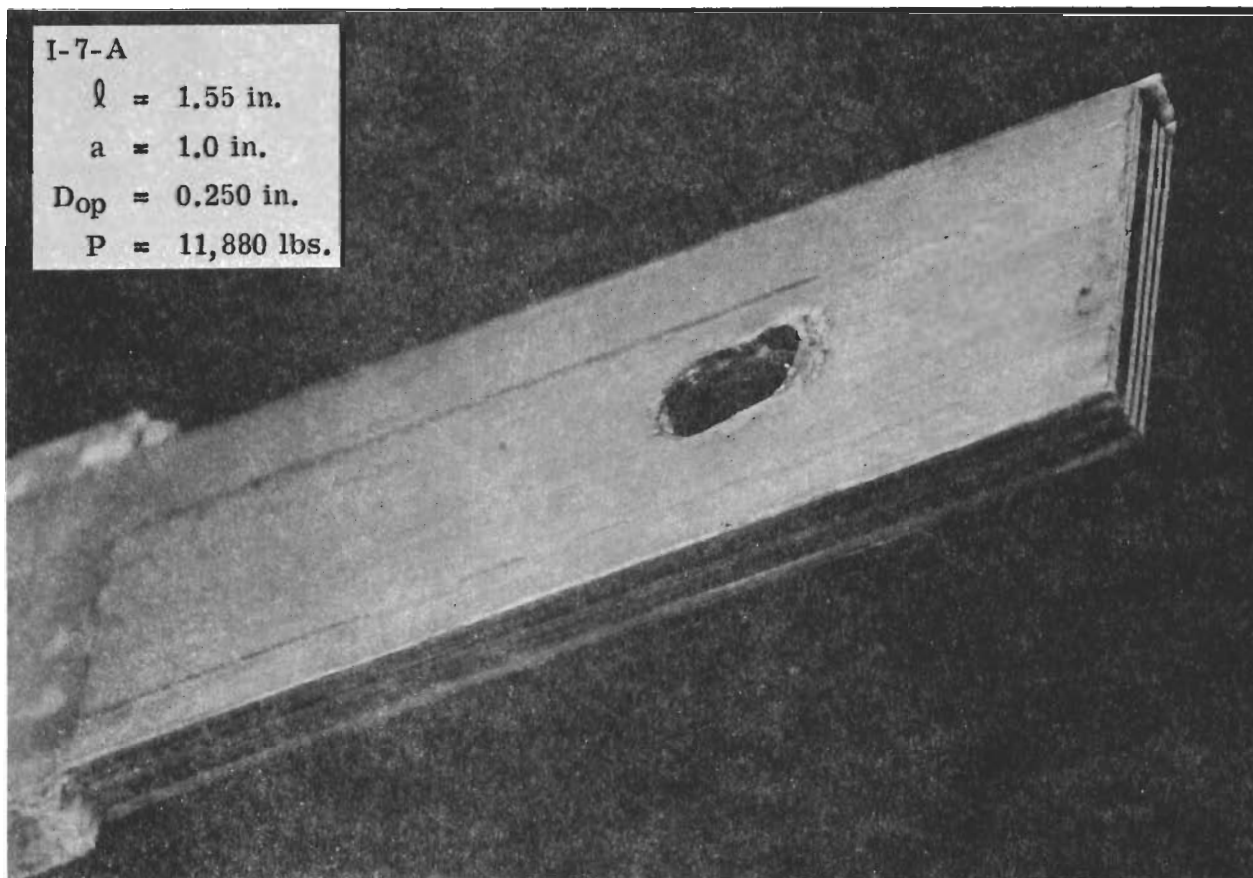


Figure 7. Flat Plate Specimens-Pin Bearing Failure

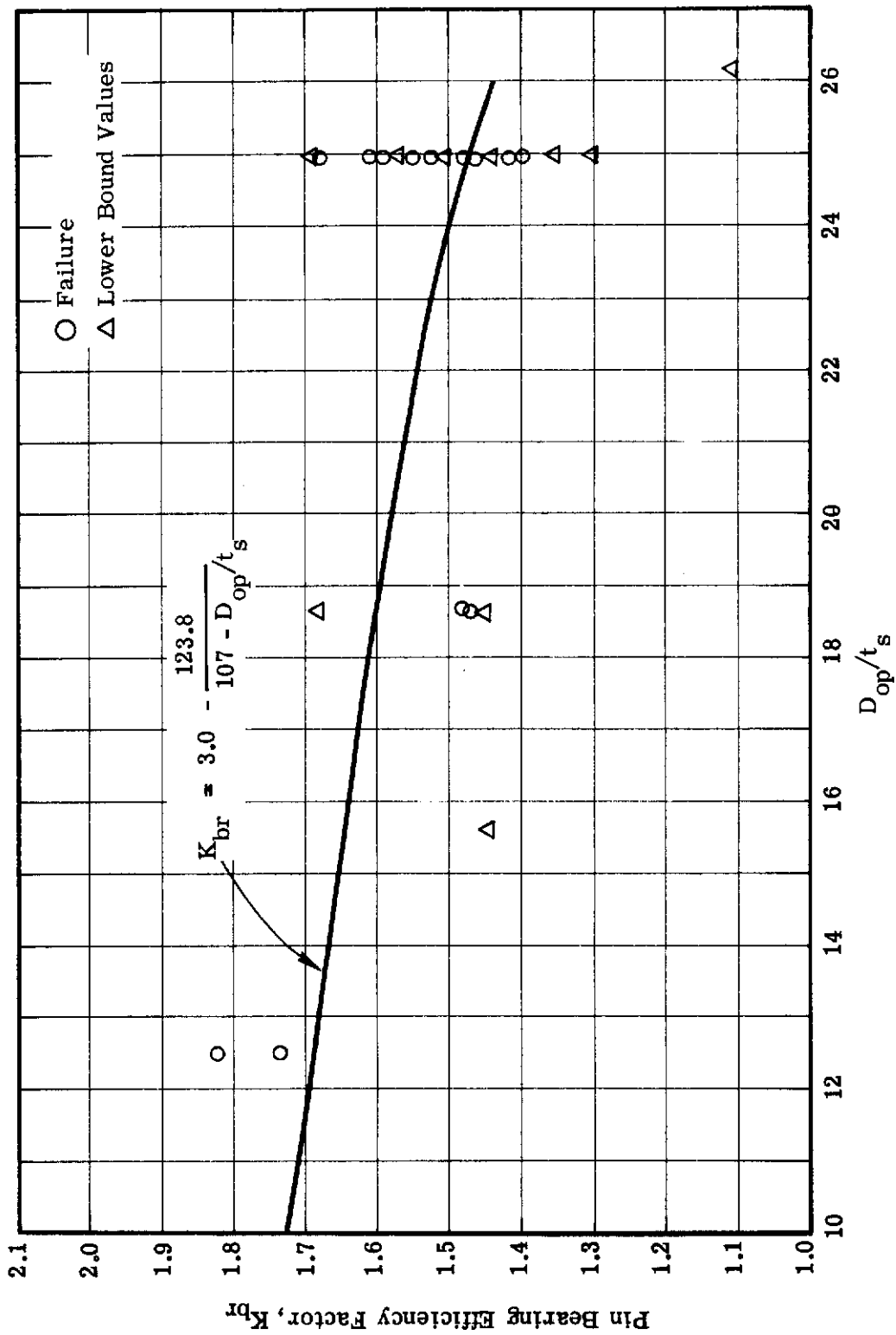


Figure 8. Pin Bearing Test Results vs.  $D_{op}/t$

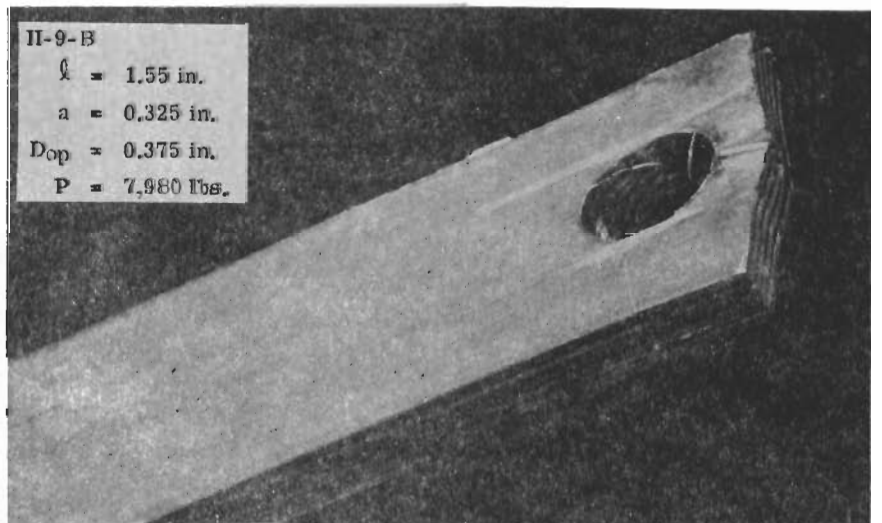
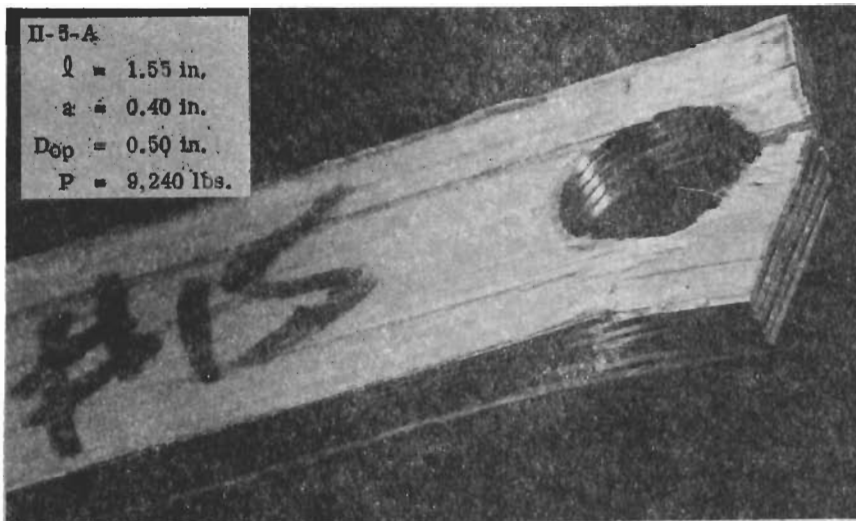
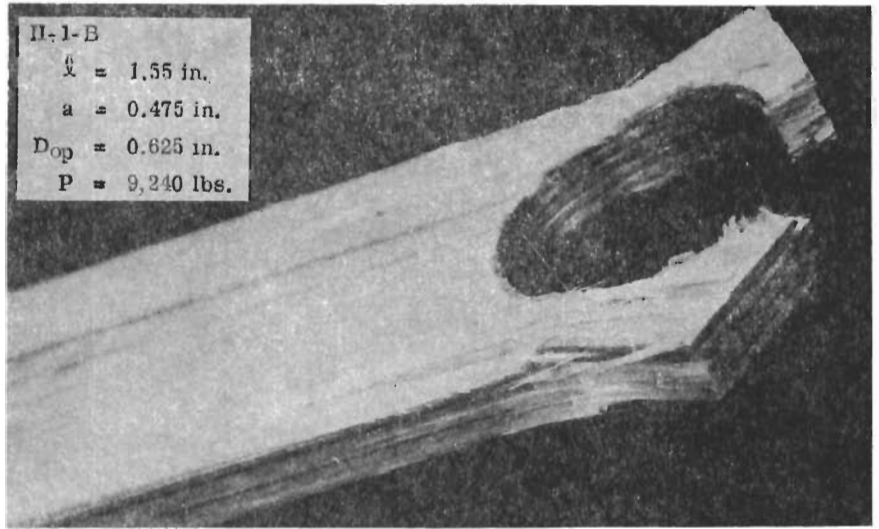


Figure 9. Flat Plate Specimens-Rupture Through Hoop Tension Area

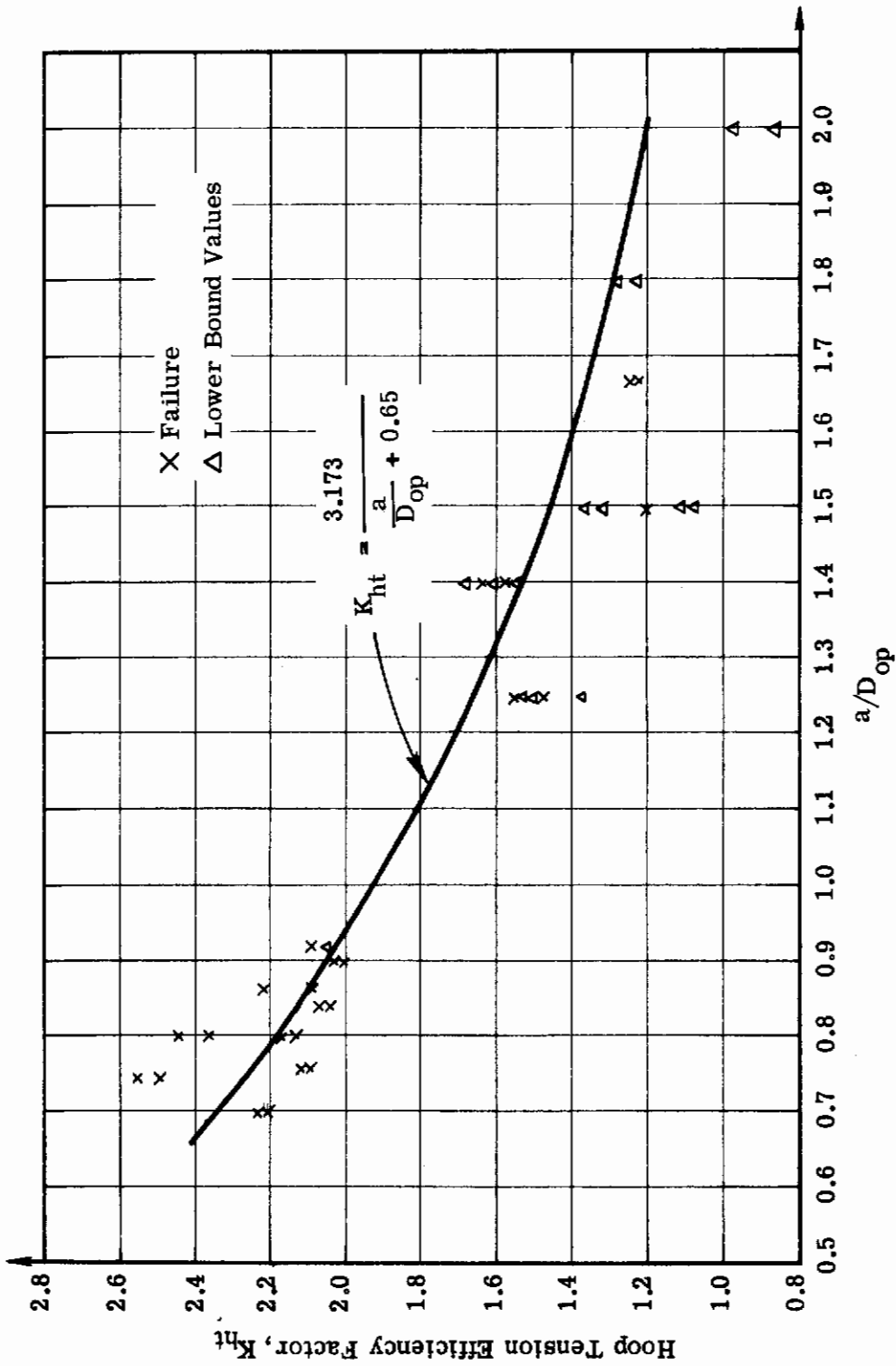


Figure 10. Hoop Tension Test Results vs.  $a/D_{op}$

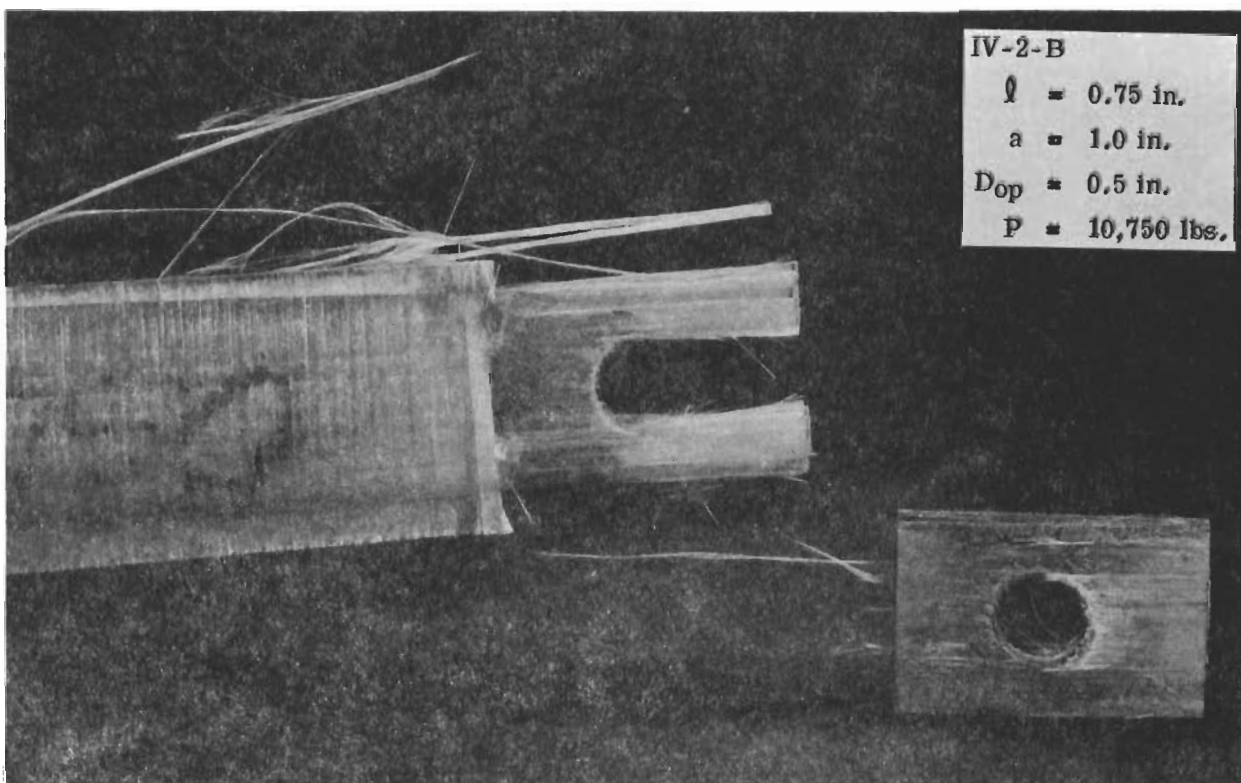
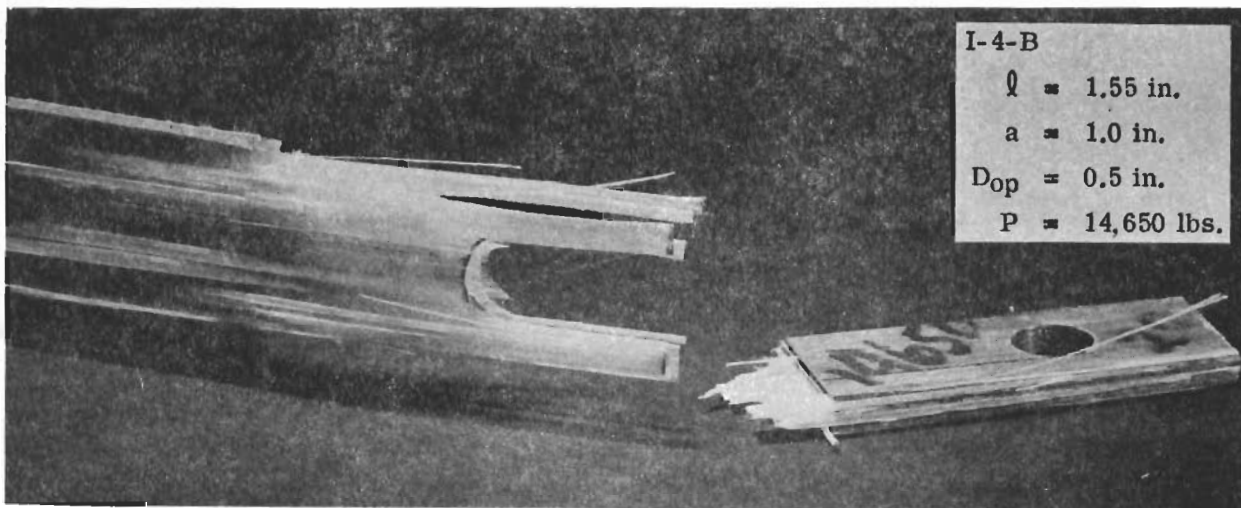


Figure 11. Flat Plate Specimens-Failure of BR-1009-49 Adhesive Joint



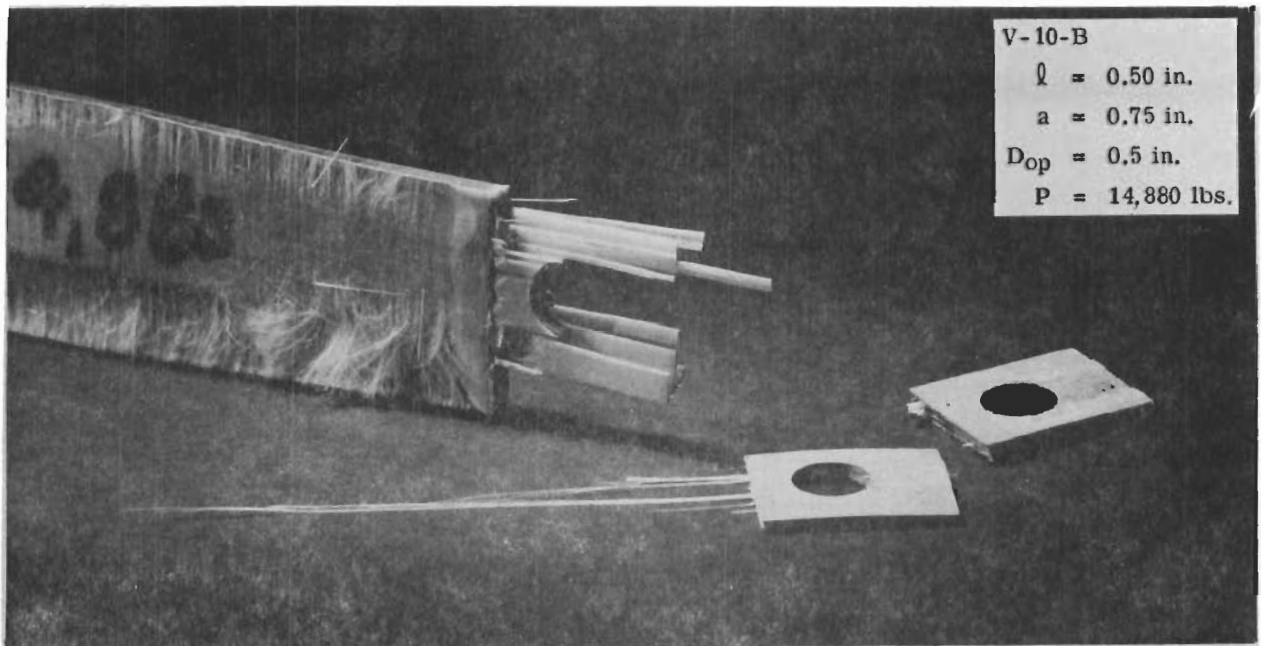
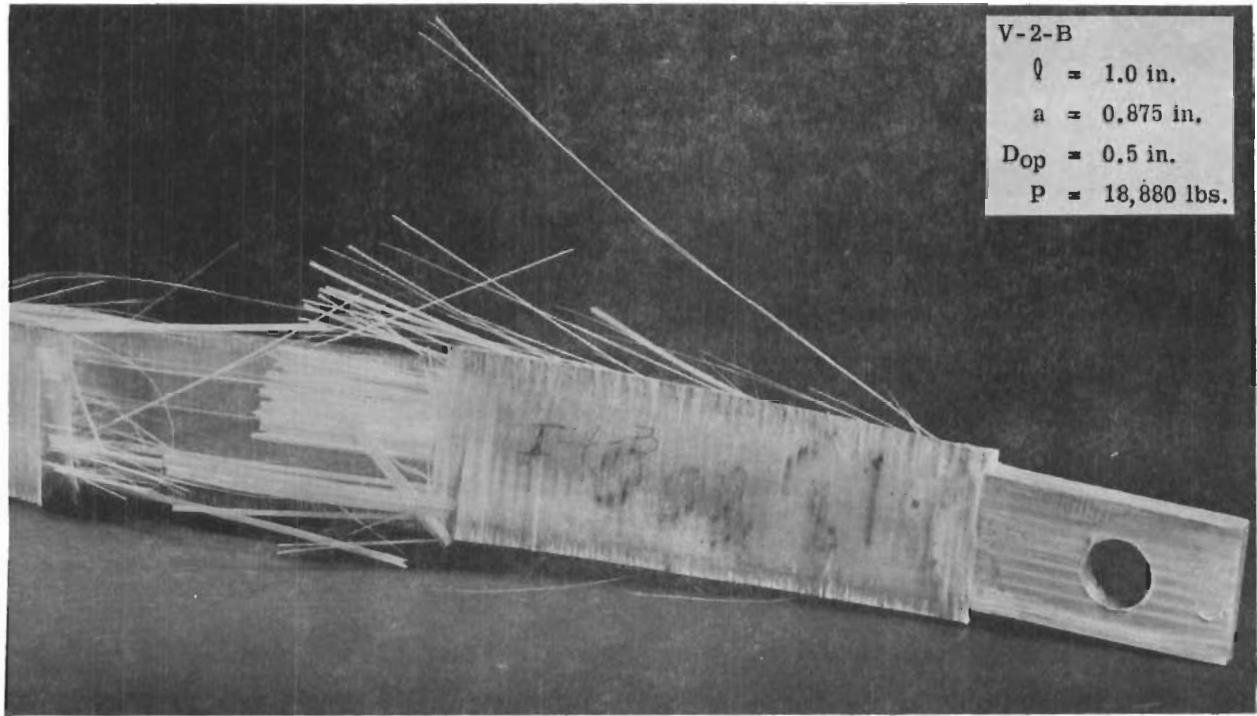


Figure 11a. Flat Plate Specimens-Failure of AF-111 Adhesive Joint

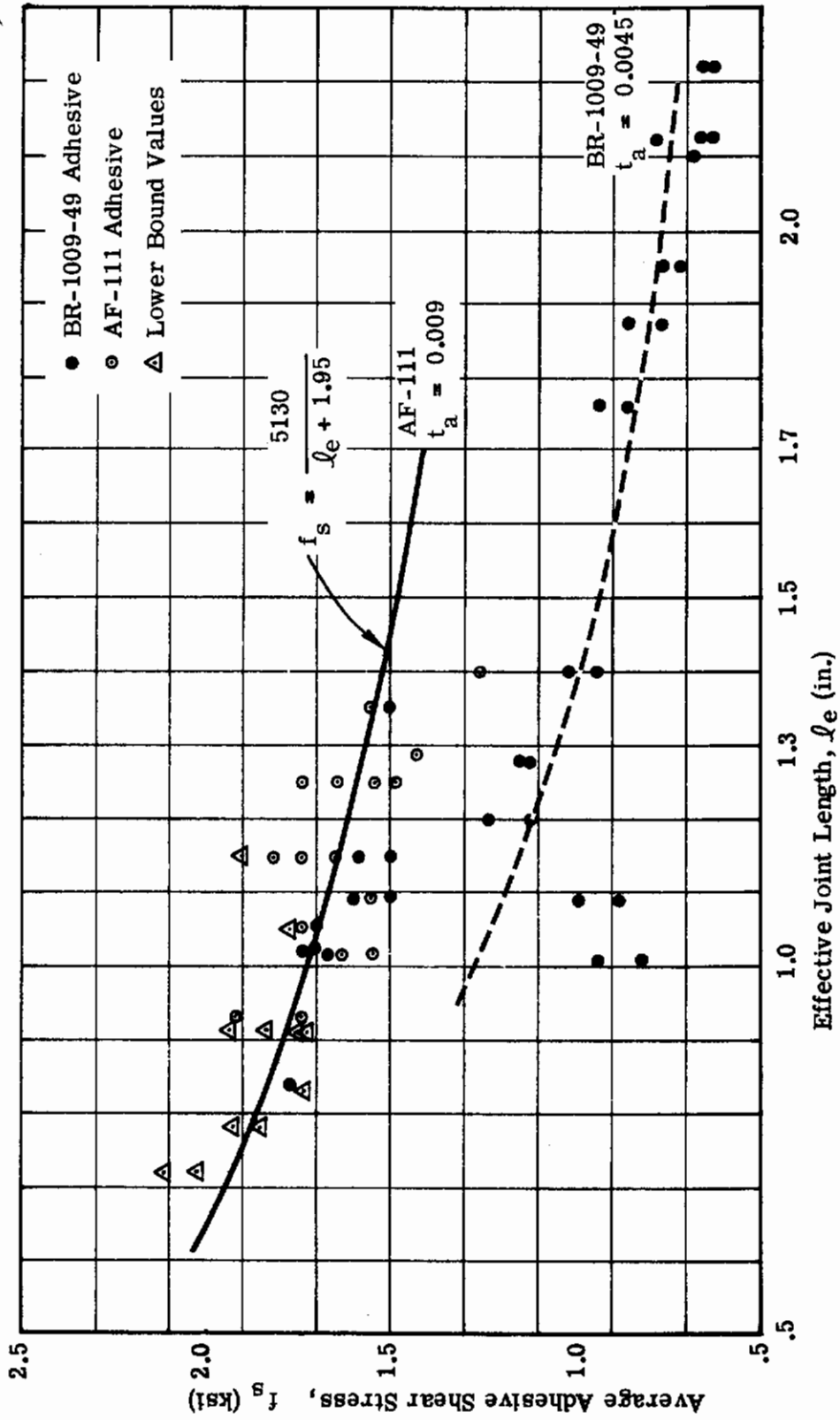


Figure 12. Average Adhesive Shear Strength vs. Effective Joint Length



# Contrails

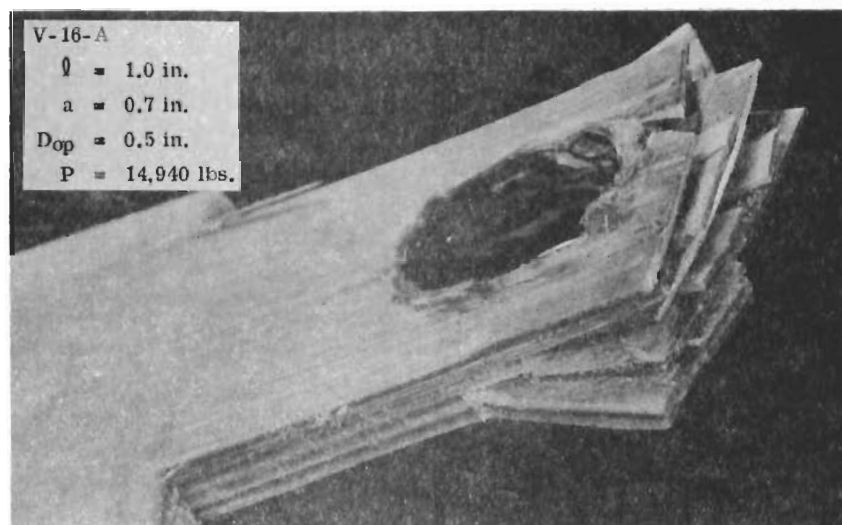
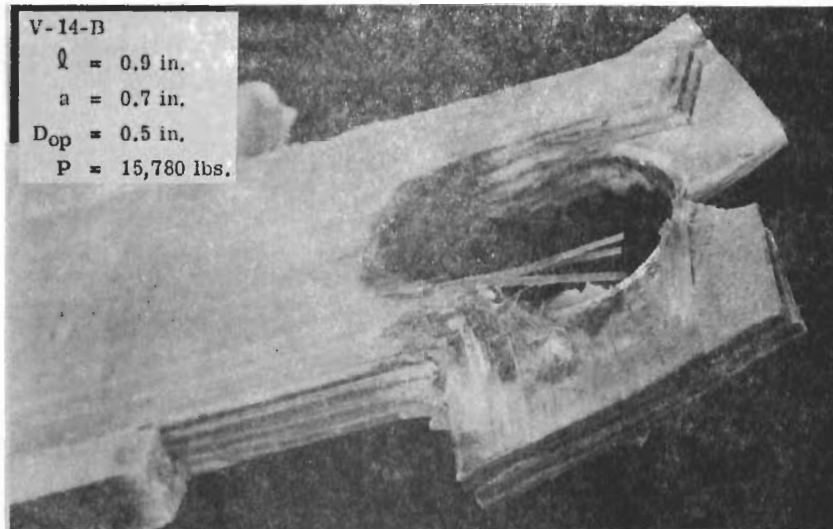


Figure 13. Flat Plate Specimens-Rupture by Combination of Failure Modes

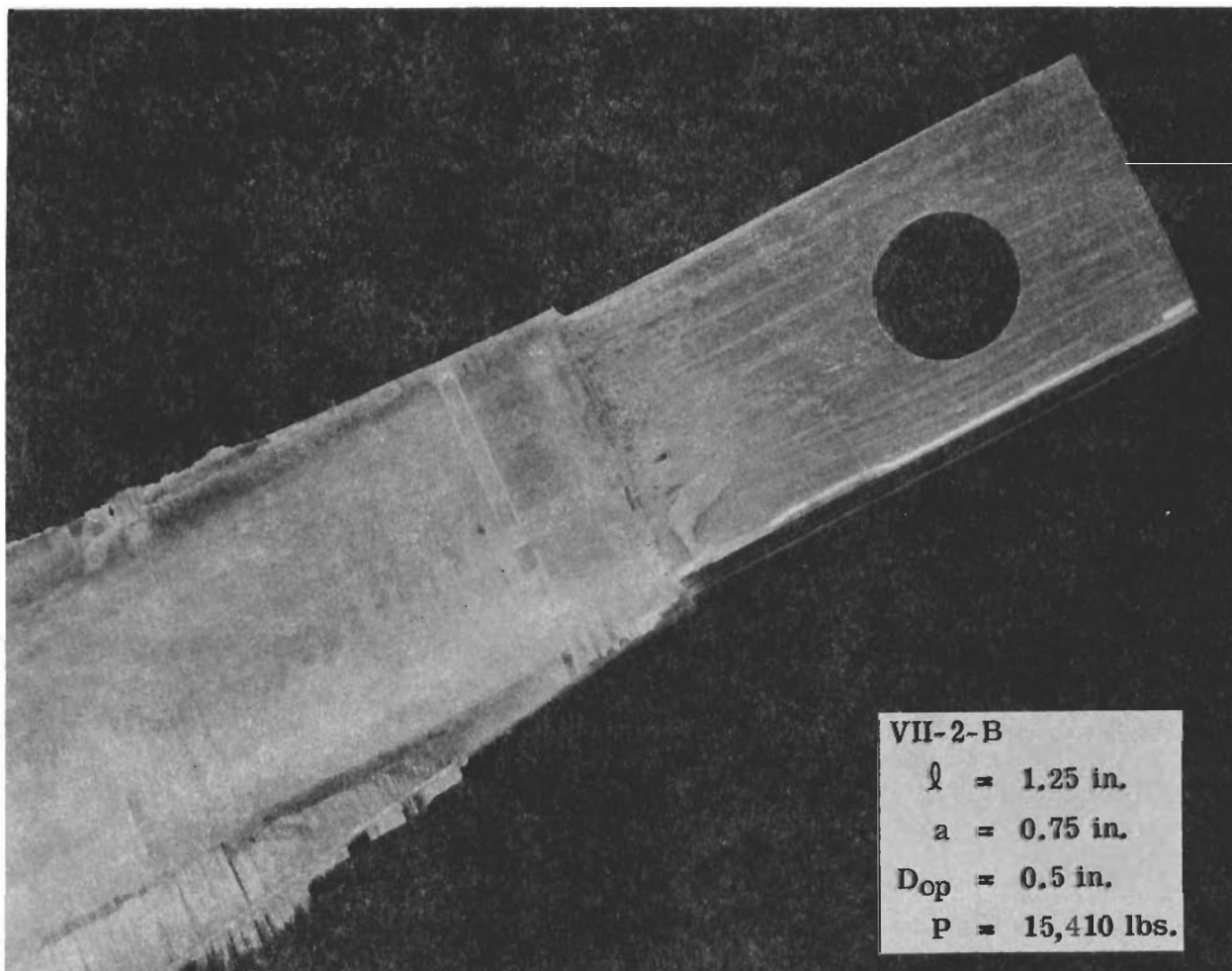


Figure 14. Flat Plate Specimens with Thickness Transition-Failure by Delamination

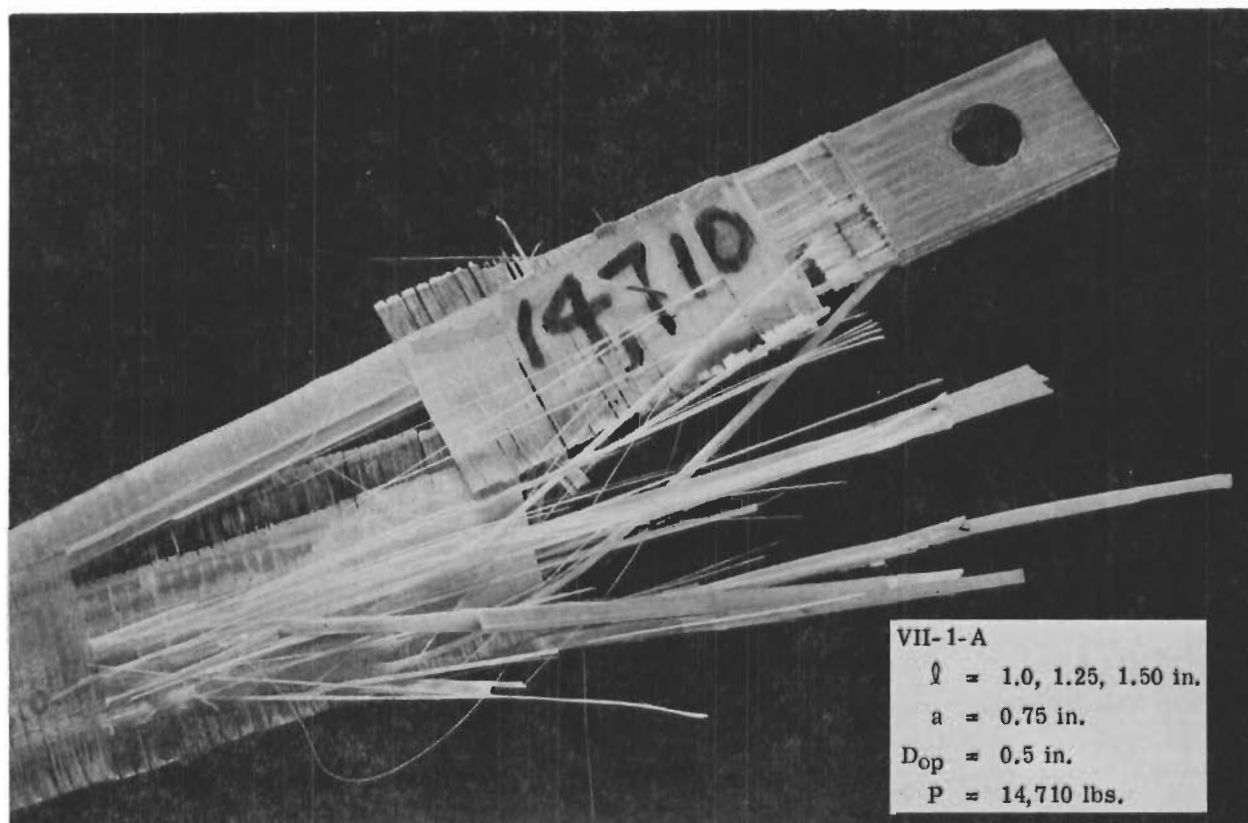


Figure 15. Flat Plate Specimen with Staggered Shim Lengths-Combination Glass and Bond Failure

SECTION IV

SHIM JOINTS FOR STRUCTURAL TUBES

4.1 DESIGN PROCEDURE

A feasible design is one that behaves satisfactorily under the specified environment. In general it is possible to find more than one feasible shim joint design for a given composite tube. If one of the design features is taken as the design objective, it is possible to find a feasible design which is most favorable as judged by the design objective. Usually the design objective of a structure is either weight or cost. In the present study, weight was chosen as the design objective. The shim joint design of minimum weight which is able to transfer a specified load to a given composite tube is termed the optimum design.

4.1.1 Design Constraints

A shim joint is considered feasible if it satisfies the following design constraints:

(a) Net section tension:

$$\left[ \frac{\pi}{2} (D_{oj} + D_{ij}) - N_p D_{op} \right] \left[ \frac{1}{2} (D_{oj} - D_{ij}) - N_{ctc} + N_s t_s \right] K_{tu} F_{tu} \geq P_{ult} \quad (24)$$

(b) Bearing:

$$N_p D_{op} N_s t_s K_{br} F_{tu} \geq P_{ult} \quad (25)$$

(c) Hoop tension:

$$N_p \left( a - \frac{1}{2} D_{op} \right) N_s t_s K_{ht} F_{tu} \geq P_{ult} \quad (26)$$

(d) Bond:

$$\pi N_s (D_{oj} + D_{ij}) l_e F_s \geq P_{ult} \quad (27)$$

(e) Circ reinforcing ring:

$$t_r \geq D_o^2 \frac{P_i - (P_i)a}{4E_f y_a} \quad (28)$$

(The derivation of this equation is given in Appendix III.)

(f) Pin:

$$\frac{\pi}{2} N_p D_p^2 (1 - R_d^2) F_{su} \geq P_{ult} \quad (29)$$

where

$$R_d = \frac{D_{1p}}{D_{op}}$$

#### 4.1.2 Objective Function

To write the objective function, the weight of each joint component is expressed in terms of the design variables:

(a) Fiber glass composite:

$$W_{fg} = \left[ \frac{\pi}{4} (D_o^2 - D_i^2) L_j - \frac{\pi}{4} D_{op}^2 N_p \left( \frac{D_o - D_i}{2} - N_c t_c \right) - N_c t_c \pi \left( \frac{D_o + D_i}{2} \right) L_j \right] \omega \quad (30)$$

(b) Shim:

$$W_s = N_s t_s \left[ \pi \left( \frac{D_{oj} + D_{ij}}{2} \right) L_s - \frac{\pi}{4} D_{op}^2 N_p \right] \omega_s \quad (31)$$

(c) Circ wrap ring:

$$W_r = \left[ 2 \pi (D_o + D_i) t_r^2 \tan \frac{\alpha}{2} \right] \omega \quad (32)$$

(d) Filler:

$$W_f = \frac{\pi}{4} (D_{oj} + D_{ij}) N_s L_t (t_s + 2 t_a) \omega_f \quad (33)$$

(e) Pin:

$$W_p = \frac{\pi}{4} D_{op}^2 (1 - R_d^2) N_p \left[ \left( \frac{D_o + D_i}{2} - N_c t_c \right) + \right.$$



$$N_s (t_s + 2 t_a) + l_p \omega_p \quad (34)$$

$l_p$  - pin length required outside shim pack to connect mating fixture.

The total joint weight  $W_t$  is the sum of equations 30 through 34:

$$W_t = W_{fg} + W_s + W_r + W_f + W_p \quad (35)$$

which includes all material within the joint length.

As a structural member, the total length of the composite tube is fixed. An increase in the joint length naturally causes a decrease in the uniform section portion of the composite tube. Consequently, the increase of weight due to longer joint length is partially compensated by a shorter basic tube section. Since the joint length is a design parameter, the total joint weight does not reflect the additional weight superimposed to the tube.

For this reason the shim joint objective function is defined as

$$W = W_t - \frac{\pi}{4} (D_o^2 - D_i^2) L_j \omega_{fg} \quad (36)$$

which is the weight added to the structural member by the attachment.

Now the design problem may be stated as:

to find the minimum of equation 36 subjected to the conditions of equations 24 through 29. There are a number of directly applicable mathematical methods for the solution of this type problem. The method selected in this study was the steepest descent. The attachment weight was taken as the objective function and the conditions equations 24 to 29 were treated as constraints. Then the objective function was minimized under the constraints by an iteration process. A description of this optimization routine is included in Appendix IV.

#### 4.2 DESIGN OF TUBULAR TEST JOINT

The optimization procedure was used to design the tubular joints for the final structural tests of this program. Using minimum allowables for 5,0°:1,90° GRP laminates\*, the ultimate load for the structural tube was determined to be 150 kips. The design allowable expressions obtained from the flat plate test data (Section III) were used in the constraint equations 24 through 29. The design was performed with the following parameters fixed:

---

\*Reference 1, Page 2-19

|            |   |                           |
|------------|---|---------------------------|
| $D_o$      | = | 3.0"                      |
| $D_i$      | = | 2.928"                    |
| $D_{oj}$   | = | 3.095"                    |
| $D_{ij}$   | = | 2.833"                    |
| $R_d$      | = | 0.8                       |
| $F_{tu}$   | = | 260 ksi (shim material)   |
| $F_{su}$   | = | 110 ksi (pin material)    |
| $t_a$      | = | .009"                     |
| $t_c$      | = | .006"                     |
| $\omega$   | = | .074 lb./in. <sup>3</sup> |
| $\omega_s$ | = | .283 lb./in. <sup>3</sup> |
| $\omega_f$ | = | .040 lb./in. <sup>3</sup> |
| $N_s$      | = | 5.0                       |
| $N_c$      | = | 2.0                       |
| $P_{ult}$  | = | 150 kips                  |

With exception of  $N_p$  (number of pins), the remaining design parameters were allowed to vary in the optimization routine. The routine does not handle discrete variables and it was impractical to treat  $N_p$  as a continuous variable. To determine the optimum number of pins, the value of  $N_p$  was varied in consecutive runs having otherwise identical input. The resulting joint designs are shown in Table 1. The table includes both, a) the weight added to the basic tube by the reinforcement and pins (objective function), and b) the total weight of the joint section. The pins were considered to be hollow ( $R_d = 0.8$ ) and made from 180 ksi UTS steel.

The objective function is plotted as a function of  $N_p$  in Figure 16. As the plot indicates, the eleven pin configuration is clearly the optimum one for the specified design problem.

#### 4.3 EFFICIENCY OF THE SHIM JOINT CONCEPT

Since shim joints are the first composite tube attachment concept to be studied in detail, it is impossible to compare them with other tube attachment concepts. A comparison can be made, however, with tubes of other materials designed to meet the same loading requirement. In Figure 17 the weights of constant strength tubes have been plotted versus tube length. The metal tubes are assumed to have identical strengths in tension and compression. Two curves are shown to reflect the different tensile and compressive strengths of 5,0°:1,90° fiber glass. The comparison of tube weights on the basis of compressive strength is not necessarily valid, however, since it does not reflect thin wall buckling and column buckling requirements. The weight of a given tube would be increased if additional wall thickness or moment of inertia were required for stability reasons.



TABLE 1. RESULTS OF PIN NUMBER VARIATION STUDY

| No. of Pins | D <sub>op</sub><br>in. | l<br>in. | a<br>in. | L <sub>t</sub><br>in. | t <sub>s</sub><br>in. | t <sub>r</sub><br>in. | Objective<br>Function<br>lb. | Total<br>Joint<br>Weight<br>lb. |
|-------------|------------------------|----------|----------|-----------------------|-----------------------|-----------------------|------------------------------|---------------------------------|
| 8           | .549                   | .685     | .686     | .461                  | .021                  | .014                  | .429                         | .518                            |
| 9           | .518                   | .680     | .681     | .447                  | .019                  | .009                  | .389                         | .477                            |
| 10          | .491                   | .702     | .667     | .424                  | .017                  | .012                  | .369                         | .457                            |
| 11          | .468                   | .722     | .661     | .409                  | .016                  | .010                  | .349                         | .436                            |
| 12          | .448                   | .740     | .663     | .414                  | .017                  | .015                  | .373                         | .461                            |
| 13          | .431                   | .753     | .664     | .422                  | .019                  | .023                  | .414                         | .502                            |

The fiber glass compression curve is dashed to indicate that not all failure modes have been considered.

The fiber glass tube weights include 0.7 pounds to reflect the weight added to both ends of the tube by the minimum weight eleven pin attachment of the previous section. The additional weight includes adhesive, steel shims and steel pins. The weight of the metallic overlap required of the mating fixture was not included because most metallic tubes used as side or drag braces also include a brazed, pinned or welded joint which causes overlapping material in the structural member. For this reason, the comparison presented is felt to be a good one.

Examination of Figure 17 reveals that for designs governed by tensile strength, fiber glass tubes are more efficient than aluminum for tube lengths of 5.0 inches or longer, and lighter than steel or titanium for tube lengths exceeding 7.5 inches. If compressive strength governs the tube design, fiber glass is more efficient than aluminum for lengths greater than 6.5 inches, and lighter than steel or titanium tube lengths exceeding 12.0 inches.

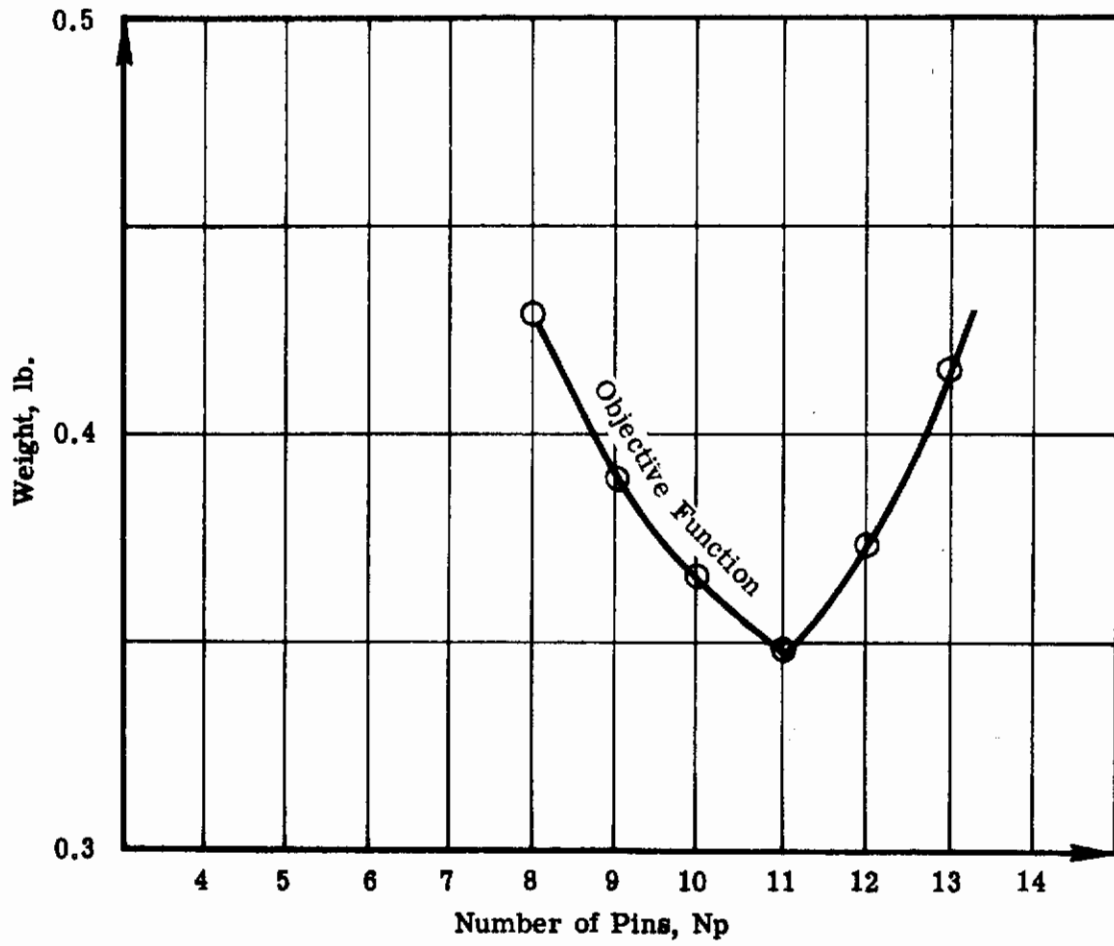


Figure 16. Increase in Weight of Structural Member Due to Joint versus Number of Pins used in Joint.

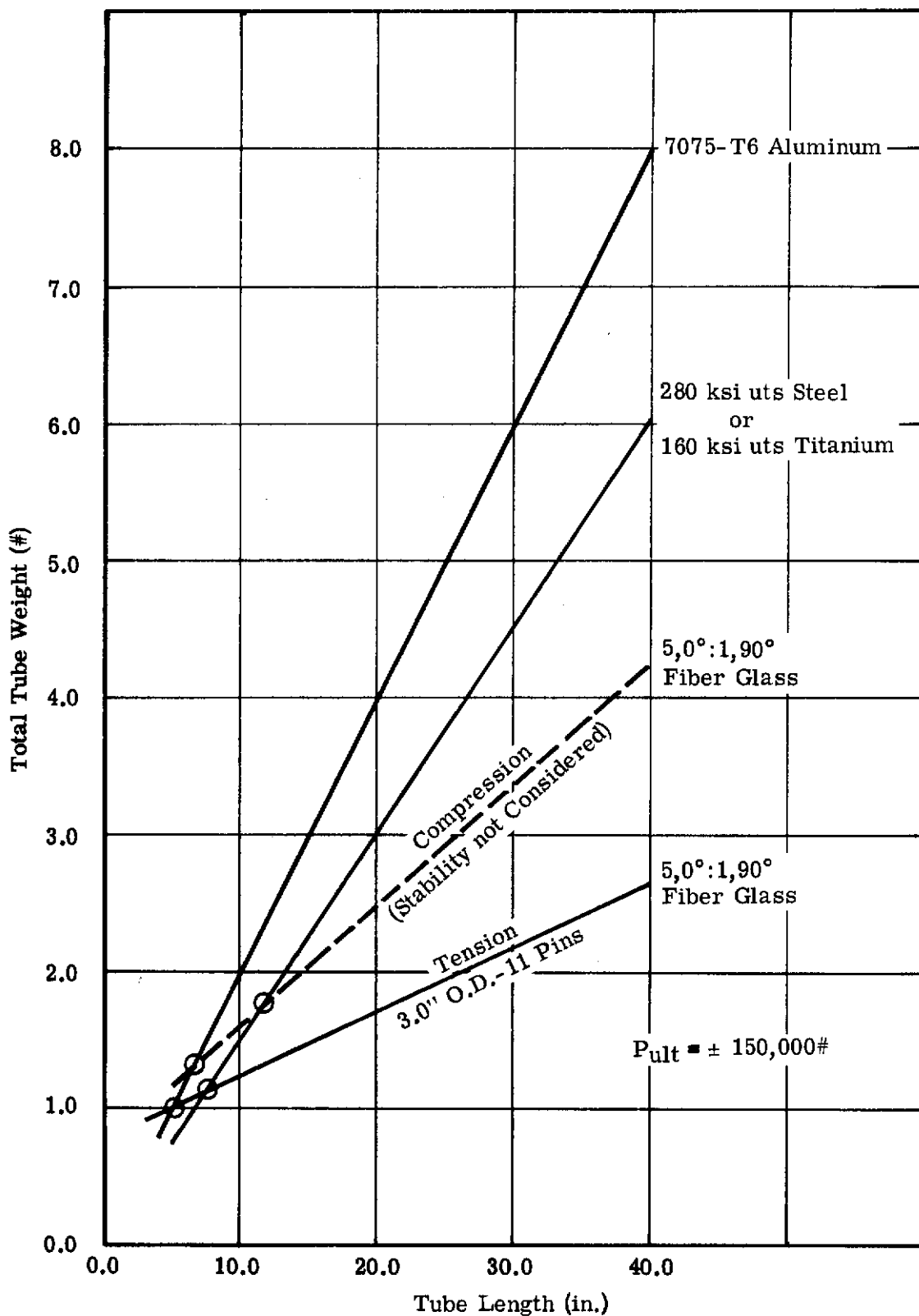


Figure 17. Weight Comparison of Constant Strength Tubes vs. Tube Length. Fiber Glass Tube Weights Include Steel End Reinforcement and Steel Pins.

SECTION V

MATERIALS AND FABRICATION

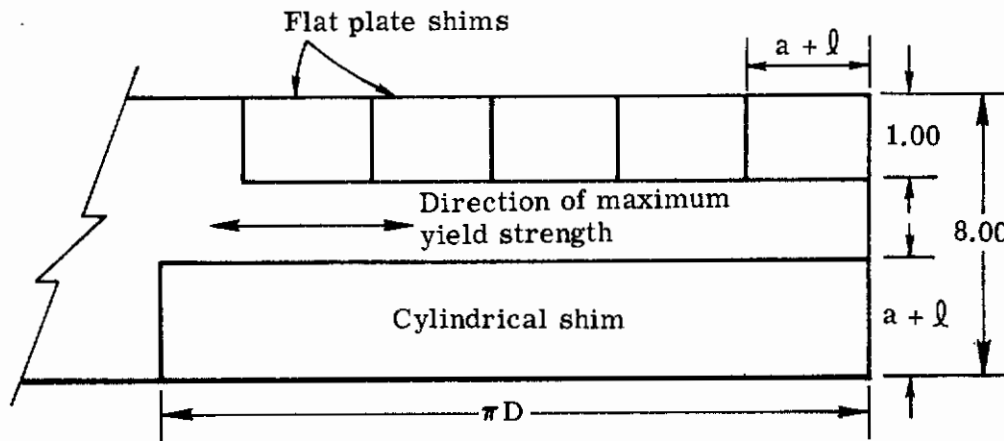
5.1 FILAMENT COMPOSITES

The filament composite materials employed in this program consisted of AF-994 glass filaments and Shell Chemical Company's 58-68R resin system.

5.2 METAL SHIMS

The metal shim material was selected to ensure adequate physical properties and ready availability. The program schedule and scope did not permit procurement of materials with excessive lead times. Several materials, such as titanium alloys, maraging steels, and corrosion resistant steels were investigated since they offered attractive strength versus weight ratios. It was found that the lead time for procurement of titanium alloy sheet was excessive. Maraging steels were eliminated since their resistance to elongation was too low for use in this application. AM-355 corrosion resistant steel was readily available and provided satisfactory material properties. The AM-355 steel was obtained from the Wasatch Division of the Thiokol Chemical Corporation where it had been originally destined for use in fabricating the large, segmented, fiberglass reinforced, plastic rocket motor case known as Project 8-150.

The AM-355 corrosion resistant steel sheet was received in a 300 pound coil. The material was eight inches wide, 0.020 inch thick, and of continuous length. Certification of the physical properties of this material is presented in Appendix VI. The material as received possessed superior yield strengths along the length of the coil as compared with the yield strengths across the eight-inch width. It was necessary, therefore, to fabricate the cylindrical shims with the greatest yield strength in the circumferential direction instead of the axial direction as desired. However, the shims utilized in the flat-plate specimens were cut from the roll such that the maximum yield strength of the material was parallel to the applied tension load, as desired. The following sketch illustrates how the shims were cut from the roll:



It would be desirable during the fabrication of production items to orient the steel sheet such that the maximum yield strength of the material would be aligned parallel to the maximum anticipated loads.

The cylindrical shims, formed of 0.020 inch thick AM-355 corrosion resistant steel sheet, were found difficult to wrap around small diameter cylinders and secure in place. An attempt was made to preform the shims to a cylindrical shape by passing them between rolls prior to assembly. The first trial resulted in a preformed diameter of approximately 24 inches when rolls of 2.5 inch diameter were employed. An analysis was performed and the curve presented in Figure 18 permitted selection of the proper size rolls to produce a preformed residual bend radius of 1.5 inches as required. The rolls selected were of one-inch diameter and satisfactorily produced preformed cylindrical shims of the proper diameter.

### 5.3 CLEANING

The shim cleaning procedure employed was originally developed and reported under the authority of Contract AF33(657)-11303, ASO Project 8-150 (Air Force Materials Laboratory, Wright-Patterson AFB, Ohio) and is summarized below:

- A. Hand wash with denatured alcohol.
- B. Trichlorethylene degrease, 20 minutes.
- C. Suspend in Prebend 700 solution, 20 minutes @ 200° F.
- D. Rinse in tap water.
- E. Check for cleanliness by water break method.
- F. Air or oven dry prior to using or placing in storage.

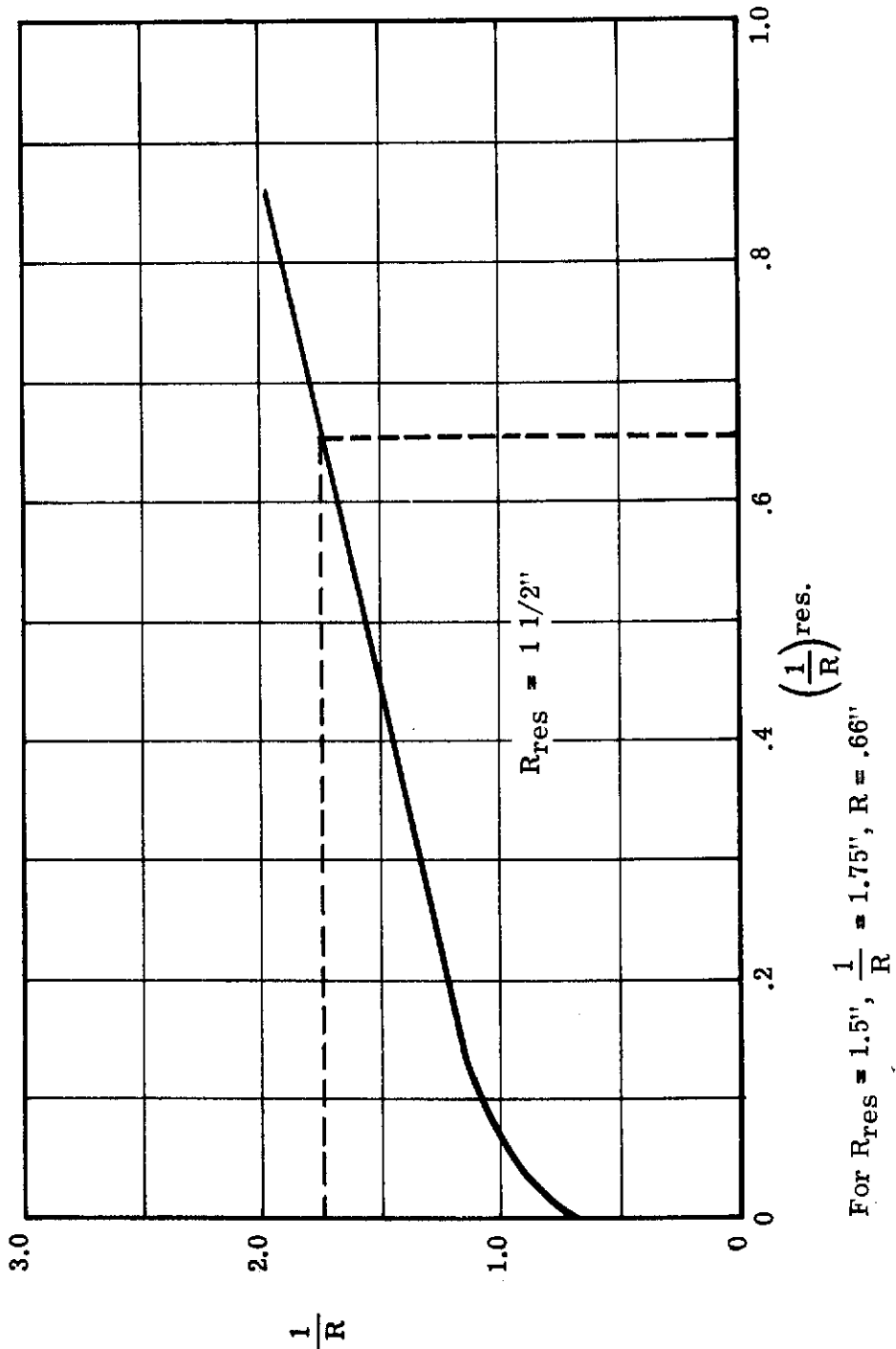


Figure 18. Bend Radius vs. Residual Bend Radius for AM-355 Sheet 0.02 Inch Thick



5.4 ADHESIVES

The bond between the corrosion resistant steel shims and the filament composite material was provided by a structural adhesive. Two types of adhesives were evaluated. The first was BR-1009-49 tack primer as supplied by the Bloomingdale Division of American Cyanamid Corporation, and the second was AF-111 structural adhesive film furnished by the 3M Corporation.

BR-1009-49 tack primer was utilized during the early phases of the program. It was originally planned to apply a uniform coat of tack primer to each shim by individually dipping each shim in the primer. However, poor results were obtained when the tack primer flowed to the bottom of the shims. The thickness of the resulting primer coat was not uniform and varied from 0.0005 to 0.0251 inch. This difficulty was obviated by allowing the bottom of the shim to contact a sheet of clean absorbent paper, such as a paper towel, immediately following removal of the shim from the primer dip tank. A primer coating of uniform thickness of approximately 0.0005 inch was obtained by this method. Subsequent to the dipping operation, the primer coat on the shims was oven cured for 60 minutes at 315° F.

AF-111 structural adhesive film was utilized during the later phases of the program to replace the BR-1009-49 tack primer. The adhesive film was applied to the steel shims, which had been cleaned in accordance with the procedure described above, by the following method:

- A. Cut portion of film to be used from roll with protective liners in place.
- B. Remove protective liner from one side of film.
- C. Place side of film from which protective liner has been removed in contact with steel shim.
- D. The protective liners still remaining on the exposed film surface should be retained to serve as protective covers over the adhesive film.
- E. Press the adhesive film against the shim by rolling with a rubber roller to ensure that no entrapped air remains between the shim and the adhesive film.
- F. Store adhesive film-coated shims at 40° F until ready for use.

5.5 DRILLING

Holes were drilled through the fiber-resin-shim-composite cylinder walls to permit insertion of shear pins. A special drilling procedure was developed and the holes were drilled in accordance with this procedure which is described as follows:

- A. A sturdy support to oppose the drill pressure must be provided inside the cylinder directly under the hole to be drilled.
- B. Drill to be carbide-tipped or full carbide.

- C. Drill speed to be approximately 90 rpm.
- D. Coolant to be iodine complex type cutting fluid.
- E. Sufficient drill pressure must be maintained to ensure continuous cutting of the AM-355 shims since insufficient pressure will permit the material to work harden ahead of the drill lips.
- F. Pilot holes can be drilled up to approximately 0.250 inch diameter.
- G. Holes larger than 0.250 inch diameter can be drilled in successive steps of approximately 0.375 inch diameter increase per step.

## 5.6 FLAT-PLATE SPECIMENS

The flat-plate filament composite test specimens utilized in this program were specially wound on a Bendix developed winding machine. The test specimens were wound over twelve-inch by two-inch aluminum mandrels, one of which is illustrated in Figure 19. Guide blocks were provided on one end of the mandrels to facilitate locating the metal shims as they were wound into the ends of the specimens.

A fluorocarbon release agent (Miller-Stephenson Chemical Company, Dry Film MS-122 or Liquid S-143) was applied to the mandrels prior to winding to facilitate removal of the specimens.

Two specimens were wound simultaneously by utilizing both sides of the mandrel. The longitudinal and transverse filaments were applied by rotating the mandrel about mutually perpendicular axes as shown in Figures 20 and 21. The location of a metal shim between the mandrel guide blocks is shown in Figure 22.

It was necessary to compress the shim areas of the specimens during curing. Upon completion of winding, rectangular aluminum blocks were placed over the shim areas between the mandrel guides. These blocks were thick enough to project above the guides. An approximately 1/4 inch thick layer of transverse windings were applied under high tension over the aluminum blocks and the guides. This layer of transverse windings served to place the shim areas under the desired compression during the curing cycle. The wrapped mandrels were then cured for four hours at 350° F.

The specimens were removed from the mandrel by cutting the glass composite along the edges with a high-speed cutting disk. The sides and ends were trimmed with a bandsaw and flat-plate disk sander.

## 5.7 TUBES

Open-end cylinders were fabricated two-at-a-time by winding a double length cylinder and then cutting it into two cylinders. The cylinders were wound over mandrels machined from salt block which was later removed by dissolving in hot water. Thin corrosion resistant steel shims, in the form of narrow circumferential bands, were wound into the cylinders on each side of the planned cut which would separate the two cylinders. Subsequent to removal of the salt mandrel, a circumferential row of holes was drilled



**Figure 19. Flat Plate Specimen Winding Mandrel**

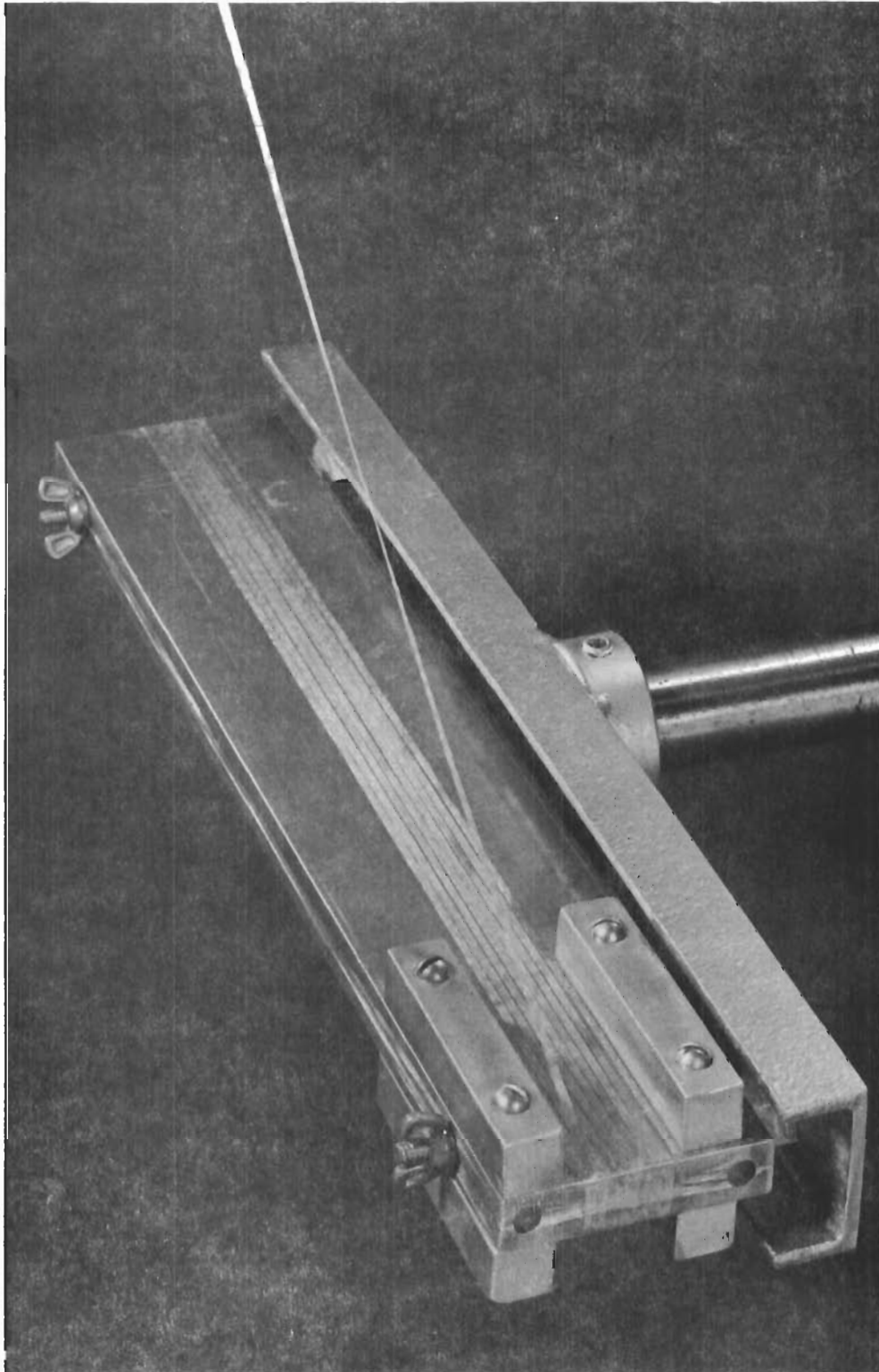


Figure 20. Winding Longitudinal Filament



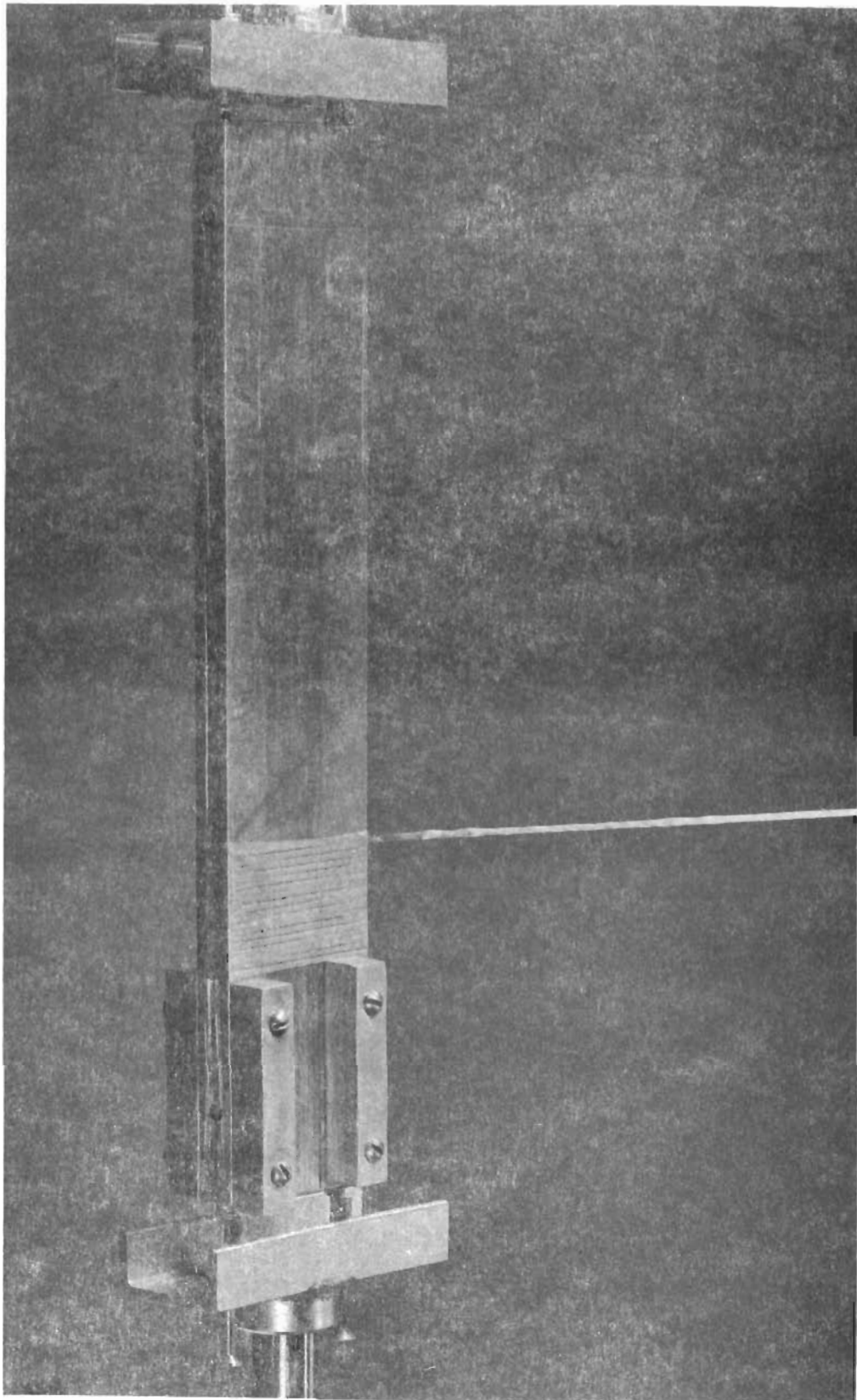


Figure 21. Winding Transverse Filament

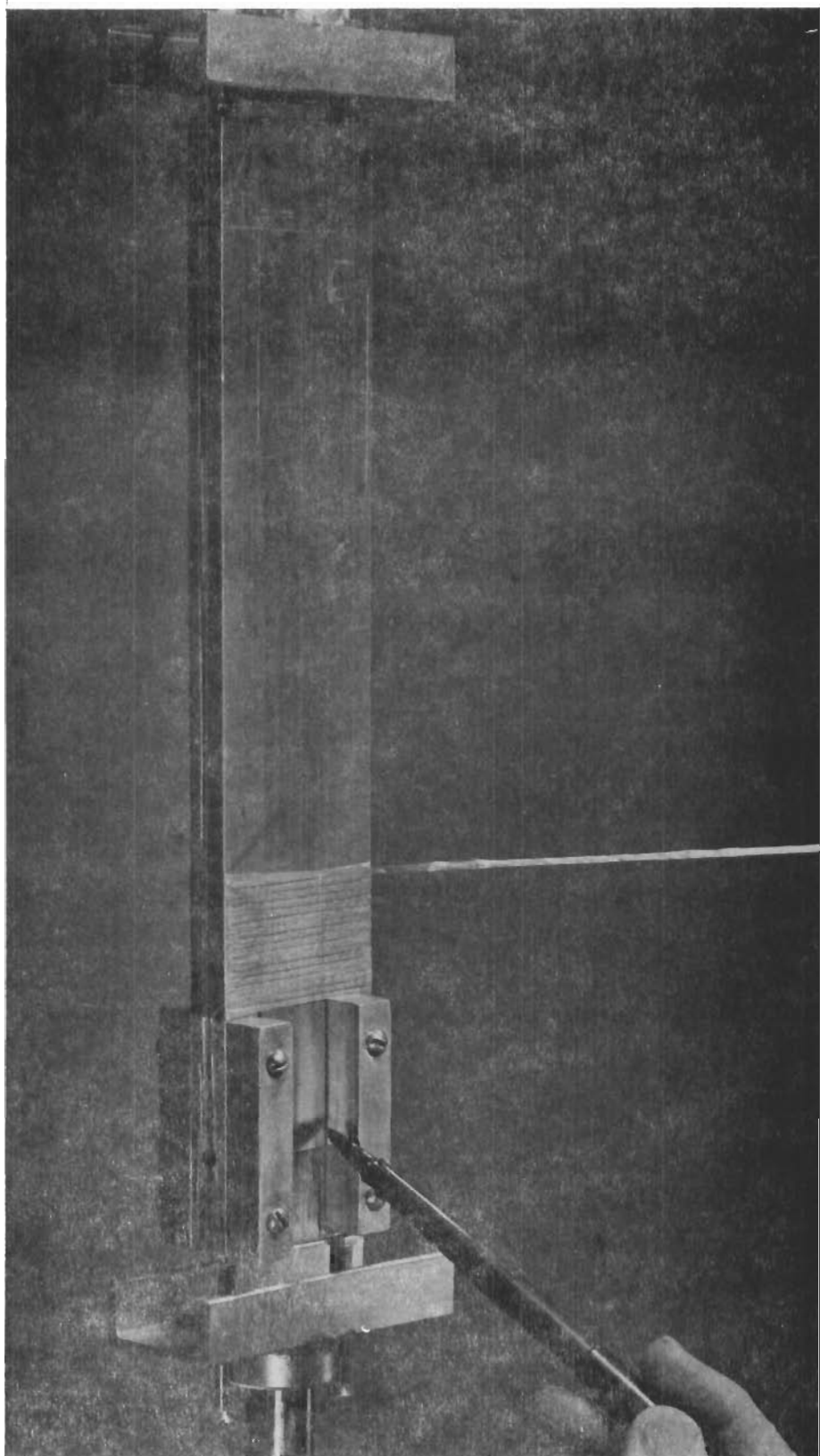


Figure 22. Location of Metal Shim



through the wall of each cylinder in the shim area for later insertion of shear pins. The necessary special drilling procedure has been previously described in the description of flat-plate specimen fabrication techniques.

The design required that five circumferential steel shims be sandwiched between alternate layers of longitudinal glass fibers. Retention of the shims during winding operations was complicated by the fact that there were no circumferential windings in the shim areas. In addition to locating and retaining the shims, it was also necessary to compact both the glass fibers and the AF-111 adhesive film in the shim area as each shim was incorporated. To satisfy these requirements, initial winding trials were conducted to develop methods of locating and retaining the shims during winding operations and of applying the necessary compressive load on the shim areas as each shim was incorporated. A successful method evolved from these winding trials, and is described below:

- A. Form shims to the required radius of curvature prior to cleaning. The circumference of the shims must be accurately controlled such that no gap or overlap exists where the ends of the shims butt together upon installation.
- B. Apply AF-111 dry film adhesive to the joint area of the cylinder.
- C. Locate cleaned shim around AF-111 dry film adhesive on cylinder joint area.
- D. Place band clamp in center of shim and tighten.
- E. Heat joint with heat lamp. The AF-111 adhesive will start to flow from under the shim at approximately 150° F. Tighten the band clamp progressively until the ends of the shim butt together.
- F. Remove the heat lamp. In approximately five minutes the band clamp can be removed and the AF-111 adhesive will hold the shim in the proper location while also compacting the glass fibers and adhesive as required.

The completed tube, prior to drilling of shear pin holes, is shown in Figures 23 and 24.

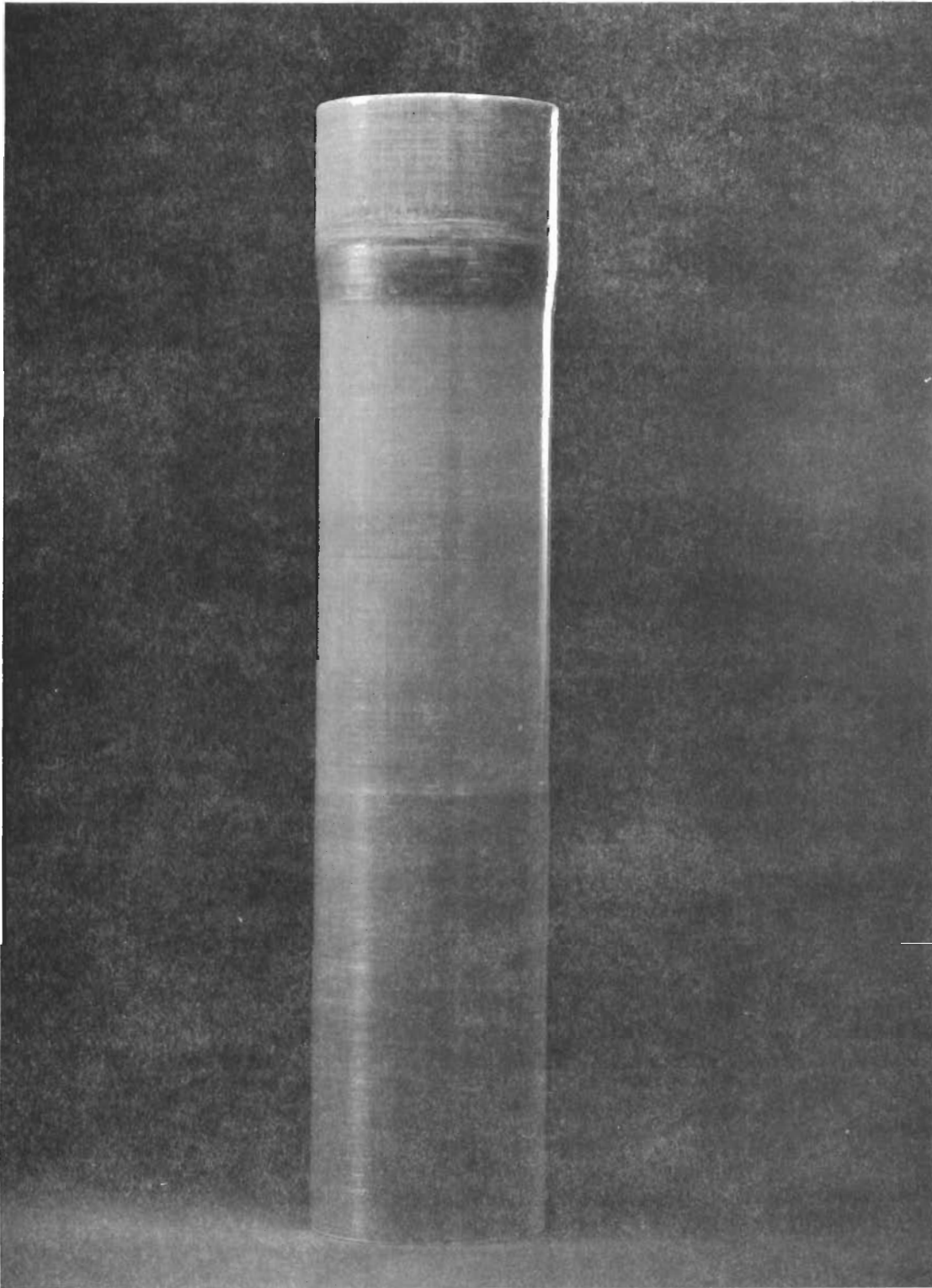


Figure 23. Tube With Shim Reinforced End

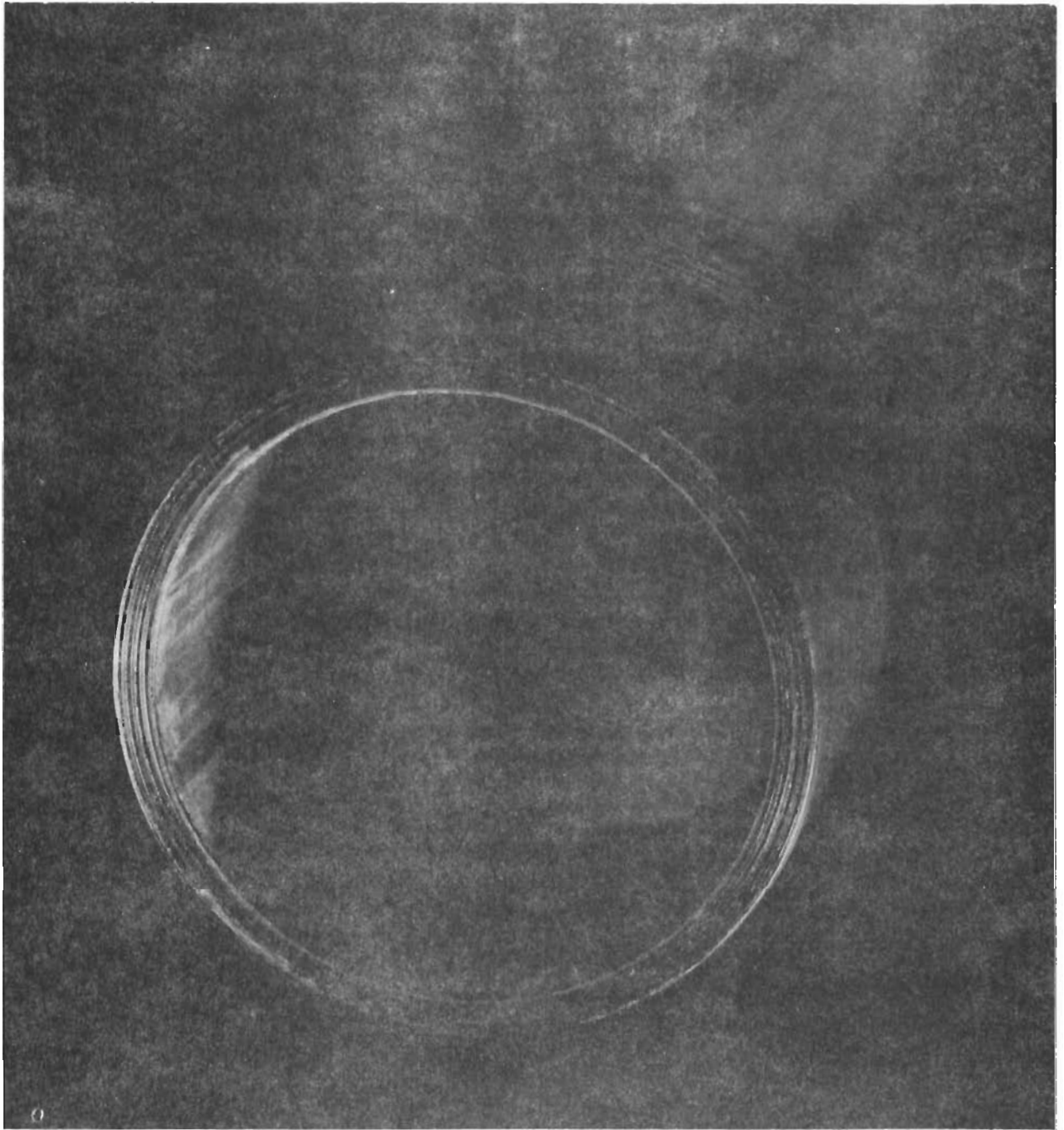


Figure 24. Shim Reinforced End of Tube



SECTION VI  
STRUCTURAL TESTS

6.1 TEST FIXTURES

Ultimate strength testing of the final tubular joint design required the fabrication of two separate test fixtures. One fixture is a clevis-type which mates with the reinforced attachment area of the tube to form the pin joint. The fixture was fabricated in two pieces to avoid the expensive machining which would be required by a monolithic assembly. The two pieces were held tightly together by a nut during drilling of the pin holes. The nut was used to insure that equal loads would be applied to the pins on the inside and outside diameter of the tube. The fixture parts are shown in Figure 25, and the assembly is shown after test in Figures 28 and 29.

The second test fixture held the opposite end of the tubular specimen which was reinforced only by four additional layers of filament material. The fixture employed a friction gripping technique developed at ECD. A detailed discussion of the gripping technique and the fixture design have been enclosed in Appendix V. A schematic of the fixture is shown in Figure 26, and the fixture is shown after test in Figures 28 and 29.

6.2 TENSION TEST OF TUBULAR JOINT

A 3.0-inch outside diameter tube was fabricated with steel reinforced end to test the shim joint concept in a full scale structural member. The design which was actually fabricated is shown in Figure 27. A nine-pin configuration was chosen so that available 1/2-inch diameter carbide tip drills and 0.02" shim stock could be used. The eleven-pin design, which was shown in Section IV to be most efficient required .468 inch pin holes and .016 inch shims. The eleven-pin design would require 15/32-inch diameter drills which were not readily available.

The test specimen was designed to fail in the attachment area since the program is oriented to refinement of shim joint design technology. The basic tube was fabricated with a 5,0°:1,90° wrap pattern to a wall thickness of 0.072 inches. The ultimate tensile load for the tube, as governed by minimum allowables\*, was found to be 150 kips. The attachment area was also designed to transfer 150 kips. The attachment design, however, was governed by the mean design allowables presented in Section III with two exceptions: a) the bond joint was designed with a safety factor of 1.1 (1.36 x 1.1 = 1.50"),

---

\*Reference 1, Page 2-19.

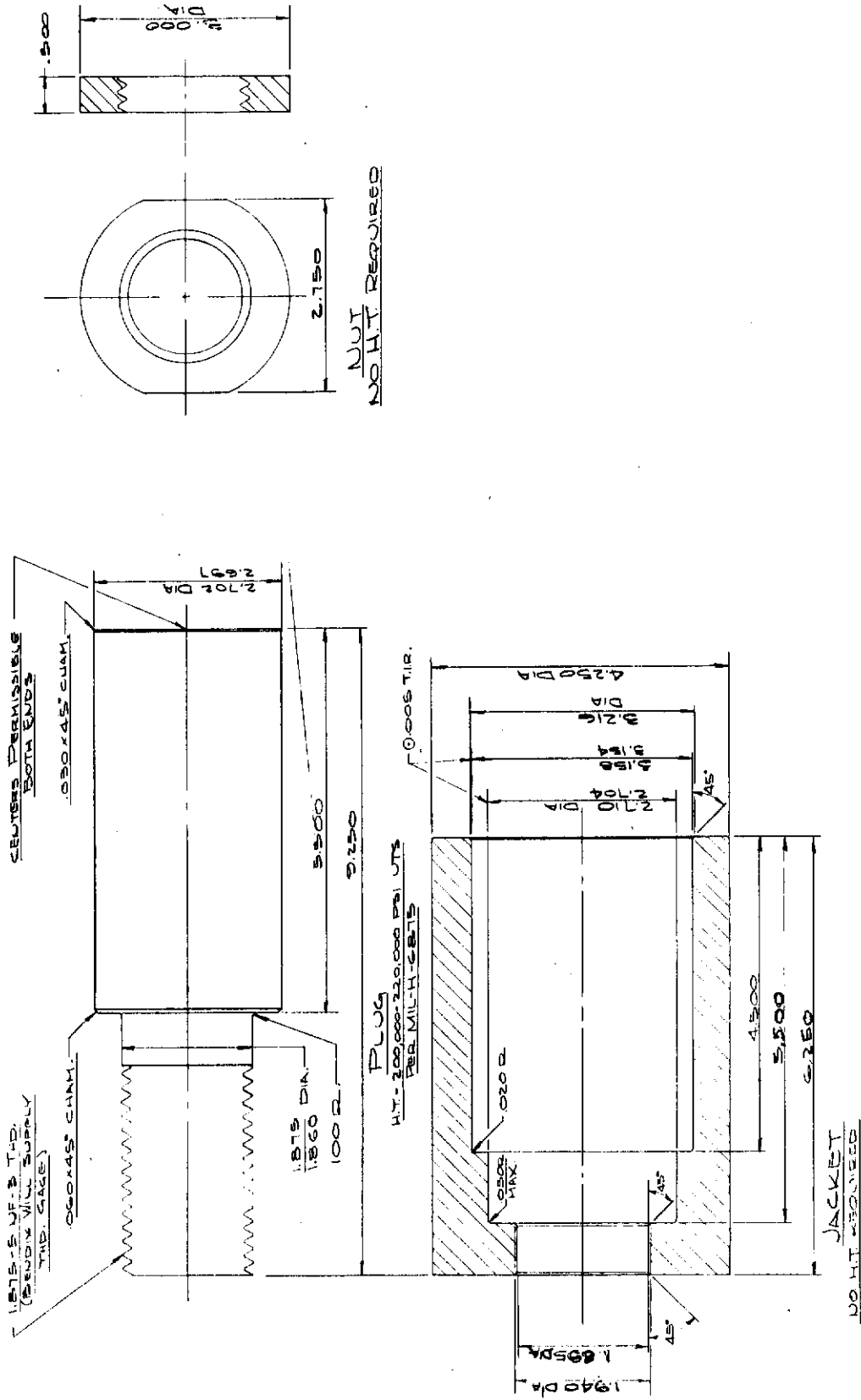


Figure 25. Joint End Test Adapter (Nonflight Weight)



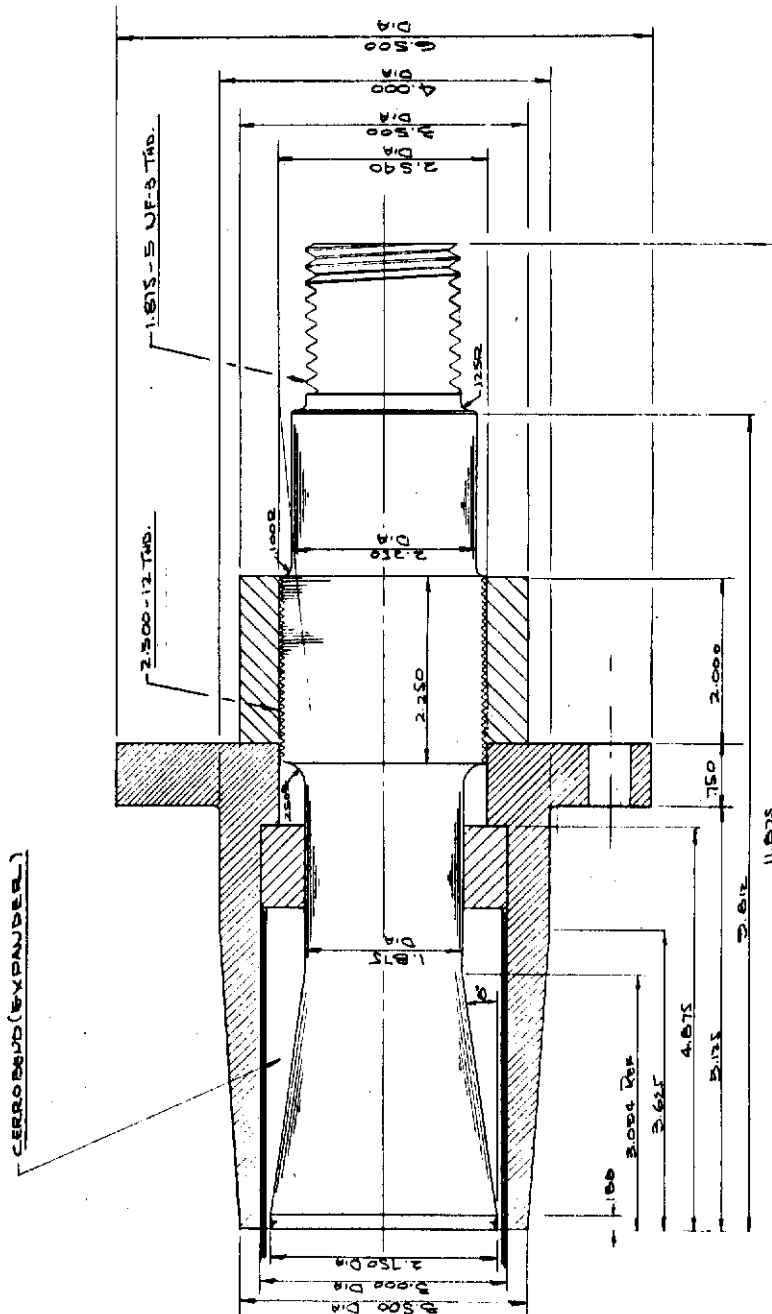


Figure 26. Tension Fixture Assembly

and b) a 1/2-inch pin diameter was used instead of 0.518 inch as called for by the nine-pin design. A safety factor was used for the bond joint because bond failure is the most catastrophic of the attachment failure modes. The smaller pin diameter was chosen so that pin bearing would be most eminent of the attachment area failure modes. Pin bearing is desirable because it is the most ductile of the attachment failure modes.

The specimen was loaded in an Olson Machine to an ultimate tension load of 135.5 kips. Fracture occurred in the outer fiber glass layer at the edge of the outside shim. The specimen is shown after failure in Figure 28. The ultimate load was about 10 percent below the expected value, but the failure mode was not an anticipated one. It is felt that the predicted load could be reached if the sharp corner was eliminated from the outside shim, and the outside fibrous layer was reinforced slightly.

### 6.3 COMPRESSION TEST OF TUBULAR JOINT

As stated in the work definition, this program was designed to develop the shim joint concept for composite tubes having primary tension and secondary compression requirements. This program was not designed, however, to study compressive joints in detail. The compressive failure modes were not studied and no design allowables unique to compressive loadings were generated. It was of interest, however, to see if a joint identical to that tested in tension could withstand the ultimate compressive load for the same tube. For this reason a compression test was conducted. Unfortunately the tube was critical in local buckling ( $D/t = 41.7$ ). The ultimate compressive load for the tube was found to be about 51.0 kips\*. An ultimate load of 84.0 kips would have been possible had the tube been compressive stress critical.

The tension clevis fixture and the jacket of the friction grip fixture were used to conduct the compression test. A Cerrobend plug was cast to reinforce the inside diameter of the nonreinforced tube end. A second tension specimen, identical to the first, was tested to an ultimate compressive load of 48.5 kips. The attachment area suffered no discernible damage. Initial failure was due to symmetrical thin wall buckling in the basic tube. Once the stability deflection became excessive, material failure did occur as shown in Figure 29.

---

\*Reference 1, Page 2-24.

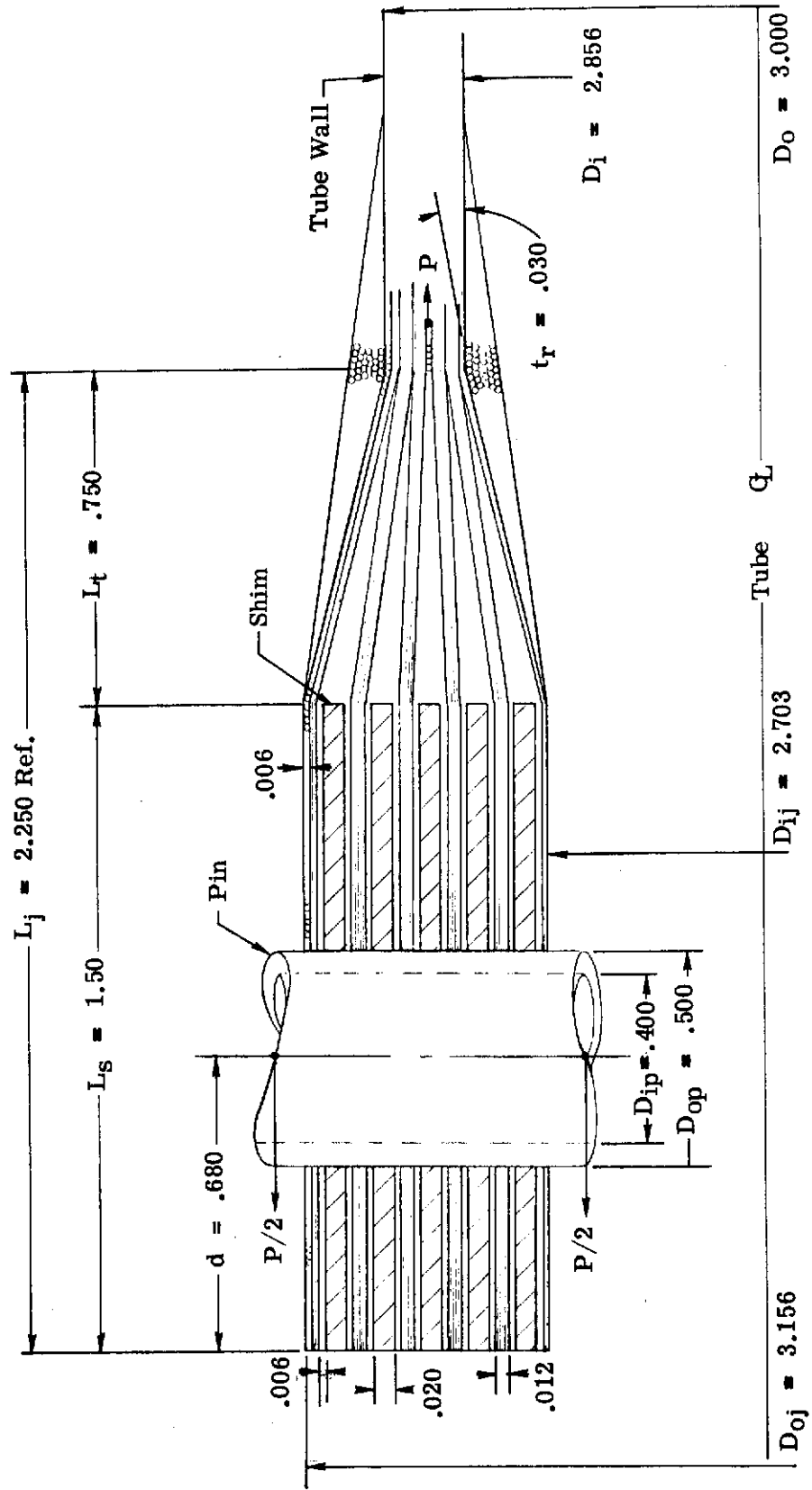


Figure 27. Tubular Joint which was Fabricated for Testing

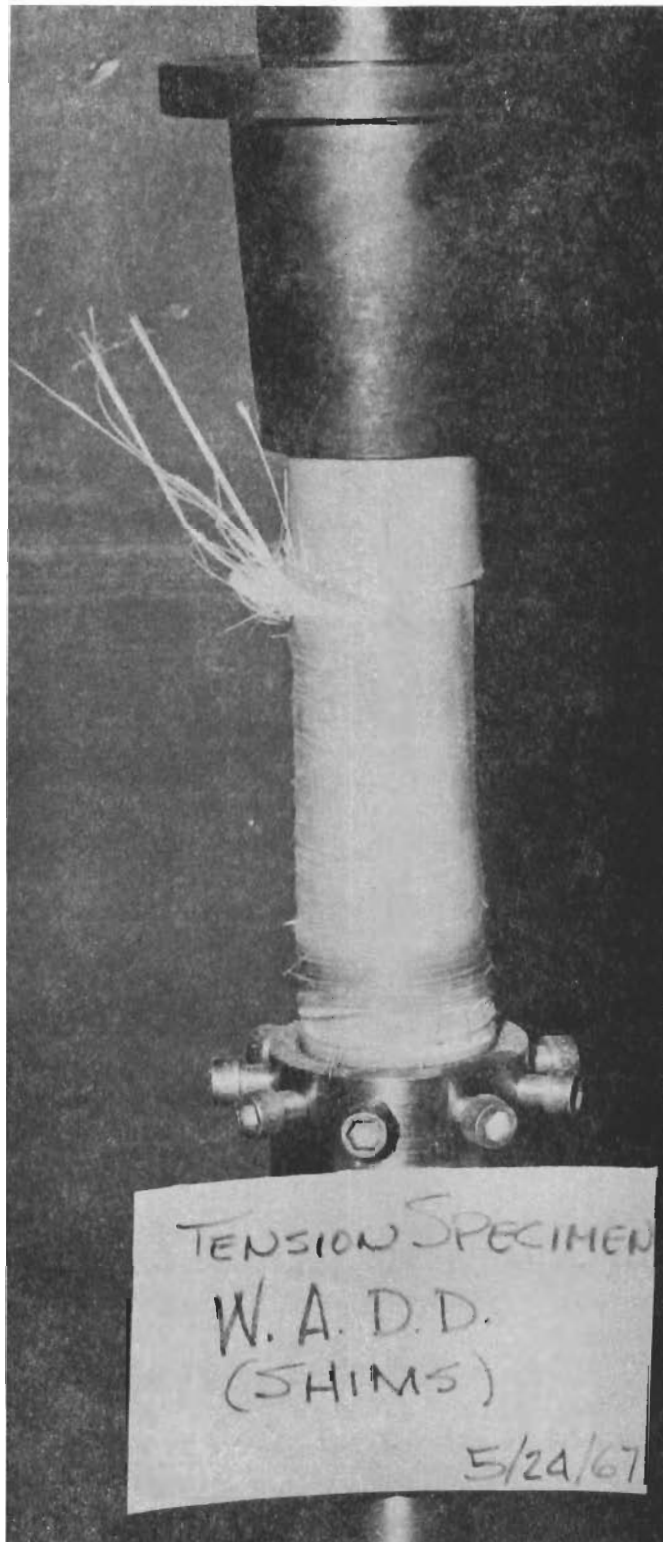


Figure 28. Tubular Shim Joint Specimen-After Tension Test

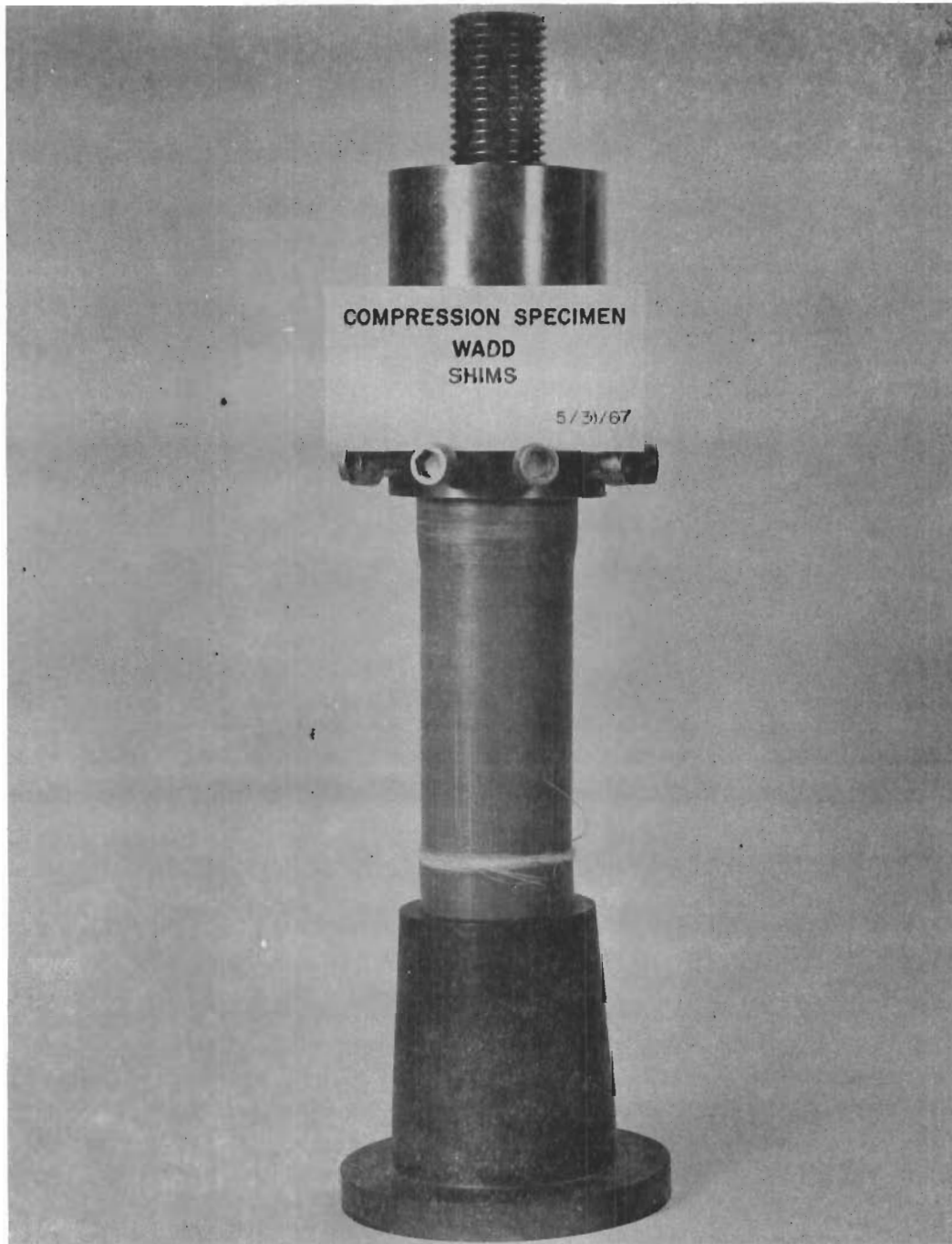


Figure 29. Tubular Shim Joint Specimen-After Compression Test

SECTION VII

CONCLUSIONS

7.1 CONCLUSIONS

The following conclusions may be made as a result of work conducted during this program:

- A. The failure modes associated with a shim joint subjected to tension have been well defined. (Paragraph 2.2.)
- B. The important design parameters associated with a shim joint under tensile loading have been defined. (Paragraph 2.1.)
- C. Most of the strength data required to design shim joints for tensile loading can be generated by testing flat plates. (Section III.)
- D. An optimum design routine has proven to be not only feasible, but highly beneficial, for designing lightweight shim joints. (Section IV.)
- E. The AM 355 corrosion resistant steel shim stock is good reinforcement shim material for glass-epoxy composites. It was successfully formed into the desired reinforcement shapes and machined in the final shim joint configurations. (Paragraph 5.2.)
- F. The use of structural adhesive tapes will significantly increase the strength of a bond joint by increasing the adhesive thickness. (Figure 12, page 31.)
- G. The shim joint concept can be used for end attachments on fiber glass structural tubes to transmit tension loads without prohibitive weight penalties. (Figure 17, page 41.)
- H. It does not appear that compression load requirements will significantly increase the weight of the shim joint configuration. (Paragraph 6.3, page 57.)



SECTION VIII  
LITERATURE SEARCH AND REFERENCE LIST

8.1 GENERAL

Prior to commencing the engineering effort to study shim joints, and continuing throughout the duration of the program, a literature search was conducted to ensure that the state-of-the-art would be advanced and to avoid duplicating the work of other researchers. To preserve the list of information sources which this search produced, the resultant reference list is presented in Table 2.

TABLE 2

LIST OF REFERENCES

1. Exploratory Application of Filament Wound Reinforced Plastics for Aircraft Landing Gear, Report No. AFML-TR-66-309, December 1966. The Bendix Corporation, Products Aerospace Division, South Bend, Indiana. Project No. 7381, USAF Contract No. AF33(615)-3080 for the Air Force Materials Laboratory, Wright-Patterson Air Force Base, Ohio.
2. Large Segmented Fiberglass Reinforced Plastic Rocket Motor Cases, Report No. ASD-IR-8-150, Volumes I through VIII, Thiokol Chemical Corporation, Wasatch Division, Contract AF33(657)-11303, ASD Project 8-150 (Air Force Materials Laboratory, Wright-Patterson AFB, Ohio).
3. Reinforced Plastic Construction Methods for Large Rocket Motor Cases, Report No. TR-63-7-858, Volume I, December 1963, Thiokol Chemical Corporation, Wasatch Division, Contract AF33(600)-42511, Project 7-858.
4. Segmented Fiberglass Motor Case Joint Design and Analysis, by Alex Brinchmann, Volume of technical papers presented at AIAA Sixth Structures and Materials Conference, Palm Springs, California, April 5-7, 1965, pages 299 through 312.
5. Photoelastic Study of Fiberglass-to-Metal Joint, by O. L. Gillette, Utah Research and Development Corporation, Presented at SESA Spring Meeting, Salt Lake City, Utah, May 6-8, 1964.
6. The Joint Stresses in Cemented Joints, by M. Goland and E. Reissner, Journal of Applied Mechanics, March 1944, pages A17 through A27.
7. Adhesive Bonding of Reinforced Plastics, by H. A. Perry, McGraw-Hill Book Company, Inc., 1959.
8. Test Results of Thick Wall and Segmented Fiberglass Cases, by D. M. Bartlett and J. Ventenbergs, Proceedings of the 19th Annual S.P.I., February 4-6, 1964, Section 7-A, pages 1 through 14.
9. Analysis of Lugs and Shear Pins, by M. A. Melcon and F. M. Hoblit, Product Engineering, May 1950 and June 1953.
10. Mechanics of Adhesive Bonded Lap-Type Joints: Survey and Review, Report No. ML-TDR-64-298, 1964, Forest Products Laboratory, Forest Service, U.S. Department of Agriculture, Madison, Wisconsin, Contract 33(657)-63-358.
11. Manufacturing Methods for Plastic Airframe Structures by Filament Winding, Technical Report IR-9-371(I), February 1967, Air Force Materials Laboratory, Wright-Patterson Air Force Base, Ohio.

TABLE . LIST OF REFERENCES (Cont.)

12. Determination of Mechanical Properties of Adhesives for Use in the Design of Bonded Joints, U. S. Forest Service Res. Note FPL-011, Forest Products Laboratory, Forest Service, U. S. Department of Agriculture, Madison, Wisconsin.
13. Design of Joints for Filament Wound Shells, Report No. EP-6984156, May 1966, Kansas City Division, The Bendix Corporation.
14. Final Report on Development of Improved Processes for Filament Wound Reinforced Plastic Structures, Technical Report No. AFML-TR-65-80, March 1965, Aerojet General Corporation.
15. Feasibility of Joining Advanced Composite Flight Vehicle Structures, First Quarterly Progress Report, August 19, 1966, Illinois Institute of Technology Research Institute, Contract Number AF33(615)-3962 (Air Force Materials Laboratory, Wright-Patterson Air Force Base, Ohio).
16. Feasibility of Joining Advanced Composite Flight Vehicle Structures, Second Quarterly Progress Report, Report Number M6151-6, October 1966, Illinois Institute of Technology Research Institute, Contract Number AF33(615)-3962 (Air Force Material Laboratory, Wright-Patterson Air Force Base, Ohio).
17. Feasibility of Joining Advanced Composite Flight Vehicle Structures, Third Quarterly Progress Report, Report No. M6151-9, February 1967, Illinois Institute of Technology Research Institute, Contract Number AF33(615)-3962 (Air Force Materials Laboratory, Wright-Patterson Air Force Base, Ohio).
18. Attachment Concepts and Problems in Fibrous Composite Aerospace Structures, Volume 10, SAMPE 10th National Symposium and Exhibit, San Diego, California, November 9-11, 1966.
19. Developments in the Analysis of Lugs and Shear Pins, by F. M. Holbit and M. A. Melcon, Product Engineering, June 1953, page 160.
20. Optimum Structural Design Concepts for Aerospace Vehicles: Bibliography and Assessment, Technical Report No. AFFDL-TR-65-9, June 1965, Allied Research Associates, Inc., Concord, Massachusetts, Contract Number AF33(615)-1840, Project Number 1467, Task Number 146704 (Air Force Flight Dynamics Laboratory, Wright-Patterson Air Force Base, Ohio).
21. Filament Wound Joint Design Study, Report No. ACF-412-256, October 13, 1965, ACF Industries, Inc., Albuquerque Division, for Sandia Corporation, Livermore, California, Sandia Purchase Order 92-1768.
22. Journal of the Structural Division, by R. A. Ridha, and R. N. Wright, ASCE, Volume 93, No. ST4, Proc. Paper 5394, August 1967, pp. 165-183.

APPENDIX I

TABULATED FLAT PLATE SPECIMEN  
GEOMETRIES AND TEST RESULTS

TABLE 3. FLAT PLATE SPECIMEN GEOMETRY - SERIES I

| Spec. Iden. | $l$ in. | $a$ in. | $l_s$ in. | $l_e$ in. | $D_{op}$ in. | Area, in. <sup>2</sup> |             |         |              | Adhesive | Remarks    |      |
|-------------|---------|---------|-----------|-----------|--------------|------------------------|-------------|---------|--------------|----------|------------|------|
|             |         |         |           |           |              | Glass                  | Net Tension | Bearing | Hoop Tension |          |            | Bond |
| I-1-A       | 1.55    | 1.0     | 2.55      | 1.579     | 0.750        | 0.041                  | 0.040       | 0.0750  | 0.0625       | 15.79    | BR-1009-49 |      |
| I-1-B       | 1.55    | 1.0     | 2.55      | 1.579     | 0.750        | 0.041                  | 0.040       | 0.0750  | 0.0625       | 15.79    | BR-1009-49 |      |
| I-2-A       | 1.55    | 1.0     | 2.55      | 1.772     | 0.625        | 0.041                  | 0.060       | 0.0625  | 0.0688       | 17.72    | BR-1009-49 |      |
| I-2-B       | 1.55    | 1.0     | 2.55      | 1.772     | 0.625        | 0.041                  | 0.060       | 0.0625  | 0.0688       | 17.72    | BR-1009-49 |      |
| I-3-A       | 1.55    | 1.0     | 2.55      | 1.863     | 0.563        | 0.041                  | 0.070       | 0.0563  | 0.0719       | 18.63    | BR-1009-49 |      |
| I-3-B       | 1.55    | 1.0     | 2.55      | 1.863     | 0.563        | 0.041                  | 0.070       | 0.0563  | 0.0719       | 18.63    | BR-1009-49 |      |
| I-4-A       | 1.55    | 1.0     | 2.55      | 1.952     | 0.500        | 0.041                  | 0.080       | 0.0500  | 0.0750       | 19.52    | BR-1009-49 |      |
| I-4-B       | 1.55    | 1.0     | 2.55      | 1.952     | 0.500        | 0.041                  | 0.080       | 0.0500  | 0.0750       | 19.52    | BR-1009-49 |      |
| I-5-A       | 1.55    | 1.0     | 2.55      | 2.120     | 0.375        | 0.041                  | 0.100       | 0.0375  | 0.0813       | 21.20    | BR-1009-49 |      |
| I-5-B       | 1.55    | 1.0     | 2.55      | 2.120     | 0.375        | 0.041                  | 0.100       | 0.0375  | 0.0813       | 21.20    | BR-1009-49 |      |
| I-6-A       | 1.55    | 1.0     | 2.55      | 2.199     | 0.312        | 0.041                  | 0.110       | 0.0312  | 0.0844       | 21.99    | BR-1009-49 |      |
| I-6-B       | 1.55    | 1.0     | 2.55      | 2.199     | 0.312        | 0.041                  | 0.110       | 0.0312  | 0.0844       | 21.99    | BR-1009-49 |      |
| I-7-A       | 1.55    | 1.0     | 2.55      | 2.276     | 0.250        | 0.041                  | 0.120       | 0.0250  | 0.0875       | 22.76    | BR-1009-49 |      |
| I-7-B       | 1.55    | 1.0     | 2.55      | 2.276     | 0.250        | 0.041                  | 0.120       | 0.0250  | 0.0875       | 22.76    | BR-1009-49 |      |



TABLE 4. FLAT PLATE SPECIMEN GEOMETRY - SERIES II

| Spec. Iden. | $l$<br>in. | $a$<br>in. | $l_s$<br>in. | $l_e$<br>in. | $D_{op}$<br>in. | Area, in. <sup>2</sup> |             |         |              | Adhesive | Remarks    |      |
|-------------|------------|------------|--------------|--------------|-----------------|------------------------|-------------|---------|--------------|----------|------------|------|
|             |            |            |              |              |                 | Glass                  | Net Tension | Bearing | Hoop Tension |          |            | Bond |
| II-1-A      | 1.55       | 0.475      | 2.025        | 1.575        | 0.625           | 0.041                  | 0.060       | 0.0625  | 0.0163       | 15.75    | BR-1009-49 |      |
| II-1-B      | 1.55       | 0.475      | 2.025        | 1.575        | 0.625           | 0.041                  | 0.060       | 0.0625  | 0.0163       | 15.75    | BR-1009-49 |      |
| II-2-A      | 1.55       | 0.525      | 2.075        | 1.594        | 0.625           | 0.041                  | 0.060       | 0.0625  | 0.0213       | 15.94    | BR-1009-49 |      |
| II-2-B      | 1.55       | 0.525      | 2.075        | 1.594        | 0.625           | 0.041                  | 0.060       | 0.0625  | 0.0213       | 15.94    | BR-1009-49 |      |
| II-3-A      | 1.55       | 0.575      | 2.125        | 1.612        | 0.625           | 0.041                  | 0.060       | 0.0625  | 0.0263       | 16.12    | BR-1009-49 |      |
| II-3-B      | 1.55       | 0.575      | 2.125        | 1.612        | 0.625           | 0.041                  | 0.060       | 0.0625  | 0.0263       | 16.12    | BR-1009-49 |      |
| II-4-A      | 1.55       | 0.350      | 1.900        | 1.627        | 0.500           | 0.041                  | 0.080       | 0.0500  | 0.0100       | 16.27    | BR-1009-49 |      |
| II-4-B      | 1.55       | 0.350      | 1.900        | 1.627        | 0.500           | 0.041                  | 0.080       | 0.0500  | 0.0100       | 16.27    | BR-1009-49 |      |
| II-5-A      | 1.55       | 0.400      | 1.950        | 1.652        | 0.500           | 0.041                  | 0.080       | 0.0500  | 0.0150       | 16.52    | BR-1009-49 |      |
| II-5-B      | 1.55       | 0.400      | 1.950        | 1.652        | 0.500           | 0.041                  | 0.080       | 0.0500  | 0.0150       | 16.52    | BR-1009-49 |      |
| II-6-A      | 1.55       | 0.450      | 2.000        | 1.677        | 0.500           | 0.041                  | 0.080       | 0.0500  | 0.0200       | 16.77    | BR-1009-49 |      |
| II-6-B      | 1.55       | 0.450      | 2.000        | 1.677        | 0.500           | 0.041                  | 0.080       | 0.0500  | 0.0200       | 16.77    | BR-1009-49 |      |
| II-7-A      | 1.55       | 0.280      | 1.830        | 1.670        | 0.375           | 0.041                  | 0.100       | 0.0375  | 0.0093       | 16.70    | BR-1009-49 |      |
| II-7-B      | 1.55       | 0.280      | 1.830        | 1.670        | 0.375           | 0.041                  | 0.100       | 0.0375  | 0.0093       | 16.70    | BR-1009-49 |      |
| II-8-A      | 1.55       | 0.300      | 1.850        | 1.682        | 0.375           | 0.041                  | 0.100       | 0.0375  | 0.0113       | 16.82    | BR-1009-49 |      |
| II-8-B      | 1.55       | 0.300      | 1.850        | 1.682        | 0.375           | 0.041                  | 0.100       | 0.0375  | 0.0113       | 16.82    | BR-1009-49 |      |
| II-9-A      | 1.55       | 0.325      | 1.875        | 1.698        | 0.375           | 0.041                  | 0.100       | 0.0375  | 0.0138       | 16.98    | BR-1009-49 |      |
| II-9-B      | 1.55       | 0.325      | 1.875        | 1.698        | 0.375           | 0.041                  | 0.100       | 0.0375  | 0.0138       | 16.98    | BR-1009-49 |      |

TABLE 5. FLAT PLATE SPECIMEN GEOMETRY - SERIES IV

| Spec. Iden. | $l$ in. | $a$ in. | $l_s$ in. | $l_e$ in. | Dop in. | Area, in. <sup>2</sup> |             |         |              | Adhesive | Remarks    |      |
|-------------|---------|---------|-----------|-----------|---------|------------------------|-------------|---------|--------------|----------|------------|------|
|             |         |         |           |           |         | Glass                  | Net Tension | Bearing | Hoop Tension |          |            | Bond |
| IV-1-A      | 0.75    | 0.750   | 1.500     | 1.027     | 0.50    | 0.041                  | 0.080       | 0.05    | 0.0500       | 10.27    | BR-1009-49 |      |
| IV-1-B      | 0.75    | 0.750   | 1.500     | 1.027     | 0.50    | 0.041                  | 0.080       | 0.05    | 0.0500       | 10.27    | BR-1009-49 |      |
| IV-2-A      | 0.75    | 0.875   | 1.625     | 1.089     | 0.50    | 0.041                  | 0.080       | 0.05    | 0.0625       | 10.89    | BR-1009-49 |      |
| IV-2-B      | 0.75    | 0.875   | 1.625     | 1.089     | 0.50    | 0.041                  | 0.080       | 0.05    | 0.0625       | 10.89    | BR-1009-49 |      |
| IV-3-A      | 0.75    | 1.000   | 1.750     | 1.152     | 0.50    | 0.041                  | 0.080       | 0.05    | 0.0750       | 11.52    | BR-1009-49 |      |
| IV-3-B      | 0.75    | 1.000   | 1.750     | 1.152     | 0.50    | 0.041                  | 0.080       | 0.05    | 0.0750       | 11.52    | BR-1009-49 |      |
| IV-4-A      | 1.80    | 0.750   | 2.550     | 2.077     | 0.50    | 0.041                  | 0.080       | 0.05    | 0.0500       | 20.77    | BR-1009-49 |      |
| IV-4-B      | 1.80    | 0.750   | 2.550     | 2.077     | 0.50    | 0.041                  | 0.080       | 0.05    | 0.0500       | 20.77    | BR-1009-49 |      |
| IV-5-A      | 1.80    | 0.875   | 2.675     | 2.139     | 0.50    | 0.041                  | 0.080       | 0.05    | 0.0625       | 21.39    | BR-1009-49 |      |
| IV-5-B      | 1.80    | 0.875   | 2.675     | 2.139     | 0.50    | 0.041                  | 0.080       | 0.05    | 0.0625       | 21.39    | BR-1009-49 |      |
| IV-6-A      | 1.80    | 1.000   | 2.800     | 2.202     | 0.50    | 0.041                  | 0.080       | 0.05    | 0.0750       | 22.02    | BR-1009-49 |      |
| IV-6-B      | 1.80    | 1.000   | 2.800     | 2.202     | 0.50    | 0.041                  | 0.080       | 0.05    | 0.0750       | 22.02    | BR-1009-49 |      |
| IV-7-A      | 1.00    | 0.625   | 1.625     | 1.214     | 0.50    | 0.041                  | 0.080       | 0.05    | 0.0375       | 12.14    | BR-1009-49 |      |
| IV-7-B      | 1.00    | 0.625   | 1.625     | 1.214     | 0.50    | 0.041                  | 0.080       | 0.05    | 0.0375       | 12.14    | BR-1009-49 |      |
| IV-8-A      | 1.00    | 0.750   | 1.750     | 1.277     | 0.50    | 0.041                  | 0.080       | 0.05    | 0.0500       | 12.77    | BR-1009-49 |      |
| IV-8-B      | 1.00    | 0.750   | 1.750     | 1.277     | 0.50    | 0.041                  | 0.080       | 0.05    | 0.0500       | 12.77    | BR-1009-49 |      |
| IV-9-A      | 1.00    | 1.000   | 2.000     | 1.402     | 0.50    | 0.041                  | 0.080       | 0.05    | 0.0750       | 14.02    | BR-1009-49 |      |
| IV-9-B      | 1.00    | 1.000   | 2.000     | 1.402     | 0.50    | 0.041                  | 0.080       | 0.05    | 0.0750       | 14.02    | BR-1009-49 |      |
| IV-10-A     | 1.55    | 0.625   | 2.175     | 1.885     | 0.375   | 0.041                  | 0.100       | 0.0375  | 0.0438       | 18.85    | BR-1009-49 |      |
| IV-10-B     | 1.55    | 0.625   | 2.175     | 1.885     | 0.375   | 0.041                  | 0.100       | 0.0375  | 0.0438       | 18.85    | BR-1009-49 |      |
| IV-11-A     | 1.55    | 0.750   | 2.300     | 1.964     | 0.375   | 0.041                  | 0.100       | 0.0375  | 0.0563       | 19.64    | BR-1009-49 |      |
| IV-11-B     | 1.55    | 0.750   | 2.300     | 1.964     | 0.375   | 0.041                  | 0.100       | 0.0375  | 0.0563       | 19.64    | BR-1009-49 |      |
| IV-12-A     | 1.55    | 1.000   | 2.550     | 2.120     | 0.375   | 0.041                  | 0.100       | 0.0375  | 0.0813       | 21.20    | BR-1009-49 |      |
| IV-12-B     | 1.55    | 1.000   | 2.550     | 2.120     | 0.375   | 0.041                  | 0.100       | 0.0375  | 0.0813       | 21.20    | BR-1009-49 |      |

TABLE 6. FLAT PLATE SPECIMEN GEOMETRY - SERIES V

| Spec. Iden. | $l$ in. | a in. | $l_s$ in. | $l_e$ in. | $D_{op}$ in. | Area, in. <sup>2</sup> |             |         |              | Adhesive | Remarks |      |
|-------------|---------|-------|-----------|-----------|--------------|------------------------|-------------|---------|--------------|----------|---------|------|
|             |         |       |           |           |              | Glass                  | Net Tension | Bearing | Hoop Tension |          |         | Bond |
| V-1-A       | 1.00    | 0.750 | 1.750     | 1.277     | 0.5          | 0.041                  | 0.080       | 0.050   | 0.0500       | 12.77    | AF-111  |      |
| V-1-B       | 1.00    | 0.750 | 1.750     | 1.277     | 0.5          | 0.041                  | 0.080       | 0.050   | 0.0500       | 12.77    | AF-111  |      |
| V-2-A       | 1.00    | 0.875 | 1.875     | 1.340     | 0.5          | 0.041                  | 0.080       | 0.050   | 0.0625       | 13.40    | AF-111  |      |
| V-2-B       | 1.00    | 0.875 | 1.875     | 1.340     | 0.5          | 0.041                  | 0.080       | 0.050   | 0.0625       | 13.40    | AF-111  |      |
| V-3-A       | 1.00    | 1.000 | 2.000     | 1.402     | 0.5          | 0.041                  | 0.080       | 0.050   | 0.0750       | 14.02    | AF-111  |      |
| V-3-B       | 1.00    | 1.000 | 2.000     | 1.402     | 0.5          | 0.041                  | 0.080       | 0.050   | 0.0750       | 14.02    | AF-111  |      |
| V-4-A       | 0.75    | 0.750 | 1.500     | 1.027     | 0.5          | 0.041                  | 0.080       | 0.050   | 0.0500       | 10.27    | AF-111  |      |
| V-4-B       | 0.75    | 0.750 | 1.500     | 1.027     | 0.5          | 0.041                  | 0.080       | 0.050   | 0.0500       | 10.27    | AF-111  |      |
| V-5-A       | 0.75    | 0.875 | 1.625     | 1.089     | 0.5          | 0.041                  | 0.080       | 0.050   | 0.0625       | 10.89    | AF-111  |      |
| V-5-B       | 0.75    | 0.875 | 1.625     | 1.089     | 0.5          | 0.041                  | 0.080       | 0.050   | 0.0625       | 10.89    | AF-111  |      |
| V-6-A       | 0.75    | 1.000 | 1.750     | 1.152     | 0.5          | 0.041                  | 0.080       | 0.050   | 0.0750       | 11.52    | AF-111  |      |
| V-6-B       | 0.75    | 1.000 | 1.750     | 1.152     | 0.5          | 0.041                  | 0.080       | 0.050   | 0.0750       | 11.52    | AF-111  |      |
| V-7-A       | 0.625   | 0.625 | 1.250     | 0.839     | 0.5          | 0.041                  | 0.080       | 0.050   | 0.0375       | 8.39     | AF-111  |      |
| V-7-B       | 0.625   | 0.625 | 1.250     | 0.839     | 0.5          | 0.041                  | 0.080       | 0.050   | 0.0375       | 8.39     | AF-111  |      |
| V-8-A       | 0.625   | 0.750 | 1.375     | 0.902     | 0.5          | 0.041                  | 0.080       | 0.050   | 0.0500       | 9.02     | AF-111  |      |
| V-8-B       | 0.625   | 0.750 | 1.375     | 0.902     | 0.5          | 0.041                  | 0.080       | 0.050   | 0.0500       | 9.02     | AF-111  |      |
| V-9-A       | 0.50    | 0.625 | 1.125     | 0.714     | 0.5          | 0.041                  | 0.080       | 0.050   | 0.0375       | 7.14     | AF-111  |      |
| V-9-B       | 0.50    | 0.625 | 1.125     | 0.714     | 0.5          | 0.041                  | 0.080       | 0.050   | 0.0375       | 7.14     | AF-111  |      |
| V-10-A      | 0.50    | 0.750 | 1.250     | 0.777     | 0.5          | 0.041                  | 0.080       | 0.050   | 0.0500       | 7.77     | AF-111  |      |
| V-10-B      | 0.50    | 0.750 | 1.250     | 0.777     | 0.5          | 0.041                  | 0.080       | 0.050   | 0.0500       | 7.77     | AF-111  |      |
| V-11-A      | 0.50    | 1.000 | 1.500     | 0.902     | 0.5          | 0.041                  | 0.080       | 0.050   | 0.0750       | 9.02     | AF-111  |      |
| V-11-B      | 0.50    | 1.000 | 1.500     | 0.902     | 0.5          | 0.041                  | 0.080       | 0.050   | 0.0750       | 9.02     | AF-111  |      |

TABLE 6. FLAT PLATE SPECIMEN GEOMETRY - SERIES V (CONT.)

| Spec. Iden. | $l$ in. | $a$ in. | $l_s$ in. | $l_e$ in. | Dop in. | Area, in. <sup>2</sup> |             |         |              | Adhesive | Remarks |      |
|-------------|---------|---------|-----------|-----------|---------|------------------------|-------------|---------|--------------|----------|---------|------|
|             |         |         |           |           |         | Glass                  | Net Tension | Bearing | Hoop Tension |          |         | Bond |
| V-12-A      | 0.80    | 0.70    | 1.50      | 1.053     | 0.5     | 0.0492                 | 0.076       | 0.040   | 0.036        | 8.42     | AF-111  |      |
| V-12-B      | 0.80    | 0.70    | 1.50      | 1.053     | 0.5     | 0.0492                 | 0.076       | 0.040   | 0.036        | 8.42     | AF-111  |      |
| V-13-A      | 0.80    | 0.90    | 1.70      | 1.153     | 0.5     | 0.0492                 | 0.076       | 0.040   | 0.052        | 9.22     | AF-111  |      |
| V-13-B      | 0.80    | 0.90    | 1.70      | 1.153     | 0.5     | 0.0492                 | 0.076       | 0.040   | 0.052        | 9.22     | AF-111  |      |
| V-14-A      | 0.90    | 0.70    | 1.60      | 1.153     | 0.5     | 0.0492                 | 0.076       | 0.040   | 0.036        | 9.22     | AF-111  |      |
| V-14-B      | 0.90    | 0.70    | 1.60      | 1.153     | 0.5     | 0.0492                 | 0.076       | 0.040   | 0.036        | 9.22     | AF-111  |      |
| V-15-A      | 0.90    | 0.90    | 1.80      | 1.253     | 0.5     | 0.0492                 | 0.076       | 0.040   | 0.052        | 10.02    | AF-111  |      |
| V-15-B      | 0.90    | 0.90    | 1.80      | 1.253     | 0.5     | 0.0492                 | 0.076       | 0.040   | 0.052        | 10.02    | AF-111  |      |
| V-16-A      | 1.00    | 0.70    | 1.70      | 1.253     | 0.5     | 0.0492                 | 0.076       | 0.040   | 0.036        | 10.02    | AF-111  |      |
| V-16-B      | 1.00    | 0.70    | 1.70      | 1.253     | 0.5     | 0.0492                 | 0.076       | 0.040   | 0.036        | 10.02    | AF-111  |      |
| V-17-A      | 1.00    | 0.90    | 1.90      | 1.353     | 0.5     | 0.0492                 | 0.076       | 0.040   | 0.052        | 10.82    | AF-111  |      |
| V-17-B      | 1.00    | 0.90    | 1.90      | 1.353     | 0.5     | 0.0492                 | 0.076       | 0.040   | 0.052        | 10.82    | AF-111  |      |

TABLE 7. FLAT PLATE SPECIMEN GEOMETRY - SERIES VII

| Spec. Iden. | $l$ in. | $a$ in. | $l_s$ in. | $l_e$ in. | $D_{op}$ in. | Area, in. <sup>2</sup> |             |         |              | Adhesive | Remarks |   |
|-------------|---------|---------|-----------|-----------|--------------|------------------------|-------------|---------|--------------|----------|---------|---|
|             |         |         |           |           |              | Glass                  | Net Tension | Bearing | Hoop Tension |          |         | Bond  |
| VII-1-A     | 1.25    | 0.75    | 2.00      | 1.527     | 0.5          | 0.041                  | 0.080       | 0.050   | 0.050        | 15.27    | AF-111  | *Staggered shims<br>$l=1.0, 1.25, 1.5, 1.25, 1.0$ in. |
| VII-1-B     | 1.25    | 0.75    | 2.00      | 1.527     | 0.5          | 0.041                  | 0.080       | 0.050   | 0.050        | 15.27    | AF-111  |   |
| VII-2-A     | *       | 0.75    | *         | 1.477     | 0.5          | 0.041                  | 0.080       | 0.050   | 0.050        | 14.77    | AF-111  |   |
| VII-2-B     | *       | 0.75    | *         | 1.477     | 0.5          | 0.041                  | 0.080       | 0.050   | 0.050        | 14.77    | AF-111  |   |



TABLE 8. FLAT PLATE TEST RESULTS

| Spec. Ident. | Ultimate Load k | Stress, ksi |             |         |              |        | Remarks                      |
|--------------|-----------------|-------------|-------------|---------|--------------|--------|------------------------------|
|              |                 | Glass       | Net Tension | Bearing | Hoop Tension | Bond   |                              |
| I-1-A        | 12.12           | 295.6       | 303.0*      | 161.6   | 193.9        | 0.768  | Pin failure.<br>Pin failure. |
| I-1-B        | 12.80           | 312.2       | 320.0*      | 170.7   | 204.8        | 0.811  |                              |
| I-2-A        | 16.48           | 402.0       | 274.7*      | 263.7   | 239.5        | 0.930* |                              |
| I-2-B        | 15.28           | 372.7       | 254.7       | 244.5   | 222.1        | 0.862* |                              |
| I-3-A        | 14.24           | 347.3       | 203.4       | 252.9   | 198.1        | 0.764* |                              |
| I-3-B        | 16.20           | 395.1       | 231.4       | 287.7   | 225.3        | 0.870* |                              |
| I-4-A        | 14.32           | 349.3       | 179.0       | 286.4   | 190.9        | 0.734* |                              |
| I-4-B        | 14.65           | 357.3       | 183.1       | 293.0   | 195.3        | 0.751* |                              |
| I-5-A        | 16.52           | 402.9       | 162.5       | 440.5   | 203.2        | 0.779* |                              |
| I-5-B        | 14.16           | 345.4       | 141.6       | 377.6   | 174.2        | 0.668* |                              |
| I-6-A        | 11.83           | 288.5       | 107.5       | 379.2   | 140.2        | 0.538  |                              |
| I-6-B        | 8.03            | 195.9       | 73.2        | 258.0   | 95.4         | 0.366  |                              |
| I-7-A        | 11.88           | 289.8       | 99.0        | 475.2*  | 135.8        | 0.522  |                              |
| I-7-B        | 11.27           | 274.9       | 93.9        | 450.8*  | 128.8        | 0.495  |                              |
|              |                 |             |             |         |              |        |                              |
| II-1-A       | 9.00            | 219.5       | 150.0       | 144.0   | 552.1*       | 0.572  |                              |
| II-1-B       | 9.24            | 225.4       | 154.0       | 147.8   | 566.9*       | 0.587  |                              |
| II-2-A       | 11.47           | 279.8       | 191.2       | 183.5   | 538.5*       | 0.720  |                              |
| II-2-B       | 11.35           | 276.8       | 189.2       | 181.6   | 532.9*       | 0.712  |                              |
| II-3-A       | 14.35           | 350.0       | 239.2       | 229.6   | 545.6*       | 0.890  |                              |
| II-3-B       | 13.92           | 339.5       | 232.0*      | 222.7   | 529.3        | 0.863  |                              |
| II-4-A       | 5.80            | 141.5       | 72.5        | 116.0   | 580.0*       | 0.357  |                              |
| II-4-B       | 5.74            | 140.0       | 71.8        | 114.8   | 574.0*       | 0.353  |                              |
| II-5-A       | 8.36            | 203.9       | 104.5       | 167.2   | 557.3*       | 0.506  |                              |
| II-5-B       | 9.24            | 225.4       | 115.5       | 184.8   | 616.0*       | 0.559  |                              |
| II-6-A       | 10.47           | 255.4       | 130.9       | 209.4   | 523.5*       | 0.624  |                              |
| II-6-B       | 10.55           | 257.3       | 131.9       | 211.0   | 527.5*       | 0.629  |                              |
| II-7-A       | 6.16            | 150.2       | 61.6        | 164.3   | 662.4*       | 0.369  |                              |
| II-7-B       | 6.03            | 147.1       | 60.3        | 160.8   | 648.4*       | 0.361  |                              |
| II-8-A       | 6.39            | 155.9       | 63.9        | 170.4   | 565.5*       | 0.380  |                              |
| II-8-B       | 7.12            | 173.7       | 71.2        | 189.9   | 630.1*       | 0.423  |                              |
| II-9-A       | 7.52            | 183.4       | 75.2        | 200.5   | 544.9*       | 0.443  |                              |
| II-9-B       | 7.98            | 194.6       | 79.8        | 212.8   | 578.3*       | 0.470  |                              |
|              |                 |             |             |         |              |        |                              |
| IV-1-A       | 9.68            | 236.1       | 121.0       | 193.6   | 193.6        | 0.943* |                              |
| IV-1-B       | 8.48            | 206.8       | 106.0       | 169.6   | 169.6        | 0.826* |                              |
| IV-2-A       | 9.54            | 232.7       | 119.3       | 190.8   | 152.6        | 0.876* |                              |
| IV-2-B       | 10.75           | 262.6       | 134.4       | 215.0   | 172.0        | 0.987* |                              |
| IV-3-A       | 18.37           | 448.0*      | 229.6       | 367.4*  | 244.9        | 1.595* |                              |
| IV-3-B       | 17.50           | 426.8*      | 218.8       | 350.0   | 233.3        | 1.519* |                              |
| IV-4-A       | 15.70           | 382.9       | 196.0*      | 315.0   | 315.0*       | 0.768  |                              |
| IV-4-B       | 14.10           | 343.9       | 176.0       | 281.0*  | 281.0        | 0.677  |                              |

NOTE: \* Denotes Failure Mode

TABLE 8. FLAT PLATE TEST RESULTS (Continued)

| Spec. Ident. | Ultimate Load k | Stress, ksi |             |         |              |        | Remarks                    |
|--------------|-----------------|-------------|-------------|---------|--------------|--------|----------------------------|
|              |                 | Glass       | Net Tension | Bearing | Hoop Tension | Bond   |                            |
| IV-5-A       | 13.76           | 335.6       | 172.0       | 275.2   | 220.0        | 0.643* | Delamination               |
| IV-5-B       | 14.50           | 353.7       | 181.5       | 290.0   | 232.0        | 0.678* |                            |
| IV-6-A       | 14.61           | 356.3       | 182.6       | 292.2   | 194.8        | 0.664* |                            |
| IV-6-B       | 13.84           | 337.6       | 173.0       | 276.8   | 184.5        | 0.629* |                            |
| IV-7-A       | 13.45           | 328.0       | 168.1       | 269.0   | 358.7        | 1.108* |                            |
| IV-7-B       | 14.96           | 364.9       | 187.0       | 299.2   | 398.9        | 1.232* |                            |
| IV-8-A       | 14.60           | 356.1       | 182.5       | 292.0   | 292.0        | 1.143* |                            |
| IV-8-B       | 14.54           | 354.6       | 181.8       | 290.8   | 290.8        | 1.139* |                            |
| IV-9-A       | 13.15           | 320.7       | 164.4       | 263.0   | 175.3        | 0.938* |                            |
| IV-9-B       | 15.38           | 375.1       | 192.3       | 307.6   | 205.1        | 1.097* |                            |
| IV-10-A      | 14.00           | 341.5       | 140.0       | 373.3   | 319.6*       | 0.743  |                            |
| IV-10-B      | 14.20           | 346.3       | 142.0       | 378.7   | 324.2*       | 0.753  |                            |
| IV-11-A      | 12.54           | 305.9       | 125.4       | 334.4*  | 222.7        | 0.639  |                            |
| IV-11-B      | 14.30           | 348.8       | 143.0       | 381.3*  | 254.0        | 0.728  |                            |
| IV-12-A      | 14.36           | 350.2       | 143.6       | 382.9*  | 176.6        | 0.677* |                            |
| IV-12-B      | 14.38           | 350.7       | 143.8       | 383.5   | 176.9        | 0.678* |                            |
| V-1-A        | 18.42           | 449.3*      | 230.3       | 368.5   | 368.5        | 1.443  | Lost Grip                  |
| V-1-B        | 17.18           | 419.0*      | 214.8       | 343.6   | 343.6        | 1.346  |                            |
| V-2-A        | 17.54           | 427.8*      | 219.3       | 350.8   | 280.6        | 1.309  |                            |
| V-2-B        | 18.80           | 458.5*      | 235.0       | 376.0   | 300.8        | 1.406  |                            |
| V-3-A        | 17.75           | 432.9*      | 221.8       | 355.0   | 236.7        | 1.266  |                            |
| V-3-B        | 17.60           | 429.3*      | 220.0       | 352.0   | 234.7        | 1.256  |                            |
| V-4-A        | 17.88           | 436.1       | 223.0       | 357.6   | 357.6        | 1.741* |                            |
| V-4-B        | 17.19           | 419.3       | 214.9       | 343.8   | 343.8        | 1.674* |                            |
| V-5-A        | 17.56           | 428.3       | 219.5       | 351.2   | 281.0        | 1.612* |                            |
| V-5-B        | 16.36           | 399.0       | 204.5       | 327.2   | 261.8        | 1.502* |                            |
| V-6-A        | 16.82           | 410.2       | 210.3       | 336.4   | 224.3        | 1.460* |                            |
| V-6-B        | 15.36           | 374.6       | 192.0       | 307.2   | 204.8        | 1.333  |                            |
| V-7-A        | 14.42           | 351.7       | 180.3       | 288.4   | 384.5*       | 1.718  |                            |
| V-7-B        | 14.57           | 355.4       | 182.1       | 291.4   | 388.5*       | 1.736* |                            |
| V-8-A        | 16.55           | 403.7       | 206.9       | 331.0   | 331.0        | 1.835* |                            |
| V-8-B        | 15.42           | 376.1       | 192.8       | 308.4   | 308.4        | 1.710* |                            |
| V-9-A        | 15.24           | 371.7       | 190.5       | 304.8   | 406.4*       | 2.134  |                            |
| V-9-B        | 14.83           | 361.7       | 185.4       | 296.6   | 395.5        | 2.076* |                            |
| V-10-A       | 14.32           | 349.3       | 179.0       | 286.4   | 286.4        | 1.843* |                            |
| V-10-B       | 14.88           | 362.9       | 186.0       | 297.6   | 297.6        | 1.916* |                            |
| V-11-A       | 15.72           | 383.4       | 196.5       | 314.4   | 209.6        | 1.743* |                            |
| V-11-B       | 17.52           | 427.3       | 219.0       | 350.4   | 233.6        | 1.943* |                            |
| V-12-A       | 14.63           | 297.4       | 192.5       | 365.8*  | 406.4        | 1.739  |                            |
| V-12-B       | 14.92           | 303.3       | 196.3*      | 373.0   | 414.4*       | 1.773* |                            |
| V-13-A       | 15.89           | 323.0       | 209.1*      | 397.3*  | 305.6        | 1.724  |                            |
|              |                 |             |             |         |              |        | Part of shims sheared out. |

NOTE: \* Denotes Failure Mode

TABLE 8. FLAT PLATE TEST RESULTS (Continued)

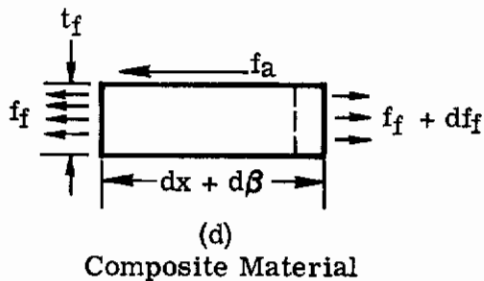
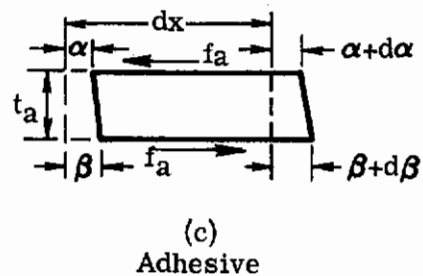
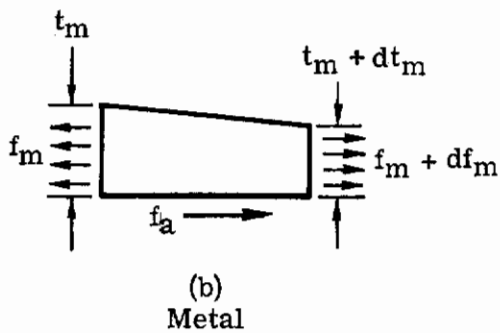
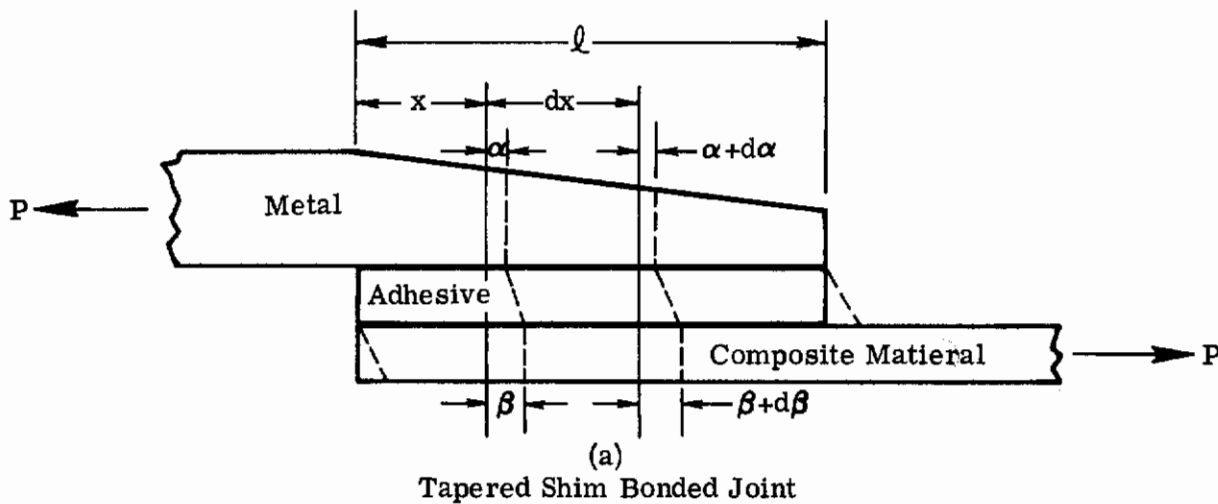
| Spec. Ident. | Ultimate Load k | Stress, ksi |             |         |              |        | Remarks |                                    |
|--------------|-----------------|-------------|-------------|---------|--------------|--------|---------|------------------------------------|
|              |                 | Glass       | Net Tension | Bearing | Hoop Tension | Bond   |         |                                    |
| V-13-B       | 17.62           | 358.1       | 231.8*      | 440.5   | 338.8        | 1.912* |         |                                    |
| V-14-A       | 15.06           | 306.1       | 198.2*      | 376.5*  | 418.3        | 1.634  |         |                                    |
| V-14-B       | 15.78           | 320.7       | 207.6*      | 394.5   | 438.3        | 1.712  |         |                                    |
| V-15-A       | 16.59           | 337.2       | 218.3*      | 414.8*  | 319.0        | 1.657  |         |                                    |
| V-15-B       | 17.45           | 354.7*      | 229.6       | 436.2*  | 335.6        | 1.742  |         |                                    |
| V-16-A       | 14.94           | 303.7       | 196.6*      | 373.5*  | 415.0*       | 1.492  |         |                                    |
| V-16-B       | 15.40           | 313.0       | 202.6*      | 385.0*  | 427.8*       | 1.538  |         |                                    |
| V-17-A       | 16.18           | 328.9       | 212.9       | 404.5*  | 311.2        | 1.496* |         |                                    |
| V-17-B       | 16.80           | 341.5       | 221.1*      | 420.0*  | 323.1        | 1.553  |         |                                    |
| VII-1-A      | 14.18           | 354.9       | 177.3       | 283.6   | 283.6        | 0.929  |         | Crack initiated at transition zone |
| VII-1-B      | 15.41           | 375.9       | 192.6       | 308.2   | 308.2        | 1.009  |         | Sudden failure                     |
| VII-2-A      | 14.71           | 358.8       | 183.9       | 294.2   | 294.2        | 0.996  |         |                                    |
| VII-2-B      | 14.60           | 356.1       | 182.5       | 292.0   | 292.0        | 0.989  |         |                                    |

NOTE: \* Denotes Failure Mode

APPENDIX II

ANALYSIS OF BONDED JOINTS

The following analysis is based on two important assumptions: a) the materials are linearly elastic, and b) the effect of bending through the joint length is small and negligible. A tapered metal sheet is considered to be bonded to a layer of fibrous composite material.



# Contrails

For a unit width, force equilibrium requires:

$$f_f t_f + f_a(dx + d\beta) = (f_f + df_f)t_f \quad (37)$$

Since  $\frac{d\beta}{dx}$  is small compared with unity:

$$f_a = t_f \frac{df_f}{dx}$$

then:

$$\frac{df_a}{dx} = t_f \frac{d^2f_f}{dx^2} \quad (38)$$

From Hooke's law:

$$\epsilon_f = \frac{f_f}{E_f} = \frac{d\beta}{dx}$$

$$\epsilon_m = \frac{f_m}{E_m} = \frac{d\alpha}{dx}$$

$$f_a = \gamma G_a$$

Thus:

$$\begin{aligned} \frac{df_a}{dx} &= G_a \frac{d\gamma}{dx} \\ &= G_a \frac{1}{t_a} \left( \frac{d\beta}{dx} - \frac{d\alpha}{dx} \right) \end{aligned}$$

$$\frac{df_a}{dx} = \frac{G_a}{t_a} \frac{f_f}{E_f} - \frac{f_m}{E_m} \quad (39)$$

Substituting equation 39 into equation 38 and rearranging:

$$\frac{d^2f_f}{dx^2} - \frac{G_a}{t_a t_f} \frac{f_f}{E_f} + \frac{G_a}{t_a t_f} \frac{f_m}{E_m} = 0 \quad (40)$$

but:

$$f_m = \frac{P - f_f t_f}{t_m}$$



hence:

$$\frac{d^2 f_f}{dx^2} - \frac{G_a}{t_a t_f} \left( \frac{1}{E_f} + \frac{t_f}{E_m t_m} \right) f_f = - \frac{G_a P}{E_m t_a t_f t_m} \quad (41)$$

which is the governing differential equation. The boundary conditions are:

$$\text{at } x = 0 \quad f_f = 0$$

$$\text{at } x = l \quad f_f = \frac{P}{t_f}$$

Introducing the following dimensionless quantities:

$$S_f = \frac{f_f}{P/t_f}$$

$$\frac{x}{l} = r$$

$$\frac{t_a}{l} = l_a$$

$$\frac{t_f}{l} = l_f \quad (42)$$

$$\frac{t_m}{l} = l_m, \text{ a function of } r$$

$$\frac{G_a}{E_f} = C_f$$

$$\frac{G_a}{E_m} = C_m$$

Then the dimensionless form of equation is:

$$\frac{d^2 S_f}{dr^2} - \frac{1}{l_a l_f} \left( C_f + \frac{l_f}{l_m} C_m \right) S_f = - \frac{C_m}{l_a l_m} \quad (43)$$

and the corresponding boundary conditions are:

$$\text{at } r = 0 \qquad S_f = 0 \qquad (44)$$

$$\text{at } r = 1 \qquad S_f = 1 \qquad (45)$$

Equations 43, 44 and 45 may be solved on a digital computer by any convenient numerical methods.

Physically the quantity  $S_f$  is a stress concentration factor for stress in the fiber. Similar quantities may be defined for the stress in metal and the shear stress in the adhesive layer

$$S_a = \frac{f_a}{P/l} \qquad (46)$$

$$S_m = \frac{f_m}{P/t_m \text{ (at } x = 0\text{)}} \qquad (47)$$

and are related to  $S_f$  by the expressions:

$$\begin{aligned} S_a &= \frac{f_a}{P/l} = \frac{t_f}{P/l} \frac{df}{dx} \\ &= \frac{d S_f}{dr} \end{aligned} \qquad (48)$$

$$\begin{aligned} S_m &= \left( \frac{P - f_f t_f}{t_m} \right) \frac{1}{P/t_m \text{ (at } x = 0\text{)}} \\ &= (1 - S_f) \frac{t_m \text{ (at } x = 0\text{)}}{t_m} \end{aligned} \qquad (49)$$

For a joint made of constant thickness layers,  $t_m$  is a constant, then equation 43 becomes:

$$\frac{d^2 S_f}{dr^2} - A S_f = -B \qquad (50)$$

where:

$$\begin{aligned} A &= \frac{1}{l_a l_f} \left( C_f + \frac{l_f}{l_m} C_m \right) \\ B &= \frac{C_m}{l_a l_m} \end{aligned} \qquad (51)$$

The general solution of equation 50 is:

$$S_f = C_1 \sinh \sqrt{A} r + C_2 \cosh \sqrt{A} r + \frac{B}{A} \quad (52)$$

and from the boundary conditions:

$$C_1 = \frac{(1 - \frac{B}{A}) + \frac{B}{A} \cosh \sqrt{A}}{\sinh \sqrt{A}}$$

$$C_2 = -\frac{B}{A}$$

Hence:

$$S_f = \frac{B}{A} + (1 - \frac{B}{A}) \frac{\sinh \sqrt{A} r}{\sinh \sqrt{A}} - \frac{B}{A} \frac{\sinh (1-r)\sqrt{A}}{\sinh \sqrt{A}} \quad (53)$$

by definitions 48 and 49,

$$S_m = 1 - S_f$$

$$S_a = (1 - \frac{B}{A}) \sqrt{A} \frac{\cosh \sqrt{A} r}{\sinh \sqrt{A}} + \frac{B}{A} \sqrt{A} \frac{\cosh(1-r)\sqrt{A}}{\sinh \sqrt{A}} \quad (54)$$

Equation 54 agrees with the well known Volkersen equation.

It can be shown that the maximum stress concentration factors are:

$$S_f \text{ max} = 1 \quad \text{at } r = 1 \quad (55)$$

$$S_m \text{ max} = 1 \quad \text{at } r = 0 \quad (56)$$

$$S_a \text{ max} = \frac{B}{A} \sqrt{A} \quad \text{at } r = 0, \text{ or} \quad (57)$$

$$= (1 - \frac{B}{A}) \sqrt{A} \quad \text{at } r = 1 \quad (58)$$

From definitions of A and B in equation      the maximum shear stress concentration factor  $S_a$  may be written:

$$S_a \text{ max} = \ell \sqrt{\frac{G_a E_f t_f}{t_a E_m t_m (E_f t_f + E_m t_m)}} \text{ at } r = 0, \text{ or} \quad (59)$$

$$S_a \text{ max} = \ell \sqrt{\frac{G_a E_m t_m}{t_a E_f t_f (E_f t_f + E_m t_m)}} \text{ at } r = 1 \quad (60)$$

It is obvious that both the magnitude and location of the maximum shear stress concentration factor depends on the relative value of  $E_f t_f$  and  $E_m t_m$ . The following discussions further illustrate the significance of this relative value.

For a joint consisting of two layers bonded together without adhesive, and  $E_f t_f$  is equal to  $E_m t_m$ , then:



$$\frac{P}{E_f t_f} = \frac{P}{E_m t_m}$$

Hooke's law implies:

$$\epsilon_f = \epsilon_m$$

in other words no differential strain in such a joint.

Equation 54 gives the shear stress concentration distribution along the bonded interval:

$$S_a = \left(1 - \frac{B}{A}\right) \sqrt{A} \frac{\cosh \sqrt{A} r}{\sinh \sqrt{A}} + \frac{B}{A} \sqrt{A} \frac{\cosh (1-r) \sqrt{A}}{\sinh \sqrt{A}}$$

A symmetrical shear distribution can be obtained if the parameters are selected such that:

$$1 - \frac{B}{A} = \frac{B}{A}$$

that is:

$$A = 2B$$

or in terms of geometry and mechanical properties:

$$\frac{G_a \ell^2}{t_a} \left( \frac{1}{E_f t_f} + \frac{1}{E_m t_m} \right) = \frac{2 G_a \ell^2}{t_a} \frac{1}{E_m t_m}$$

which implies the condition that  $E_f t_f$  should equal  $E_m t_m$ .

Since  $E_f t_f$  does not equal to  $E_m t_m$  in general, a study of the relative magnitude of these two quantities is of practical interest. Let the larger of the two quantities,  $E_f t_f$  and  $E_m t_m$ , be  $\phi$ , the small one be  $\psi$ , and the ratio of  $\phi$  to  $\psi$  be  $n$ , then  $n$  is always greater than unity:

$$\max (E_f t_f, E_m t_m) = \phi$$

$$\min (E_f t_f, E_m t_m) = \psi$$

$$\frac{\phi}{\psi} = n \quad n > 1$$

In terms of these notations, the maximum shear stress concentration factor is:

$$S_a = \ell \sqrt{\frac{G_a n \psi}{t_a \psi^2 (n + 1)}} = \ell \sqrt{\frac{G_a}{t_a \psi}} \cdot \sqrt{\frac{n}{n + 1}} \quad (61)$$

$$\text{at } r = 0 \quad \text{if } \phi = E_f t_f$$

$$\text{at } r = 1 \quad \text{if } \phi = E_m t_m$$

Then the influence of  $n$  may be plotted as shown in Figure . For given values of  $\ell$ ,  $G_a$ ,  $t_a$  and  $\psi$ , the shear stress corresponding to any  $n$  ratio is given by the curve in Figure 30.

As indicated by the curve,  $S_a$  is quite sensitive to changes in the  $n$  ratio for  $n$  equal 1.0 to  $n$  equal 5.0.



# Contrails

The results of the bond joint analysis are further illustrated in Figures 31 through 34. Figure 31 shows the effect of joint length on the adhesive shear stress distribution in a typical bond joint. Note that the maximum stress value is independent of the bond length. Similarly, Figures 32, 33 and 34 show the effect of bond length, adhesive thickness and metal elastic modulus on the distribution of the shear stress concentration factor.

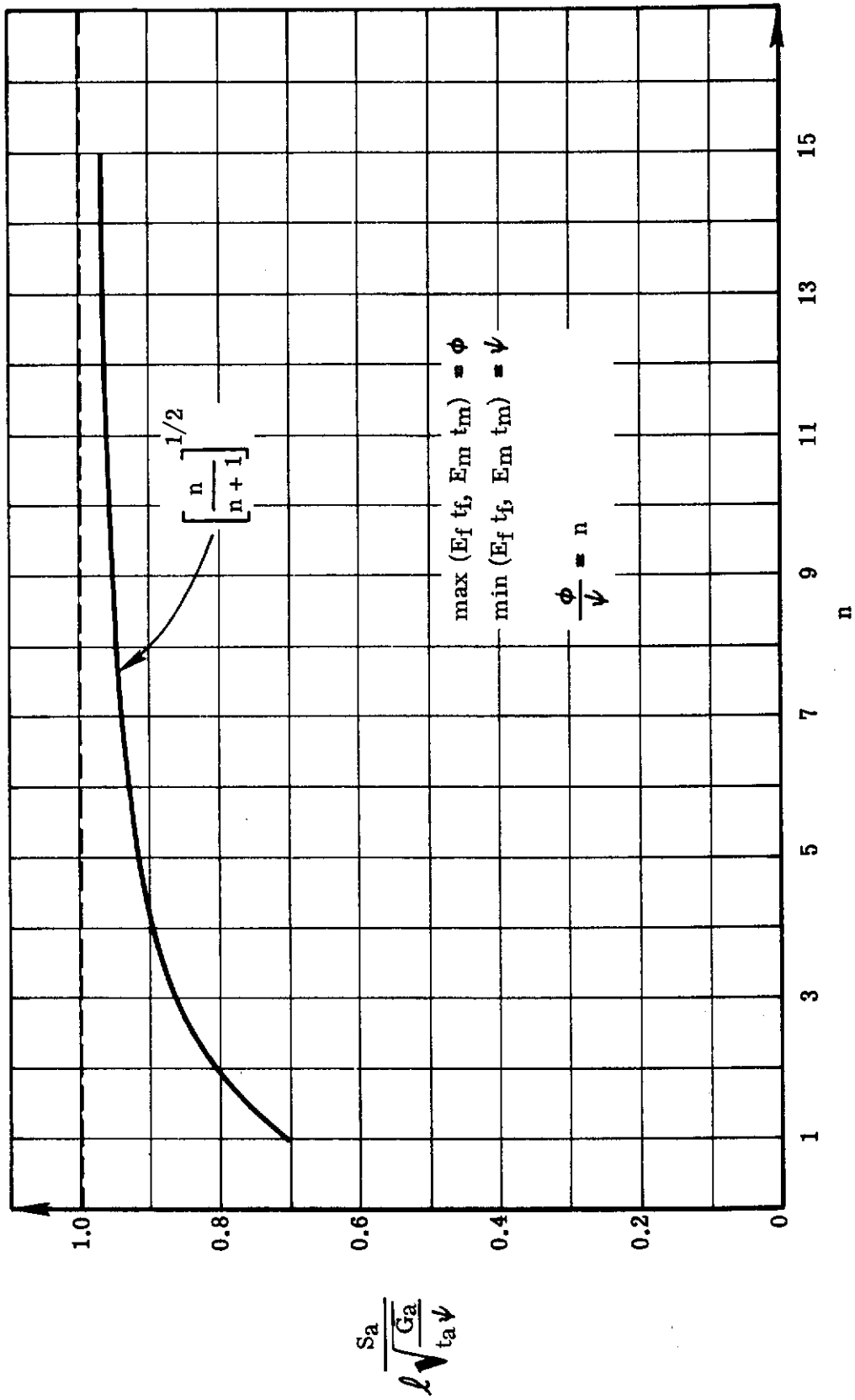


Figure 30. Effect of n Ratio on the Shear Stress Concentration Factor

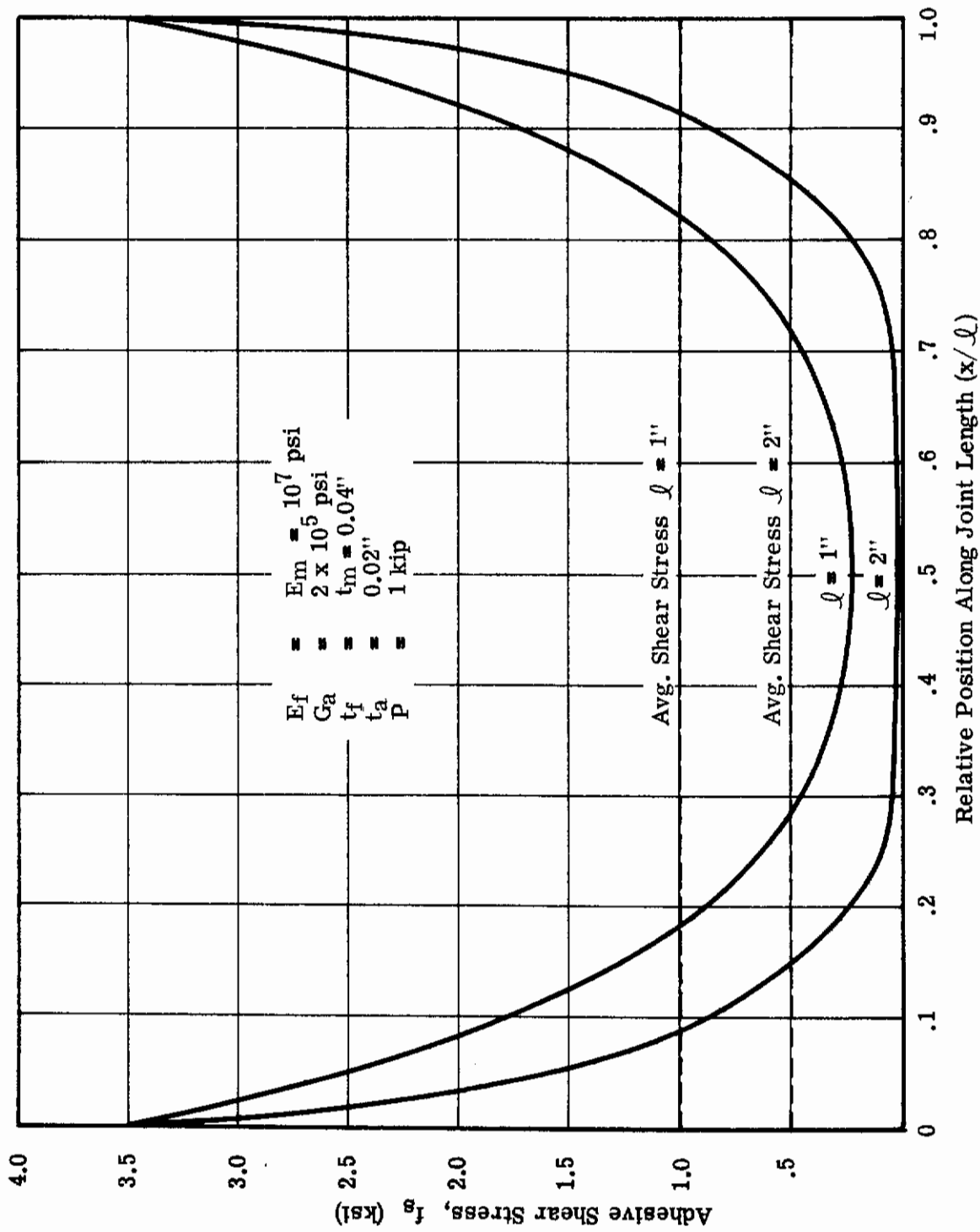


Figure 31. Effect of Joint Length on Distribution of Shear Stress

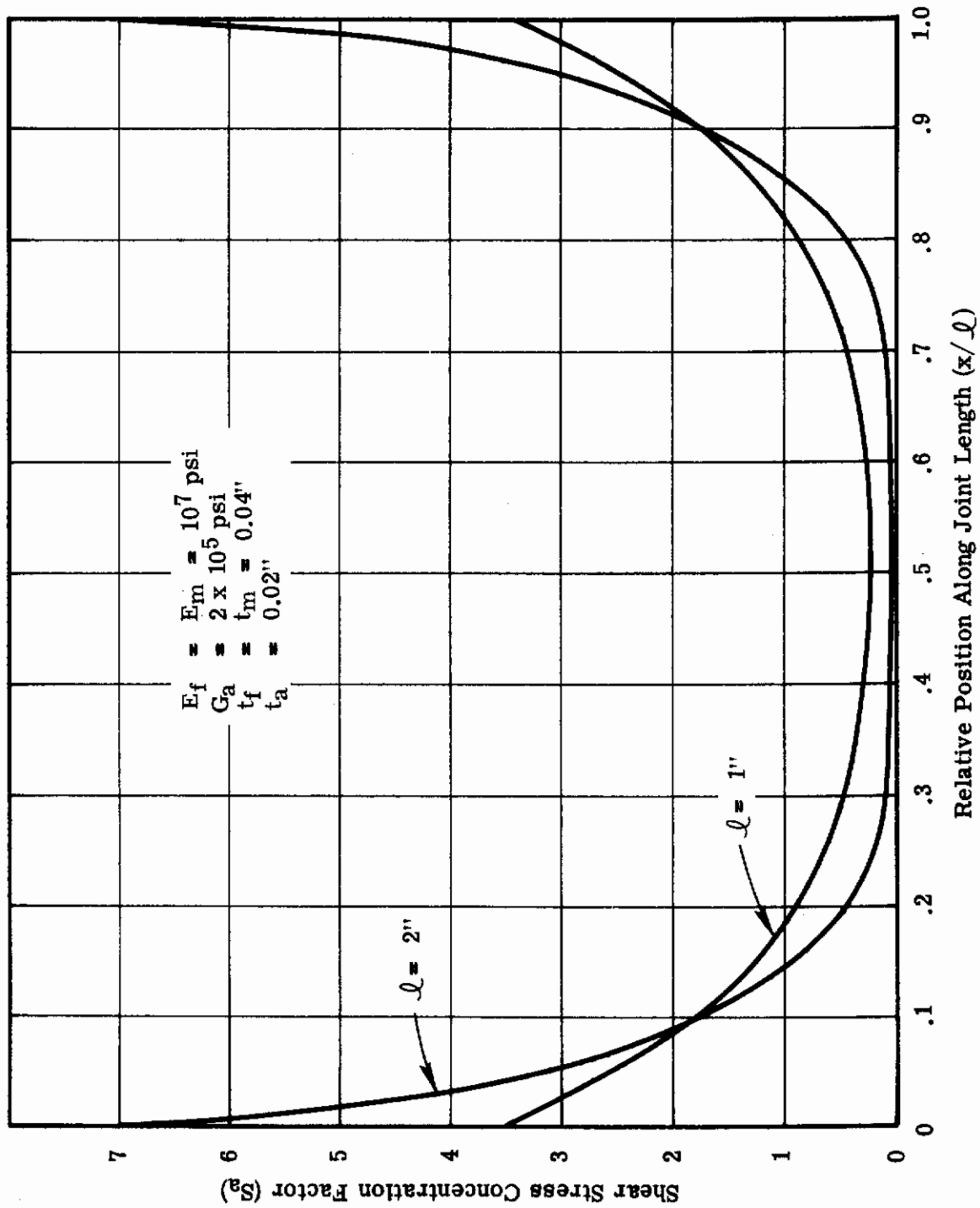


Figure 32. Effect of Joint Length on Distribution of Shear Stress Concentration Factor

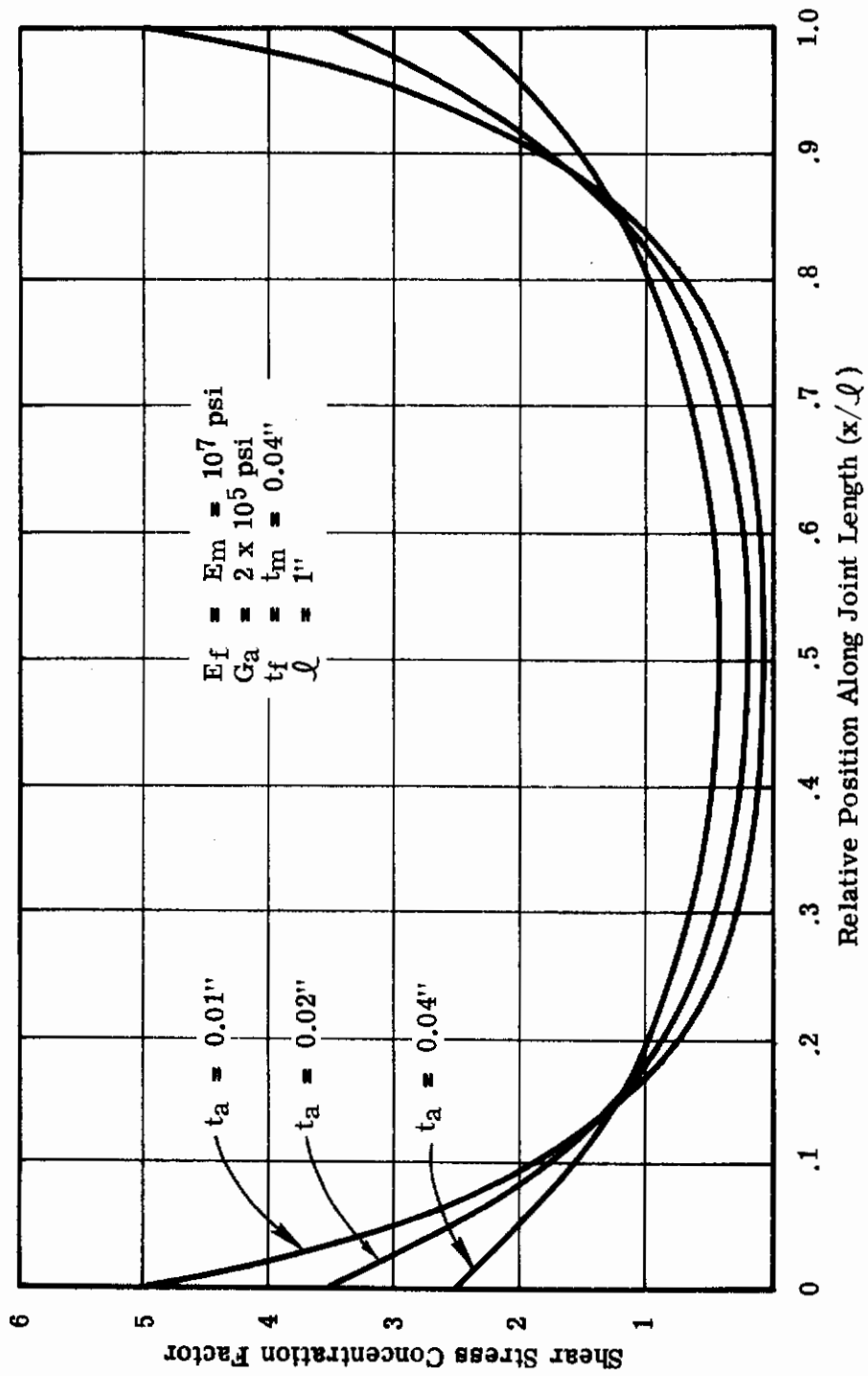


Figure 33. Effect of Adhesive Thickness on Distribution of Shear Stress Concentration Factor



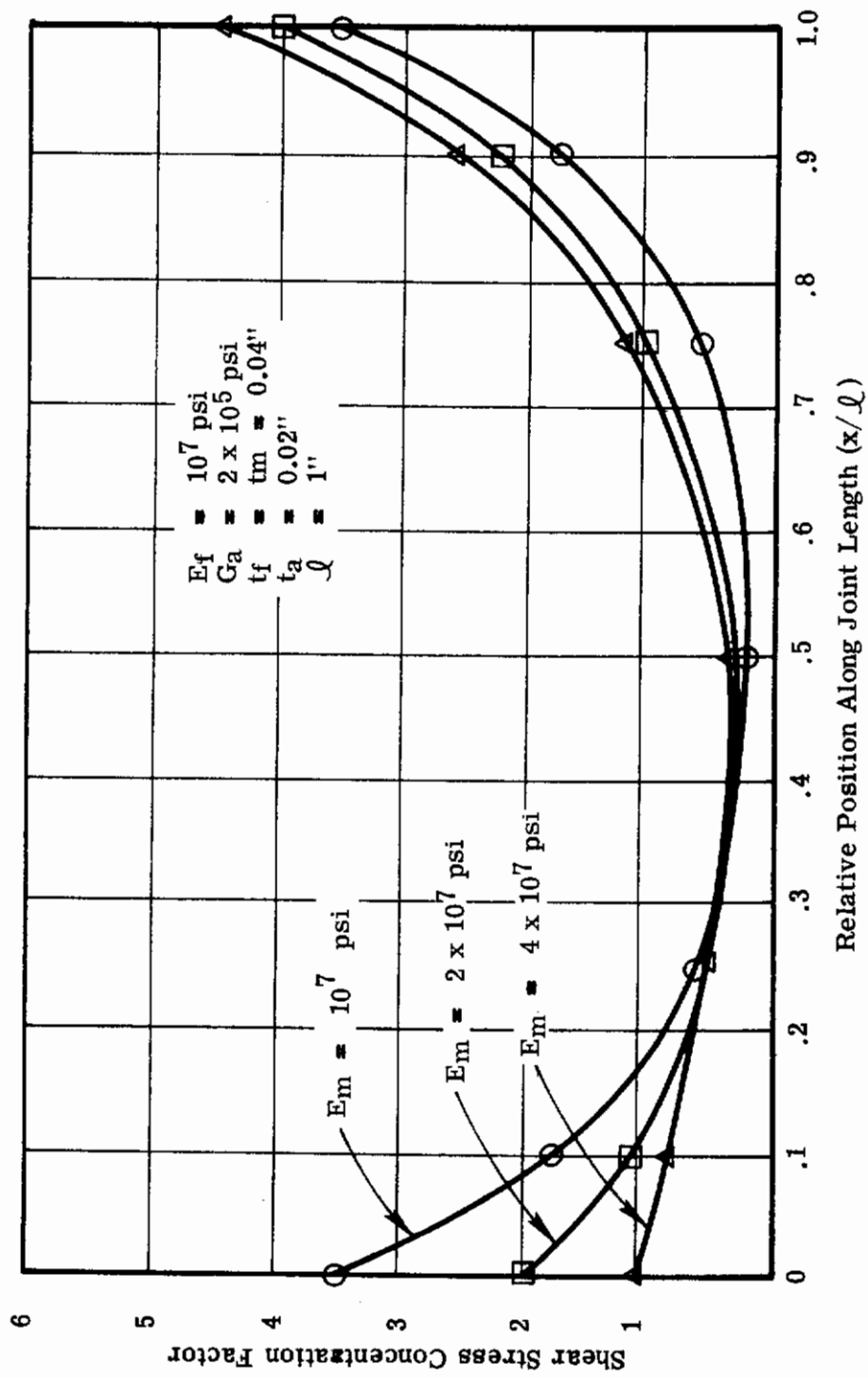


Figure 34. Effect of Metal Elastic Modulus on Distribution of the Shear Stress Concentration Factor

APPENDIX III

ANALYSIS OF TRANSITION ZONE

Due to change of geometry, high stresses exist in the transition zone and may cause delamination. This type of failure was observed on flat plate specimen VII-1-B (Figure 14). A properly designed ring located at the intersection of transition zone and tube may prevent delamination.

The transition zone was analyzed by the ECD finite element program on a digital computer. The model used in the finite element analysis is shown in Figure 35. Note that the location of separation points for adjacent layers is staggered as expected in fabrication. For practical joint arrangements, the following interesting results were observed from the computer studies:

- A. The uplifting (radial) force in the exterior layer is approximately 85 percent of that calculated based on simple geometry and neglecting continuity between layers. (Figure 36.)
- B. The maximum radial strain of the adhesive layers occurs at the exterior layer.
- C. The radial strain at the exterior adhesive layer is proportional to uplifting force at the same location. (Figure 37.)
- D. The radial displacement of the exterior layer is proportional to uplifting force. (Figure 38.)

Based on results from computer studies, the following procedure is suggested for the design of transition zone circ wrap ring thickness.

The uplifting force in the exterior layer  $P'$  is assumed to be 85 percent of the force calculated from a simple model that isolates the exterior layer.

$$P' = 0.85 P \sin \alpha \quad (62)$$

where  $\alpha$  is the angle between the exterior layer and the longitudinal tube axis.

The ultimate radial strain of the exterior adhesive layer may be determined experimentally. For this study the average allowable radial strain is set as 1.4 percent.

$$\epsilon_a = 0.014 \quad (63)$$

Figure 39 indicates that the 58-68R has an ultimate strain value of 2.0 percent. This indicates the presence of a strain concentration factor of 1.43 which seems reasonable. Then, according to the computer analyses for the constituent materials studied:

$$(P_i')_a = C_1 \epsilon_a \quad (64)$$

$$y_a = \frac{(P_i')_a}{C_2} \quad (65)$$

where  $(P_i')_a$  and  $y_a$  are the allowable uplifting force and displacement at the exterior adhesive layer as limited by the allowable strain;  $C_1$  and  $C_2$  are coefficients depending on geometry and mechanical properties.

Then the thickness of transition zone circ wrap ring is given by:

$$t_r = \frac{D^2 [P_i' - (P_i')_a]}{4E_f y_a} \quad (66)$$

where  $t_r$  is the ring thickness,  $D$  the diameter and  $E_f$  the modulus of fiber. It is also recommended that at least one layer of fiber should be used, i.e., 0.006 inch minimum in this case.

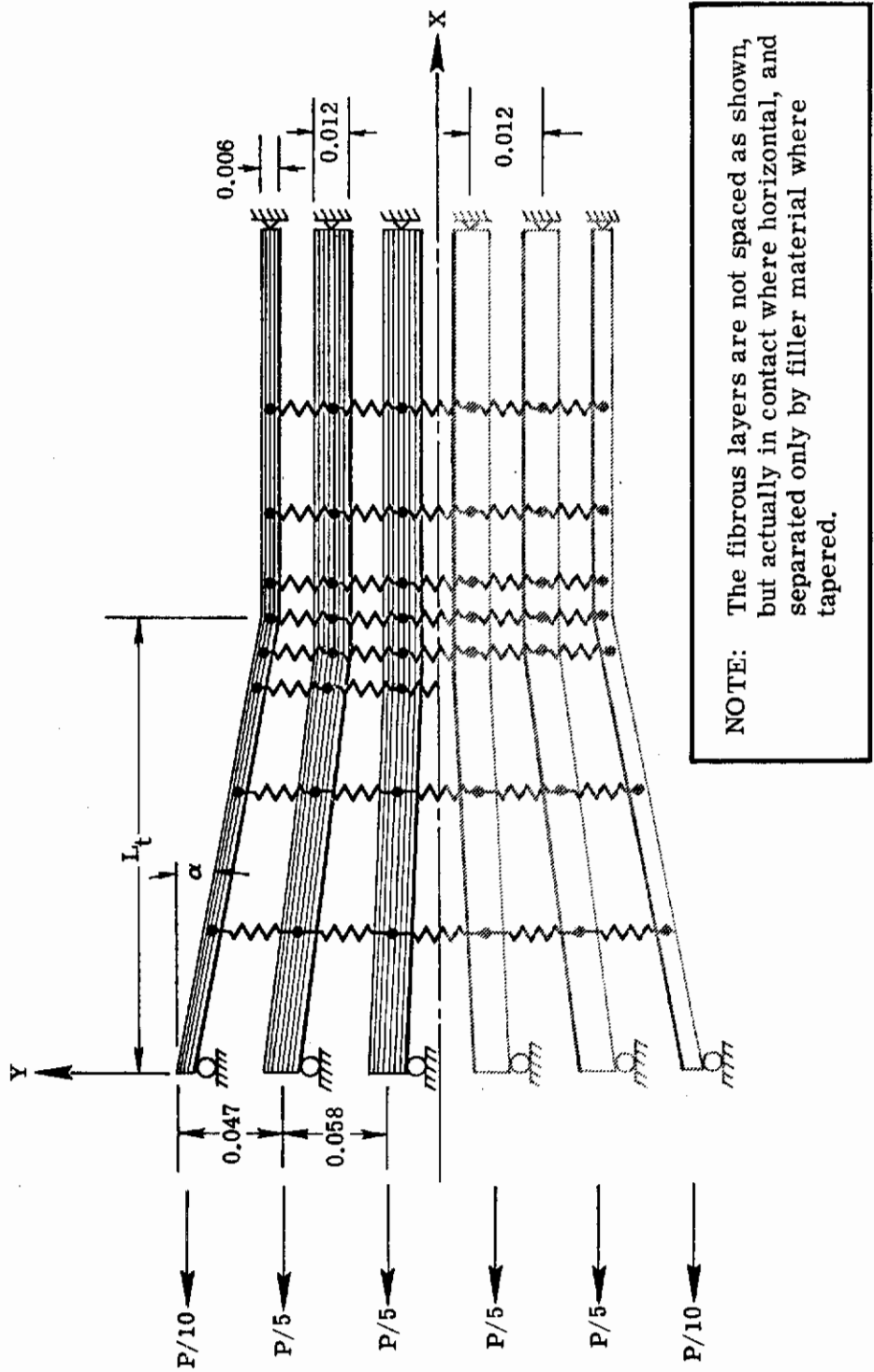


Figure 35. Finite Element Model Used in Computer Studies

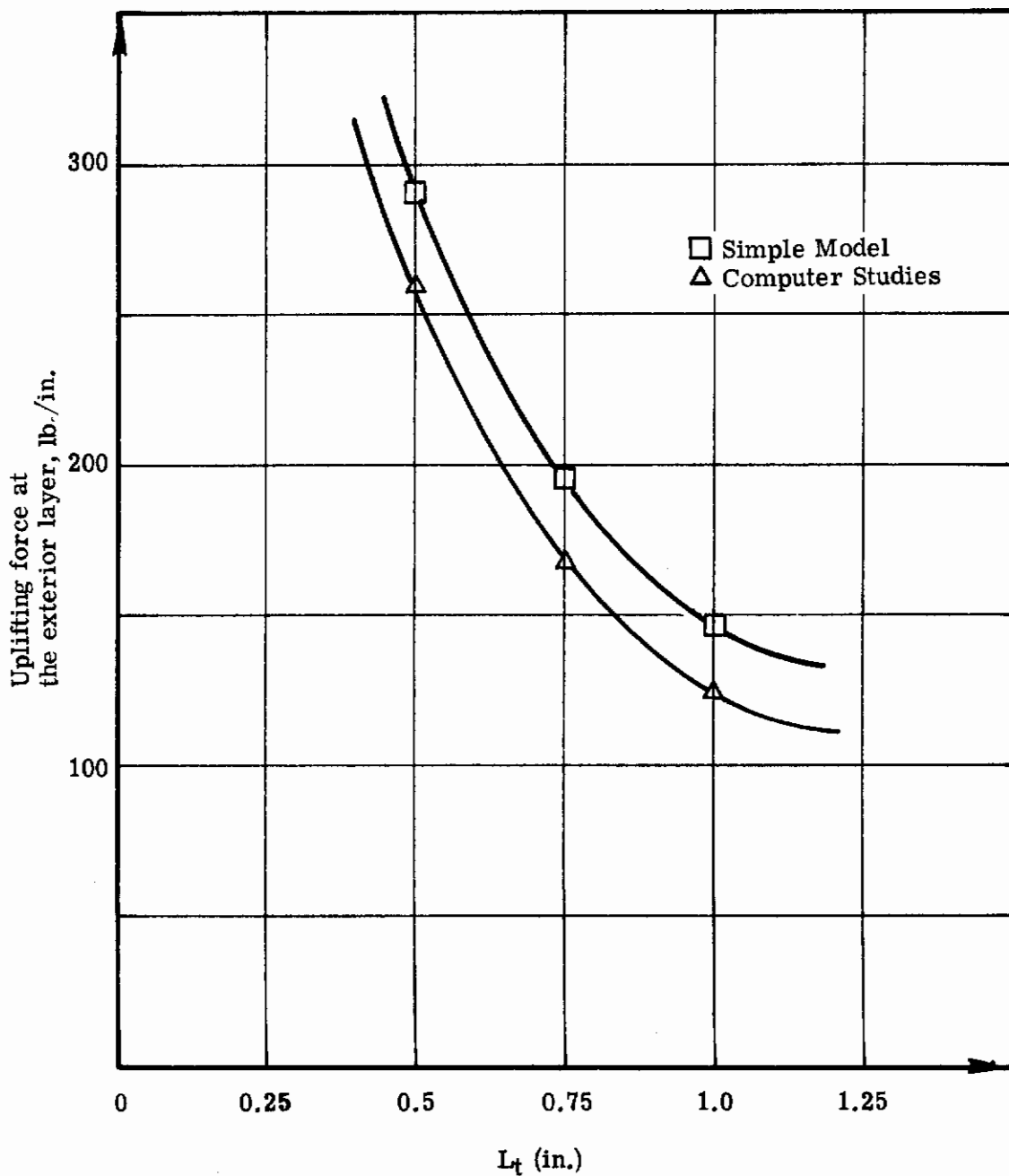


Figure 36. Uplifting Force vs. Transition Zone Length



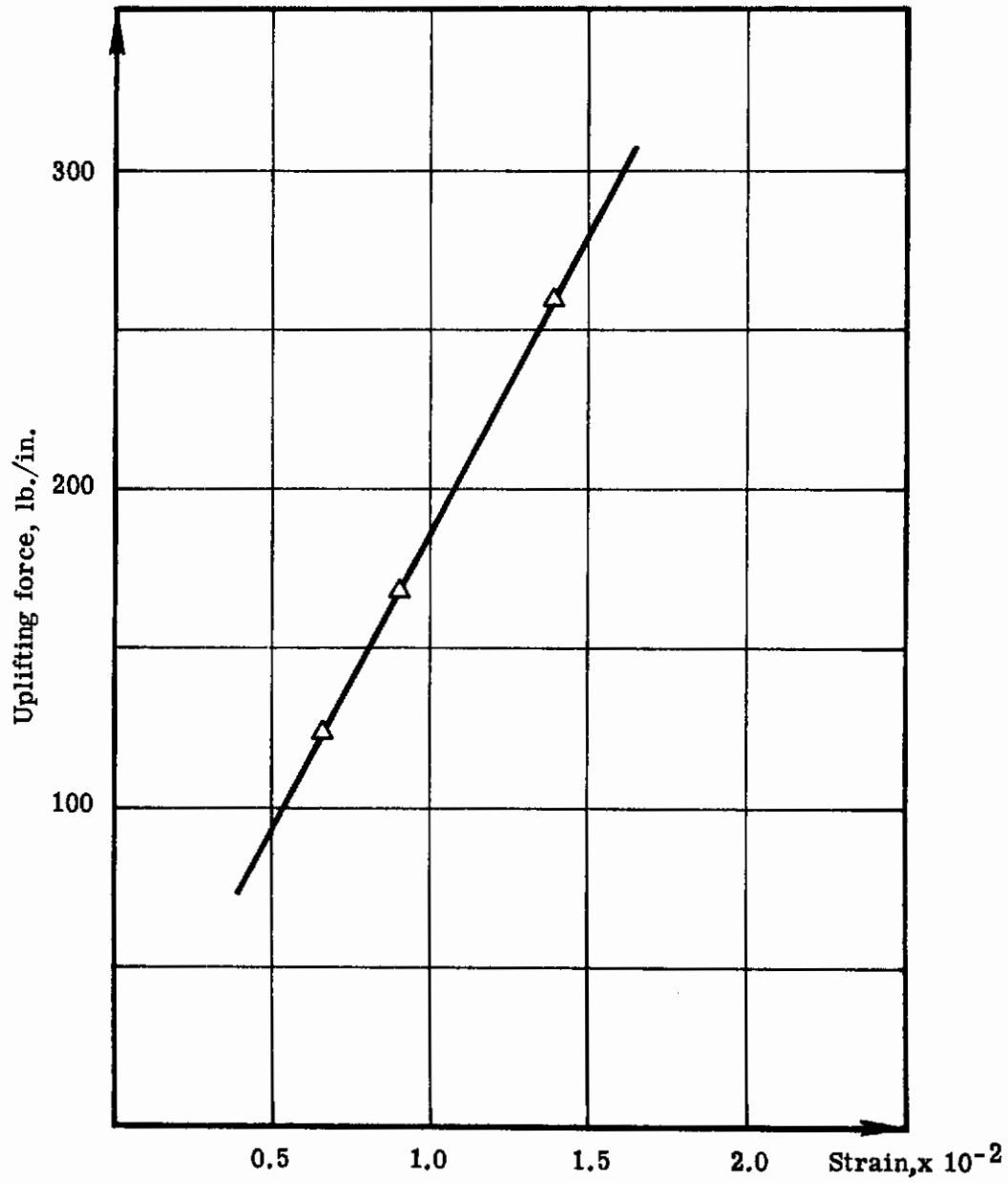


Figure 37. Uplifting Force vs. Resin Strain At Exterior Layer

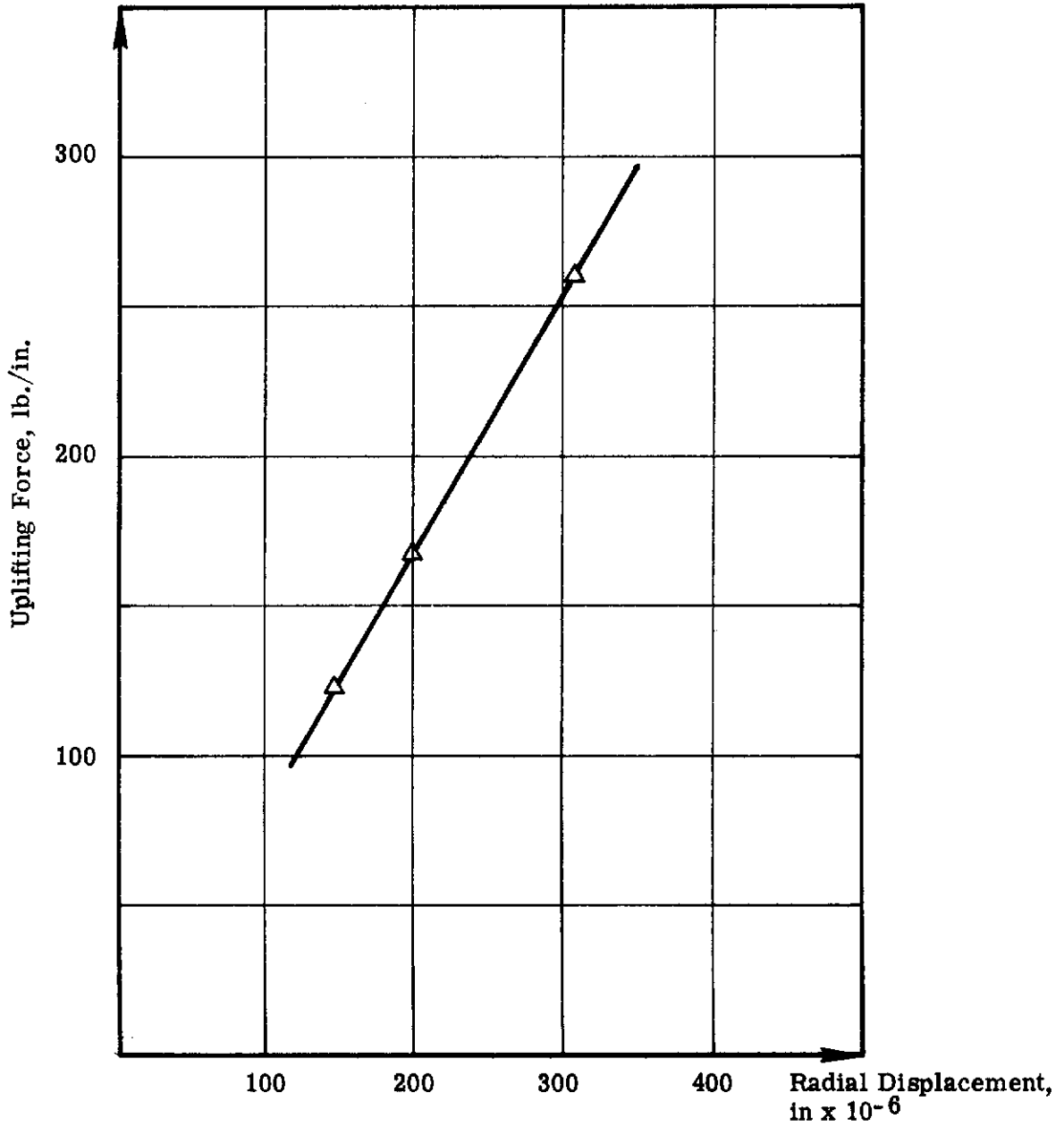


Figure 38. Uplifting Force vs. Radial Displacement at Exterior Layer

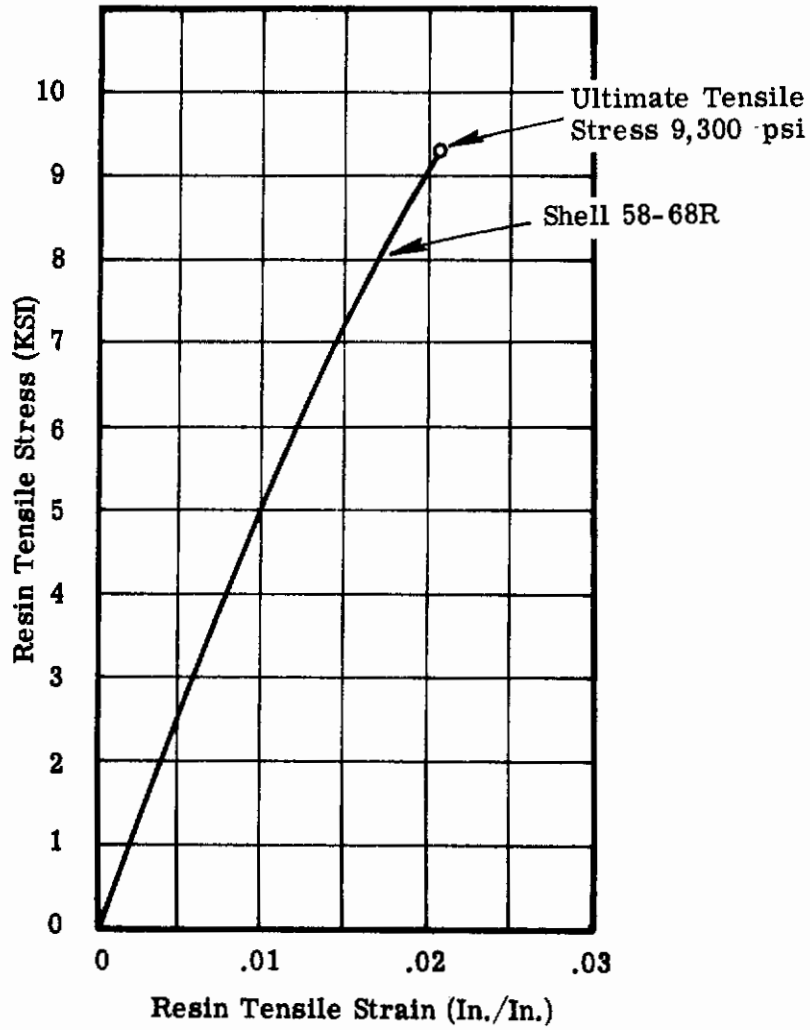


Figure 39. Tensile Stress Strain Curve for Shell 58-68R Resin

APPENDIX IV

OPTIMUM DESIGN PROCEDURE

An optimization problem is generally one of finding the set of variables  $x_i (i = 1, m)$  which minimizes the "objective function"  $f(x_i)$  subjected to the "constraint,"  $G_j(x_i) \geq 0 (j = 1, n)$ .

In design problems, each design specifies the values of the variables  $x_i (i = 1, m)$ . If an  $m$ -dimensional space is considered, a design is defined by a point in that space. Each equation  $G_j(x_i)$  plots as a surface dividing the space into two parts, one of which satisfies  $G_j(x_i) \geq 0$ . Considering all the constraints, a domain is established in which  $G_j(x_i) \geq 0 (j = 1, n)$ . This is the "feasible domain." The equation  $f(x_i) = c$  plots as a contour surface. The distance of the contour surface from the origin depends on the value of  $c$ . The optimization problem involves finding a point in the feasible domain which minimizes the objective function.

The method used on this project is a descent routine using vector analysis. Starting with an initial solution, steps are taken towards new points at which the value of the objective function is improved. The iteration process continues until a minimum is reached.

The direction of movement and the step length depend on the location of the current point. If the point is within the feasible domain, the direction of movement is along the admissible direction of steepest descent, i.e., the negative of the gradient of the objective function. The step length is determined by the first constraint surface encountered upon the movement. The step length is found by the binary chopping technique. If the point is on the boundary, some of the constraints are equally satisfied. The admissible direction of steepest descent at such a point is obtained by sweeping out of the direction of steepest descent the components along the gradients of these constraints.

If some constraints are violated at the current point, movement back to the feasible domain is along the resultant of the gradients of the violated constraints.

When a minimum is reached, the admissible direction of steepest descent is a zero vector and the iteration process stops.

The procedure described above has been programmed in Fortran IV to form the basic ECD optimization routine. The routine has been successfully used for numerous design problems at ECD. When applied to the design of shim joints the input consists of :

# Constraints

1. Number of design parameters, number of constraints.
2. Limit of iterative cycles.
3. Initial step length.
4. Tolerance range for each constraint.
5. Applied load.
6. Tube geometry.
7. Mechanical properties of materials.
8. Design constraints.
9. Initial design parameters.
10. Optional information.

If allowable stress is expressed as a function of design parameters, it is convenient to incorporate allowable stress expressions in the program as design constraints. The program output consists of:

1. Design parameters.
2. Information concerning any violation of constraints.
3. Direction of movement.
4. Weight of each shim joint component.
5. Value of the objective function.

The program was executed on an IBM 360/44 computer at the BECD Computing Center. For six design variables and eleven constraints (including artificial constraints for convenience) the average running time was five to six minutes. It was observed that usually after twenty-five iterations the variation of objective function was in the order of one thousandth of a pound. For all practical purpose the objective function obtained in twenty-five iterations may be taken as the minimum and the corresponding design parameters the optimum design.

APPENDIX V

DESIGN OF FRICTION GRIP TEST FIXTURE

A. Physical Nature of the Fixture.

Figure 26 shows the various elements of the fixture, namely: plug, expander, spacer, jacket and nut. All the elements except the expander are made of high strength steel. The expander is composed of four segments which are made of a woods metal with the trade name of Cerrobend. The part of the tapered plug surface which is in contact with the expander has a relatively smooth finish. The filament test specimen as well as the inside surface of the jacket have comparatively rough finishes. In order for the grip to work properly the fixture must be preloaded. Preloading is accomplished by pulling on the plug and bearing in the opposite direction on the top of the housing until the Cerrobend begins to flow and seats against the inside diameter of the filament tube end. The nut is for the purpose of maintaining the preload while the specimen is mounted in the test machine. If the preloading is sufficiently large, there will be no slipping of the test specimen when tension loads are applied. In fact, any tensile force, acting between the plug and the test specimen, larger than the preload will further tighten the grip. The low friction between the plug and the expander allows the plug to move relative to the expander while the expander is nearly fixed to the test specimen. This movement will increase the intensities of the normal pressures which in turn produce a higher friction force to stretch the test specimen. The expander has a low shear strength of 3500 psi and deforms readily. Yet a high uniform pressure can be developed in the expander because it is confined by the spacer, plug and jacket. In order for the fixture to function properly, it is important to have a proper combination of plug taper, coefficients of friction on the various surfaces, and adequate strength in the elements.

B. Stress Analysis.

1. Plug.

a) Tensile stress at the critical section in the threaded region:

$$\text{Critical sectional area} = \pi \left( \frac{1.875}{2} \right)^2 = 2.76 \text{ sq. in.}$$

For a design maximum load of 200,000 pounds, the average tensile stress at the section is:

$$\frac{200,000}{2.76} = 72,500 \text{ psi}$$



# Contrails

The maximum elastic stress concentration factor occurs near the root of the first thread and has a value of 6.0. The fixture will be used for a limited number of times (less than one thousand times). Therefore, yielding in localized areas may be permitted. The yielding causes a reduction of the stress concentration factor to 3.0. Then the maximum stress is:

$$3 \times 72,500 = 217,500 \text{ psi}$$

which is less than the ultimate material strength.

b) Normal stress at the tapered section of the plug.

The surface area of the tapered section is:

$$A_S = \frac{\pi}{2} (3.00 + 1.873) \cdot 3.1 = 23.4 \text{ sq. in.}$$

The taper has a value of eight degrees, assuming the coefficient of friction,  $\mu$ , between the plug and the expander to be 0.5, then the axial force  $P$  and the normal stress  $f_n$  follow the relationship:

$$\begin{aligned} P &= f_n (\sin 8^\circ + \mu \cos 8^\circ) A_S \\ &= 16.0 f_n \end{aligned}$$

Thus the ultimate normal stress is:

$$f_n = \frac{P}{16.0} = \frac{200,000}{16.0} = 12,500 \text{ psi}$$

The Cerrobend material has a maximum tensile stress of 6,000 psi and a maximum shear strength of 3500 psi. According to this limiting shear strength:

$$P = (f_n \sin 8^\circ + 3500) A_S$$

From which:

$$\begin{aligned} f_n &= \frac{1}{\sin 8^\circ} \left( \frac{P}{A_S} - 3500 \right) \\ &= \frac{1}{0.14} \left( \frac{200,000}{23.4} - 3500 \right) = 36,000 \text{ psi} \end{aligned}$$

Therefore, the maximum normal stress may have a value of 36,000 psi, which is also the maximum internal pressure acting on the jacket.

## 2. Jacket.

The critical stress in the jacket is the hoop stress caused by the internal pressure. The internal pressure may not be uniformly distributed. However, the pressure at the

thinner section of the jacket will be lower than that at the thicker section because of the flexibility of the wall. Therefore, it is adequate to consider the average internal pressure and hoop stress. The average wall thickness,  $t$ , of the jacket is:

$$t = \frac{1}{2} (0.691 + 0.428) = 0.56 \text{ inch}$$

The average hoop stress,  $f_h$ , is:

$$f_h = \frac{f_n R}{t} = \frac{36,000 \times 2}{0.56} = 128,000 \text{ psi}$$

The Cerrobend material creeps even at a low tensile stress of 300 psi. When the fixture sustains the static load for a certain duration, the creep may release the shear strength. Assuming further a reduction of shear strength by 50 percent, the normal stress or the internal pressure may be:

$$f_n = \frac{1}{\sin 8^\circ} \left( \frac{P}{A_S} - \frac{3500}{2} \right)$$

$$= 48,600 \text{ psi}$$

Then the hoop stress has a value of:

$$f_h = \frac{48,600 \times 2}{0.56} = 174,000 \text{ psi}$$

which is also less than the allowable stress.

### 3. Spacer.

The spacer transfers the load from the plug to the jacket and then to the test specimen. It also serves the purpose of confining the expander. The spacer is subjected to bearing stress and torsion caused by the eccentric forces (see sketch). The bearing area,  $A_b$ , is:

$$A_b = \pi (\overline{1.509}^2 - \overline{1.27}^2) = 2.08 \text{ sq. in.}$$

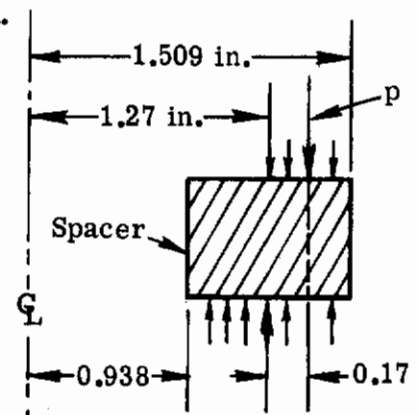
The bearing stress,  $S_b$ , is:

$$S_b = \frac{200,000}{2.08} = 96,600 \text{ psi}$$

which is less than the allowable bearing strength.

The load,  $p$ , per unit length of the spacer is:

$$p = \frac{200,000}{2\pi \times \frac{1}{2} \times (1.509 + 1.270)}$$



$$= 22,900 \text{ lb./in.}$$

The torque,  $M_t$ , per unit length of the spacer is:

$$\begin{aligned} M_t &= 22,900 \times \left( \frac{1.509 + 1.27}{2} - \frac{1.509 + 0.938}{2} \right) \\ &= 22,900 \times 0.17 = 3900 \text{ in.lb./in.} \end{aligned}$$

The maximum bending moment,  $M$ , contributed by the distributed torques is:

$$\begin{aligned} M &= M_t R \\ &= 3900 \times \frac{1}{2} (1.509 + 0.938) \\ &= 4,760 \text{ in. lb.} \end{aligned}$$

The spacer has a depth of 0.75 inch. Thus the maximum bending stress,  $f_b$ , is:

$$\begin{aligned} f_b &= \frac{Mc}{I} = \frac{4760 \times \frac{1}{2} \times 0.75}{\frac{1}{12} \times 0.56 \times 0.75^3} \\ &= 121,500 \text{ psi} \end{aligned}$$

which is an acceptable value.

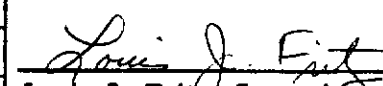
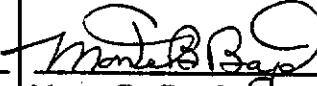
#### 4. Nut.

The nut is used for the purpose of preloading. When the tensile force exceeds the pre-load, there will be no force acting on the nut.

It is to be noted that conservatism has been exercised in making the design and stress analysis.

APPENDIX VI

QUALIFICATION CHECKS ON AM-355 SHEET

| <b>METCUT RESEARCH ASSOCIATES INC.</b>  |              |   |   |                       |               |             |              |           |                   |                       |               |        |       |              |     |     |    |        |       |              |     |     |    |        |       |              |     |     |    |        |       |            |     |     |    |        |       |            |     |     |    |        |       |            |     |     |    |
|---|--------------|---|---|-----------------------|---------------|-------------|--------------|-----------|-------------------|-----------------------|---------------|--------|-------|--------------|-----|-----|----|--------|-------|--------------|-----|-----|----|--------|-------|--------------|-----|-----|----|--------|-------|------------|-----|-----|----|--------|-------|------------|-----|-----|----|--------|-------|------------|-----|-----|----|
| 3980 Rosslyn Drive<br>Telephone:<br>(513)-271-5100  |              |   | Cincinnati, Ohio 45209<br>Teletype:<br>513-577-1785 |                       |               |             |              |           |                   |                       |               |        |       |              |     |     |    |        |       |              |     |     |    |        |       |              |     |     |    |        |       |            |     |     |    |        |       |            |     |     |    |        |       |            |     |     |    |
| <u>LABORATORY REPORT</u>  |              |   |   |                       |               |             |              |           |                   |                       |               |        |       |              |     |     |    |        |       |              |     |     |    |        |       |              |     |     |    |        |       |            |     |     |    |        |       |            |     |     |    |        |       |            |     |     |    |
| DATE  |              | April 23, 1964  |   | NUMBER                |               |             |              |           |                   |                       |               |        |       |              |     |     |    |        |       |              |     |     |    |        |       |              |     |     |    |        |       |            |     |     |    |        |       |            |     |     |    |        |       |            |     |     |    |
|   |              |   |   | 656-5762-5            |               |             |              |           |                   |                       |               |        |       |              |     |     |    |        |       |              |     |     |    |        |       |              |     |     |    |        |       |            |     |     |    |        |       |            |     |     |    |        |       |            |     |     |    |
| CLIENT  |              |   | %   |                       |               |             |              |           |                   |                       |               |        |       |              |     |     |    |        |       |              |     |     |    |        |       |              |     |     |    |        |       |            |     |     |    |        |       |            |     |     |    |        |       |            |     |     |    |
| The B. F. Goodrich Company  |              |   | Mr. W. G. Thomas                                    |                       |               |             |              |           |                   |                       |               |        |       |              |     |     |    |        |       |              |     |     |    |        |       |              |     |     |    |        |       |            |     |     |    |        |       |            |     |     |    |        |       |            |     |     |    |
| ADDRESS   |              |   | AUTHORIZATION                                       |                       |               |             |              |           |                   |                       |               |        |       |              |     |     |    |        |       |              |     |     |    |        |       |              |     |     |    |        |       |            |     |     |    |        |       |            |     |     |    |        |       |            |     |     |    |
| 500 South Main<br>Akron, Ohio   |              |   | DD 244404   |                       |               |             |              |           |                   |                       |               |        |       |              |     |     |    |        |       |              |     |     |    |        |       |              |     |     |    |        |       |            |     |     |    |        |       |            |     |     |    |        |       |            |     |     |    |
| PROJECT   |              |   |   |                       |               |             |              |           |                   |                       |               |        |       |              |     |     |    |        |       |              |     |     |    |        |       |              |     |     |    |        |       |            |     |     |    |        |       |            |     |     |    |        |       |            |     |     |    |
| Qualification Checks on AM-355 Sheet (Coil #1A) <span style="float: right;">BFG<br/>FL</span>   |              |   |   |                       |               |             |              |           |                   |                       |               |        |       |              |     |     |    |        |       |              |     |     |    |        |       |              |     |     |    |        |       |            |     |     |    |        |       |            |     |     |    |        |       |            |     |     |    |
| CONCLUSIONS   |              |   |   |                       |               |             |              |           |                   |                       |               |        |       |              |     |     |    |        |       |              |     |     |    |        |       |              |     |     |    |        |       |            |     |     |    |        |       |            |     |     |    |        |       |            |     |     |    |
| A. Tensile Test (6) Sheet Specimens Manufactured to Metcut D/N 610921-1<br>From Material Supplied by B. F. Goodrich<br>Nominal Gage Section: 0.02" x 0.25" x 1.00" Temp.: R. T.<br>Strain Rate through 0.2% Yield: 0.005 in./in./min.<br>Head Rate thence to Failure: 0.05 in./min.   |              |   |   |                       |               |             |              |           |                   |                       |               |        |       |              |     |     |    |        |       |              |     |     |    |        |       |              |     |     |    |        |       |            |     |     |    |        |       |            |     |     |    |        |       |            |     |     |    |
| <table border="1" style="width: 100%; border-collapse: collapse;"> <thead> <tr> <th style="text-align: center;">MRAI<br/>No.</th> <th style="text-align: center;">Spec.<br/>No.</th> <th style="text-align: center;">Direction</th> <th style="text-align: center;">U. T. S.<br/>(ksi)</th> <th style="text-align: center;">.2%<br/>Y. S.<br/>(ksi)</th> <th style="text-align: center;">Elong.<br/>(%)</th> </tr> </thead> <tbody> <tr> <td style="text-align: center;">T-1976</td> <td style="text-align: center;">1A-AL</td> <td style="text-align: center;">Longitudinal</td> <td style="text-align: center;">255</td> <td style="text-align: center;">250</td> <td style="text-align: center;">13</td> </tr> <tr> <td style="text-align: center;">T-1977</td> <td style="text-align: center;">1A-BL</td> <td style="text-align: center;">Longitudinal</td> <td style="text-align: center;">257</td> <td style="text-align: center;">255</td> <td style="text-align: center;">13</td> </tr> <tr> <td style="text-align: center;">T-1978</td> <td style="text-align: center;">1A-CL</td> <td style="text-align: center;">Longitudinal</td> <td style="text-align: center;">258</td> <td style="text-align: center;">253</td> <td style="text-align: center;">21</td> </tr> <tr> <td style="text-align: center;">T-1979</td> <td style="text-align: center;">1A-DT</td> <td style="text-align: center;">Transverse</td> <td style="text-align: center;">258</td> <td style="text-align: center;">228</td> <td style="text-align: center;">15</td> </tr> <tr> <td style="text-align: center;">T-1980</td> <td style="text-align: center;">1A-ET</td> <td style="text-align: center;">Transverse</td> <td style="text-align: center;">259</td> <td style="text-align: center;">228</td> <td style="text-align: center;">15</td> </tr> <tr> <td style="text-align: center;">T-1981</td> <td style="text-align: center;">1A-FT</td> <td style="text-align: center;">Transverse</td> <td style="text-align: center;">260</td> <td style="text-align: center;">228</td> <td style="text-align: center;">15</td> </tr> </tbody> </table> |              |   |   |                       |               | MRAI<br>No. | Spec.<br>No. | Direction | U. T. S.<br>(ksi) | .2%<br>Y. S.<br>(ksi) | Elong.<br>(%) | T-1976 | 1A-AL | Longitudinal | 255 | 250 | 13 | T-1977 | 1A-BL | Longitudinal | 257 | 255 | 13 | T-1978 | 1A-CL | Longitudinal | 258 | 253 | 21 | T-1979 | 1A-DT | Transverse | 258 | 228 | 15 | T-1980 | 1A-ET | Transverse | 259 | 228 | 15 | T-1981 | 1A-FT | Transverse | 260 | 228 | 15 |
| MRAI<br>No.   | Spec.<br>No. | Direction   | U. T. S.<br>(ksi)                                   | .2%<br>Y. S.<br>(ksi) | Elong.<br>(%) |             |              |           |                   |                       |               |        |       |              |     |     |    |        |       |              |     |     |    |        |       |              |     |     |    |        |       |            |     |     |    |        |       |            |     |     |    |        |       |            |     |     |    |
| T-1976  | 1A-AL        | Longitudinal  | 255   | 250                   | 13            |             |              |           |                   |                       |               |        |       |              |     |     |    |        |       |              |     |     |    |        |       |              |     |     |    |        |       |            |     |     |    |        |       |            |     |     |    |        |       |            |     |     |    |
| T-1977  | 1A-BL        | Longitudinal  | 257   | 255                   | 13            |             |              |           |                   |                       |               |        |       |              |     |     |    |        |       |              |     |     |    |        |       |              |     |     |    |        |       |            |     |     |    |        |       |            |     |     |    |        |       |            |     |     |    |
| T-1978  | 1A-CL        | Longitudinal  | 258   | 253                   | 21            |             |              |           |                   |                       |               |        |       |              |     |     |    |        |       |              |     |     |    |        |       |              |     |     |    |        |       |            |     |     |    |        |       |            |     |     |    |        |       |            |     |     |    |
| T-1979  | 1A-DT        | Transverse  | 258   | 228                   | 15            |             |              |           |                   |                       |               |        |       |              |     |     |    |        |       |              |     |     |    |        |       |              |     |     |    |        |       |            |     |     |    |        |       |            |     |     |    |        |       |            |     |     |    |
| T-1980  | 1A-ET        | Transverse  | 259   | 228                   | 15            |             |              |           |                   |                       |               |        |       |              |     |     |    |        |       |              |     |     |    |        |       |              |     |     |    |        |       |            |     |     |    |        |       |            |     |     |    |        |       |            |     |     |    |
| T-1981  | 1A-FT        | Transverse  | 260   | 228                   | 15            |             |              |           |                   |                       |               |        |       |              |     |     |    |        |       |              |     |     |    |        |       |              |     |     |    |        |       |            |     |     |    |        |       |            |     |     |    |        |       |            |     |     |    |
| B. Hardness measurements were made using Rockwell 15N superficial scale.<br>Random readings and their average are given below: <span style="float: right;">Rockwell 'c'<br/>49</span><br>85.1, 85.4, 85.2 Average: 85.2   |              |   |   |                       |               |             |              |           |                   |                       |               |        |       |              |     |     |    |        |       |              |     |     |    |        |       |              |     |     |    |        |       |            |     |     |    |        |       |            |     |     |    |        |       |            |     |     |    |
| C. Density check was performed by F. C. Broeman & Co., Cincinnati, Ohio:<br>Density (g/cc): 7.77  |              |   |   |                       |               |             |              |           |                   |                       |               |        |       |              |     |     |    |        |       |              |     |     |    |        |       |              |     |     |    |        |       |            |     |     |    |        |       |            |     |     |    |        |       |            |     |     |    |
| No heat treatment was performed by Metcut.  |              |   |   |                       |               |             |              |           |                   |                       |               |        |       |              |     |     |    |        |       |              |     |     |    |        |       |              |     |     |    |        |       |            |     |     |    |        |       |            |     |     |    |        |       |            |     |     |    |
| APPROVED  |              | BY  |   |                       |               |             |              |           |                   |                       |               |        |       |              |     |     |    |        |       |              |     |     |    |        |       |              |     |     |    |        |       |            |     |     |    |        |       |            |     |     |    |        |       |            |     |     |    |
| <br>Louis J. Fritz, Supervisor<br>Mechanical Testing   |              | <br>Monte B. Boyd,<br>Laboratory Technician |   |                       |               |             |              |           |                   |                       |               |        |       |              |     |     |    |        |       |              |     |     |    |        |       |              |     |     |    |        |       |            |     |     |    |        |       |            |     |     |    |        |       |            |     |     |    |
| Sheet   | 1            |   |   |                       |               |             |              |           |                   |                       |               |        |       |              |     |     |    |        |       |              |     |     |    |        |       |              |     |     |    |        |       |            |     |     |    |        |       |            |     |     |    |        |       |            |     |     |    |
| of  | 1            |   |   |                       |               |             |              |           |                   |                       |               |        |       |              |     |     |    |        |       |              |     |     |    |        |       |              |     |     |    |        |       |            |     |     |    |        |       |            |     |     |    |        |       |            |     |     |    |



ALLEGHENY LUDLUM STEEL CORPORATION  
Special Steels for Industry

PLEASE REMIT TO: P.O. BOX 2159, PITTSBURGH 30, PENNSYLVANIA

|                   |            |              |                |                       |            |           |                   |
|-------------------|------------|--------------|----------------|-----------------------|------------|-----------|-------------------|
| ADDRESS TO        | MESSAGE NO | INQUIRY DATE | SHIPMT REG'D   | NOT BEFORE            | MILL ORDER |           |                   |
| GOVT CONTRACT NO  |            |              | VENDOR CODE NO | CUSTOMER ORDER NUMBER | AND DATE   | NO. ITEMS | DATE NUMBER       |
| 09AF-35-657-11303 |            |              |                | DD-214113             |            |           | 32-403-125        |
| PRIORITY          | DEST       | IND          | CUST CODE      | PRODUCT               | MATL       | SLSM      | DIST              |
| 000139            | 024644     | 425504       | 00229          | 127102332             |            |           |                   |
|                   |            |              |                |                       |            |           | ACCEPTING MILL    |
|                   |            |              |                |                       |            |           | DRACKENRIDGE, PA. |

S  
I  
D  
E  
S  
I  
D  
E  
S  
I  
D  
E

D.F. GOODRICH COMPANY  
500 S. MAIN ST.  
AKRON, OHIO



CERTIFICATE  
OF TEST

S  
I  
D  
E  
S  
I  
D  
E  
S  
I  
D  
E

D.F. GOODRICH COMPANY  
DEPT. #3  
505 W. WILBETH ROAD  
AKRON, OHIO

AL STAINLESS STEEL TYPE AM-355 COLD ROLLED STRIP SPEC MPS-815-7 REV A  
TYPE B

|                       |            |              |
|-----------------------|------------|--------------|
| INVOICE NUMBER & DATE |            | DATE SHIPPED |
| R-37744               |            | 3-31-64      |
| CAR INVOICE NO        | GROSS TARE | NET          |
| 3181#                 | 121#       | 3060#        |

| ITEM                     | WEIGHT SHIPPED | QUANTITY SHIPPED | WIDTH DIA O D INCHES | GA THICK WALL NUMBER | LENGTH OR PART NO |
|--------------------------|----------------|------------------|----------------------|----------------------|-------------------|
| 1                        | 3060           | 8                | 8                    | .020                 | COIL              |
| HEAT TEST<br>55571 J1753 |                |                  |                      |                      |                   |
| 2 SKIDS                  |                |                  |                      |                      |                   |
| NET WEIGHT OF INVOICE    |                | 3060             |                      |                      |                   |

CERTIFIED CHEMICAL ANALYSIS AND PHYSICAL PROPERTIES  
ON REVERSE SIDE



ALLEGHENY LUDLUM STEEL CORPORATION  
CERTIFICATE OF TEST

CHEMICAL ANALYSIS

32-403-125

| ITEM | HEAT NO. | C   | MN  | P    | S    | SI  | CR    | NI   | MO   | N2  |  |  |  |  |
|------|----------|-----|-----|------|------|-----|-------|------|------|-----|--|--|--|--|
|      | 55571    | .13 | .74 | .018 | .012 | .32 | 15.60 | 4.30 | 2.74 | .10 |  |  |  |  |

PHYSICAL PROPERTIES

| ITEM | HEAT | TEST | YIELD STRENGTH | TENSILE STRENGTH | ELONG % | ROCKWELL | COLD BEND |  |  |
|------|------|------|----------------|------------------|---------|----------|-----------|--|--|
|      |      |      |                |                  |         |          |           |  |  |

CORE LOSS TEST

10000 B - 15000 B

60 CYCLES

| ITEM | LOT NUMBER | WATTS PER POUND | ITEM | LOT NUMBER | WATTS PER POUND |
|------|------------|-----------------|------|------------|-----------------|
|      |            |                 |      |            |                 |

CORE LOSS IN ACCORDANCE WITH THE AMERICAN SOCIETY FOR TESTING MATERIALS SPECIFICATION A-34

RESULT AS ABOVE CERTIFIED  
ALLEGHENY LUDLUM STEEL CORPORATION  
*J. J. Donnelly*  
CHIEF INSPECTOR

DISTRIBUTION LIST

FOR REPORT NO. AFFDL-TR-67-116 CONTRACT F33615-67-C-1263

Wright-Patterson Air Force Base  
Ohio, 45433

Attn: AFFDL (FDFM) (2 Cys)  
AFFDL (FDTC)  
AFML (MAA)  
AFML (MAAE) (2 Cys)  
AFML (MAAM)  
AFML (MAC)  
AFML (MAM)  
AFML (MAN)  
AFML (MAT)  
AFML (MAY)  
AFML (MAX)(Dr. Tanner)  
AFAL (AVTM)  
AFAPL (API)  
AFAPL (APT)  
AFAPL (APFT)  
SEG (SEPIE)  
SEG (SEFL)  
SEG (SEFSA)  
SEG (SELA)  
SEG (SENXLF-1)  
SEG (SENY ZF)  
SEG (SESSV-R. STALDER)  
BWFRR

Hq. USAF (AFXSAI)  
Air Battle Analysis Center  
Deputy Director of Plans for War  
Directorate of Plans, DC5/P&D  
Washington, D. C. 20330

Hq. USAF (AFRSTF)  
Washington, D.C. 20330

Hq. USAF (AFCSAI)  
Washington, D. C. 20330

Hq. USAF (SAFRD)  
Washington, D. C. 20330

# Contrails

Air Force Rocket Propulsion Lab.  
(RPRPT)  
Edwards Air Force Base, California 93523

Air Force Special Weapons Center  
Kirkland AFB, New Mexico  
Attn: SWO1

Eglin AFB, Florida  
APGC (PGTR1 TECH LIBRARY)

AIR University Library  
Maxwell Air Force Base  
Alabama

Army Rocket and Guided Missile Agency  
Redstone Arsenal, Oklahoma  
Attn: Tech. Library

Dept. of the Army  
Ordnance Corps.  
Springfield Arsenal  
Springfield, Massachusetts  
Attn: R&D D. V.

Commanding Officer  
USA TRECOM  
Attn: J. E. Forehand  
Ft. Eustis, Virginia

U. S. Army  
Ft. Eustis, Virginia  
Attn: USAAML Dr. R. Echols  
USAAML Lt. E. B. Paxson (Bldg. 401)

Dept. of the Army  
Picatinny Arsenal  
Dover, New Jersey  
Attn: PLASTECH Mr. A. Slobodzinski  
PLASTECH Mr. H. Peibly  
Plastics and Packaging Lab. Mr. M. Eig  
Mr. G. R. Rugger  
Mr. J. Scavuzzo

Naval Ordnance Lab.  
White Oaks  
Silver Springs, Maryland  
M. A. Kinna/S. Prosen

Naval Air Engineering Center  
Philadelphia, Pennsylvania 19112  
Aeronautical Structures Lab.  
Attn: T. Manno

Naval Air Systems Command  
Washington, D. C. 20360  
Attn: Code AIR-52032D M. Stander  
Code AIR-530321 R. W. Wills  
Code AIR-5302

NASA  
Lewis Lab.  
21000 Brookpark Road  
Cleveland 35, Ohio  
Attn: Morgan Hansen - Mail 49-1  
J. Burkner - Mail 500-209

NASA Ames Research Center  
Muffett Field, California  
Attn: R. B. Clapper Bldg. 218

NASA Headquarters  
Operation Section  
P.O. Box 5700  
Bethesda, Maryland 20014  
ST/Din (SAK/DL)

NASA  
Space Flight Center  
Huntsville, Alabama  
Attn: J. T. Schell

NASA  
Flight Research Center  
P. O. Box 273  
Edwards Air Force Base  
California 93523  
Attn: Jean L. Jones - Librarian

U. S. Atomic Energy Commission  
Office of Tech. Information Extension  
P. O. Box 62  
Oak Ridge, Tennessee

# Contrails

Sandia Corporation  
Sandia Base  
Attn: Tech. Library  
Albuquerque, New Mexico

Sandia Corporation  
Livermore Laboratory  
P. O. Box 969  
Livermore, California 94551  
Attn: A. L. Skinrood

The Bendix Corporation  
Kansas City Division  
P. O. Box 1159  
Kansas City, Missouri  
Attn: R. Palmer, Dept. 834

Federal Aviation Agency  
Washington, D. C.  
Attn: Engr. and Mfg. Division FS-120  
B. Grochal

Defense Document Center (20 Cys)  
Cameron Station  
Alexandria, Virginia

DISTRIBUTION LIST

FOR REPORT NO. AFFDL-TR-67-116

Aerojet General Corporation  
P. O. Box 296  
Azusa, California 91703  
Attn: F. Darms  
Tech. Library

Aerospace Corporation  
1111 East Mill Street  
San Bernadino, California 92400  
Attn: Dr. L. Rubin

Aeronutronics  
Materials Dept.  
Ford Road  
Newport Beach, California  
Attn: Librarian

Aerospace Corporation  
Applied Mechanics Division  
P. O. Box 95085  
Los Angeles, California 90045  
Attn: H. F. Prime  
Tech. Library

Aerospace Corporation  
El Segundo, California 90245  
Attn: E. Robert Ryder

Aerospace Industries Associations  
1725 DeSales St., N.W., Ste. 600  
Washington, D. C. 20036  
Attn: J. P. Reese, Tech. Services

AVCO Corporation  
201 Lowell Street  
Wilmington, Massachusetts 01887  
Attn: Dr. R. A. Cocozella



# Contracts

Battelle Memorial Institute  
Defense Metals Information Center  
505 King Avenue  
Columbus, Ohio 43201

Beech Aircraft Corporation  
Wichita 1, Kansas  
Attn: Chester A. Rembleske  
Chief, Administrative Engr.

Bell Aerospace Corporation  
Aerosystems Division  
P. O. Box 1  
Buffalo, New York 14205  
Attn: Tech. Library  
D. Earl  
A. Krevitsky

The Boeing Company  
P. O. Box 3733  
Seattle, Washington 98124  
Attn: Ruth E. Peerenboom (Library)  
R. Lacali

The Boeing Company  
P. O. Box 3707  
Seattle, Washington 98124  
Attn: J. Cashin  
W. Plommer

The Boeing Company  
Airplane Division  
P. O. Box 707  
Renton, Washington  
Attn: Harry B. Hightchew - Mail Stop 59-89  
R. J. Hilton - Mail Stop 77-44  
G. F. Harbord - Research Engr. Mfg.

The Boeing Airplane Company  
Wichita 1, Kansas  
Attn: Mr. Al Paxhia

The Boeing Company  
Vertol Division  
Morton, Pennsylvania 19070  
Attn: R. H. Pinckney

The Bendix Corporation  
Energy Controls Division  
South Bend, Indiana 46620  
Attn: A. L. Courtney

Brush Beryllium Company  
17876 St. Clair Avenue  
Cleveland, Ohio 44110

Chrysler Corporation  
Missile Division  
16 Mile Road at Von Dyke  
Detroit, Michigan  
Attn: H. W. Haugen

Cleveland Pneumatic Tool Company  
3781 East 77th Street  
Cleveland, Ohio 44105  
Attn: B. E. Nye  
Z. Barson

Curtiss-Wright Corporation  
Curtiss Division  
Box 351  
Caldwell, New Jersey 07006  
Attn: Engineering Librarian

Douglas Aircraft Company Inc.  
Missile and Space System Division  
3000 Ocean Park Boulevard  
Santa Monica, California 90291  
Attn: Dr. Howard Dixon

Douglas Aircraft Company, Inc.  
Aircraft Division  
Long Beach, California 90801  
Attn: Technical Library  
Dr. Steven Yurenka  
R. Palmer  
K. W. DuBois

Douglas Aircraft Company, Inc.  
Tulsa Division  
2000 North Memorial Drive  
Tulsa, Oklahoma  
Attn: H. E. Felix, Director  
Product Development

# Contrails

Fairchild-Hiller Corporation  
Republic Aviation Division  
Farmingdale, Long Island, New York 11735  
Attn: R. G. Melrose

Forest Products Laboratory  
Madison, Wisconsin  
Attn: Ed Huenzi

Franklin Institute Lab. for R&D  
20th Street and Parkway  
Philadelphia, Pennsylvania 19103

General Dynamic  
Convair Division  
P. O. Box 1950  
San Diego, California 92112  
Attn: Engineering Library (Mail Zone 6-157)  
Bud Perl  
Seth Gunthrop

General Dynamics  
Astronautics  
P. O. Box 1128  
San Diego, California 92112  
Attn: Library and Information Service  
Dept. 128-000  
T. T. Tanalski-Mail Zone 592-10  
D. E. Diller

General Dynamics/Fort Worth  
P. O. Box 748  
Fort Worth, Texas 76101  
Attn: P. R. DeTonnancour  
C. W. Rogers

General Dynamics-Pomona  
Pomona, California 91769  
Attn: Herbert A. Swift - Mail Zone 6-56  
Chief of Structures and Materials

General Electric Company  
Missile and Space Division  
P. O. Box 8555  
Philadelphia, Pennsylvania 19101  
Attn: Lawrence I. Chasen

General Electric Company  
Advanced Technology Laboratories  
1 River Road  
Schenectady, New York 12305  
Attn: J. L. Michaelson

B. F. Goodrich Company  
Aerospace and Defense Products Division  
Wheel and Brake Plant  
Troy, Ohio  
Attn: W. J. Le Blanc

B. F. Goodrich Company  
Research Center  
Brecksville Road  
Brecksville, Ohio 44141  
Attn: J. Sidles  
H. Dietrick

B. F. Goodrich Company  
500 S. Main Street  
Akron, Ohio 44318  
Attn: W. N. Dickerson  
H. W. Stevenson

Goodyear Aircraft Corporation  
Akron, Ohio 44316  
Attn: M. C. Hoffman  
R. A. Burkley (2 Copies)

Grumman Aircraft Engineering Corporation  
Bethpage, L. I., New York 11714  
Attn: Engineering Library  
F. J. Turek  
W. B. Atcheson  
Grant Hedrick

Hercules Powder Company  
P. O. Box 210  
Cumberland, Maryland  
Attn: R. E. Randolph  
James A. Kerns

Hughes Aircraft Company  
Technical Documents Center  
Building 6, Mail Station E-110  
Culver City, California 90232  
Attn: Dr. Colner

IIT Research Institute  
Technology Center  
10 West 35th Street  
Chicago, Illinois 60616  
Attn: Dr. R. Cornish

Ling-Temco-Vought, Inc.  
Aeronautics Division  
P. O. Box 5907  
Dallas, Texas 75222  
Attn: G. A. Starr  
    Dr. B. A. Forcht - Material Tech. Group  
    James E. Martin - Chief of Structures

Lockheed-Georgia Company  
86 South Cobb Drive  
Marietta, Georgia 30061  
Attn: C. K. Bauer  
    J. Osterman  
    W. Lassiter  
    W. A. Boggs  
    H. P. Gilpin

Lockheed-California Company  
10445 Glenoaks Boulevard  
Pacoima, California 91331  
Attn: D. L. Kelly  
    K. S. Carter  
    George Stump

Lockheed-California Company  
Central Library  
Department 72-25, Building 63-1,  
Plant A-1  
Burbank, California 91503  
Attn: Plastics Department  
    V. D. Moss  
    W. J. Crichlow

Lockheed Aircraft Corporation  
Missiles and Space Division  
3251 Hanover Street  
Palo Alto, California  
Attn: Tech. Information Center

Lockheed Missile and Space Division  
Dept. 83-31, Box 504  
Sunnyvale, California  
Attn: James E. Gaughan

Lockheed Aircraft Corporation  
7701 Woodley Avenue  
Van Nuys, California  
Attn: Structures Department

McDonnell Aircraft Corporation  
P. O. Box 516  
St. Louis, Missouri 63166  
Attn: Engineering Library  
Al Drake

Martin Company  
Middle River, Maryland 21220  
Attn: Harry Turner

Martin Company  
Middle River, Science-Tech. Library  
Mail 398  
Baltimore, Maryland 21203  
Attn: Dr. I. Pincus

Martin Company  
Denver Division  
Denver, Colorado 20801  
Attn: Research Library, Mail A-52

Martin Company  
Orlando, Florida  
Attn: Tech. Library

Massachusetts Institute of Tech.  
Dept. of Civil Engineering  
Cambridge 39, Massachusetts  
Attn: Prof. F. J. McGarry

Menasco Manufacturing Company  
805 S. San Fernando Boulevard  
Burbank, California 91502  
Attn: W. J. Eaton



North American Aviation, Inc.  
Space & Information Systems Division  
12214 Lakewood Boulevard  
Downey, California 90241  
Attn: L. M. Foster (Library)  
R. W. Spencer

North American Aviation, Inc.  
International Airport  
Los Angeles, California 90009  
Attn: LAD Library, Dept. 262  
R. F. Shank  
Tom Goebel  
N. Klimmick

North American Aviation, Inc.  
Columbus Division  
4300 East 5th Street  
Columbus, Ohio  
Attn: L. Hackman, Dept. 56

North American Aviation Inc.  
S&ID Division  
2000 North Memorial Drive  
Tulsa 2, Oklahoma  
Attn: James E. Hayes

North American Aviation Inc.  
Rocketdyne Division  
6633 Canoga Avenue  
Canoga Park, California  
Attn: Library  
R. R. Moran

Northrop Space Laboratories  
3401 West Broadway  
Hawthorne, California 90250  
Attn: NSL Library 412-61

Northrop Corporation  
Norair Division  
3901 West Broadway  
Hawthorne, California 90250  
Attn: Tech. Library

Owens Corning Fiberglass Corporation  
Government Services Office  
Suite 508  
900 17th Street, N. W.  
Washington D. C. 20006

Ryan Aeronautical Company  
Lindberg Field  
San Diego 12, California

Southwest Research Institute  
8500 Culebra Road  
San Antonio, Texas 78228  
Attn: L. U. Rastrelli

Space Technology Laboratories, Inc.  
One Space Park  
Redondo Beach, California 90278  
Attn: STL Technical Library

United Aircraft Corporation  
Sikorski Aircraft Division  
Stratford, Connecticut 06497  
Attn: George A. Dmitroff

Whittaker Corporation  
Narmaco R&D Division  
3540 Aero Court  
San Diego, California 92123  
Attn: B. L. Duft

# *Contrails*

UNCLASSIFIED  
Security Classification

| DOCUMENT CONTROL DATA - R&D   |   |  |
|---|---|--|
| <i>(Security classification of title, body of abstract and indexing annotation must be entered when the overall report is classified)</i>   |   |  |
| 1. ORIGINATING ACTIVITY (Corporate author)<br>Energy Controls Division of<br>The Bendix Corporation<br>South Bend, Indiana 46620  |   | 2a. REPORT SECURITY CLASSIFICATION<br>Unclassified |
|   |   | 2b. GROUP  |
| 3. REPORT TITLE<br>Development of the Shim Joint Concept for Composite Structural Members   |   |  |
| 4. DESCRIPTIVE NOTES (Type of report and inclusive dates)<br>Final Report (15 December 1966 to 30 June 1967)  |   |  |
| 5. AUTHOR(S) (Last name, first name, initial)<br>Analytical Mechanics Department<br>Energy Controls Division of<br>The Bendix Corporation   |   |  |
| 6. REPORT DATE<br>August 1967   | 7a. TOTAL NO. OF PAGES<br>108   | 7b. NO. OF REFS<br>21                              |
| 8a. CONTRACT OR GRANT NO.<br>F33615-67-C-1263   | 9a. ORIGINATOR'S REPORT NUMBER(S)   |  |
| b. PROJECT NO.<br>6M26499   | 9b. OTHER REPORT NO(S) (Any other numbers that may be assigned this report)<br>AFFDL-TR-67-116                    |  |
| c.  |   |  |
| d.  |   |  |
| 10. AVAILABILITY/LIMITATION NOTICES<br>This document is subject to special export controls and each transmittal to foreign governments or foreign nationals may be made only with prior approval of AF Flight Dynamics Laboratory (FDFM), WPAFB, Ohio 45433   |   |  |
| 11. SUPPLEMENTARY NOTES   | 12. SPONSORING MILITARY ACTIVITY<br>Air Force Flight Dynamics Laboratory<br>Wright-Patterson Air Force Base, Ohio |  |
| 13. ABSTRACT<br><p>Several methods have been proposed for attaching to the ends of structural tubes fabricated from composite materials, but few have been studied in detail. This program was initiated to study the shim joint concept in detail as subjected to tension loads. The shim joint concept permits a conventional pin joint between the composite tube end and a mating metal fitting by reinforcing the composite material with thin metallic layers. Shim joints were studied during this program as applied to glass reinforced plastic tubes. Corrosion resistant steel (AM 355, 260 ksi) was used as a reinforcement material.</p> <p>An attempt was made to extend shim joint technology by (a) defining through analyses the critical failure modes and pertinent design parameters for tension loads, (b) establishment of design allowables for each of the failure modes through tensile testing of single pin, flat plate specimens, (c) development of a rational design procedure for the shim reinforced tube end, (d) development of improved methods for fabrication and machining of the reinforced tube end, and (e) fabrication and test of full scale tubular joints in test weight end fittings.</p> <p>It was shown during this program that glass composite tubes can be successfully reinforced with AM 355 foil to develop the ultimate load in the tube without prohibitive attachment weight penalties. An optimization routine was used in the design procedure to aid in determining the minimum weight configuration. The bond joint strength was increased significantly during the program by incorporating an adhesive film between the metallic and fibrous layers. A joint, designed to transmit 150 kips to a 3.0 inch OD tube, added only 0.35 pound to the basic tube weight.</p> <p>This abstract has been approved for public release.<br/>Its distribution is unlimited.</p> |   |  |

| 14 | KEY WORDS   | LINK A |    | LINK B |    | LINK C |    |
|----|---|--------|----|--------|----|--------|----|
|    |   | ROLE   | WT | ROLE   | WT | ROLE   | WT |
|    | Filament Composites<br>Filament Winding<br>Filament Tubes<br>Structures<br>Fibers - Glass<br>Fibers - Boron<br>Aircraft Landing Gears<br>Tension<br>Compression<br>Joints |        |    |        |    |        |    |

**INSTRUCTIONS**

1. **ORIGINATING ACTIVITY:** Enter the name and address of the contractor, subcontractor, grantee, Department of Defense activity or other organization (*corporate author*) issuing the report.
- 2a. **REPORT SECURITY CLASSIFICATION:** Enter the overall security classification of the report. Indicate whether "Restricted Data" is included. Marking is to be in accordance with appropriate security regulations.
- 2b. **GROUP:** Automatic downgrading is specified in DoD Directive 5200.10 and Armed Forces Industrial Manual. Enter the group number. Also, when applicable, show that optional markings have been used for Group 3 and Group 4 as authorized.
3. **REPORT TITLE:** Enter the complete report title in all capital letters. Titles in all cases should be unclassified. If a meaningful title cannot be selected without classification, show title classification in all capitals in parenthesis immediately following the title.
4. **DESCRIPTIVE NOTES:** If appropriate, enter the type of report, e.g., interim, progress, summary, annual, or final. Give the inclusive dates when a specific reporting period is covered.
5. **AUTHOR(S):** Enter the name(s) of author(s) as shown on or in the report. Enter last name, first name, middle initial. If military, show rank and branch of service. The name of the principal author is an absolute minimum requirement.
6. **REPORT DATE:** Enter the date of the report as day, month, year, or month, year. If more than one date appears on the report, use date of publication.
- 7a. **TOTAL NUMBER OF PAGES:** The total page count should follow normal pagination procedures, i.e., enter the number of pages containing information.
- 7b. **NUMBER OF REFERENCES:** Enter the total number of references cited in the report.
- 8a. **CONTRACT OR GRANT NUMBER:** If appropriate, enter the applicable number of the contract or grant under which the report was written.
- 8b, 8c, & 8d. **PROJECT NUMBER:** Enter the appropriate military department identification, such as project number, subproject number, system numbers, task number, etc.
- 9a. **ORIGINATOR'S REPORT NUMBER(S):** Enter the official report number by which the document will be identified and controlled by the originating activity. This number must be unique to this report.
- 9b. **OTHER REPORT NUMBER(S):** If the report has been assigned any other report numbers (*either by the originator or by the sponsor*), also enter this number(s).
10. **AVAILABILITY/LIMITATION NOTICES:** Enter any limitations on further dissemination of the report, other than those

imposed by security classification, using standard statements such as:

- (1) "Qualified requesters may obtain copies of this report from DDC."
- (2) "Foreign announcement and dissemination of this report by DDC is not authorized."
- (3) "U. S. Government agencies may obtain copies of this report directly from DDC. Other qualified DDC users shall request through \_\_\_\_\_."
- (4) "U. S. military agencies may obtain copies of this report directly from DDC. Other qualified users shall request through \_\_\_\_\_."
- (5) "All distribution of this report is controlled. Qualified DDC users shall request through \_\_\_\_\_."

If the report has been furnished to the Office of Technical Services, Department of Commerce, for sale to the public, indicate this fact and enter the price, if known.

11. **SUPPLEMENTARY NOTES:** Use for additional explanatory notes.
12. **SPONSORING MILITARY ACTIVITY:** Enter the name of the departmental project office or laboratory sponsoring (*paying for*) the research and development. Include address.
13. **ABSTRACT:** Enter an abstract giving a brief and factual summary of the document indicative of the report, even though it may also appear elsewhere in the body of the technical report. If additional space is required, a continuation sheet shall be attached.  
  
It is highly desirable that the abstract of classified reports be unclassified. Each paragraph of the abstract shall end with an indication of the military security classification of the information in the paragraph, represented as (TS), (S), (C), or (U).  
  
There is no limitation on the length of the abstract. However, the suggested length is from 150 to 225 words.
14. **KEY WORDS:** Key words are technically meaningful terms or short phrases that characterize a report and may be used as index entries for cataloging the report. Key words must be selected so that no security classification is required. Identifiers, such as equipment model designation, trade name, military project code name, geographic location, may be used as key words but will be followed by an indication of technical context. The assignment of links, rules, and weights is optional.